SOLUTIONS AND METHODS OF SOLUTIONS FOR PROBLEMS ENCOUNTERED IN THE THERMAL DESIGN OF SPACECRAFT

by

Richard E. Turner

Thesis submitted to the Graduate Faculty of the

Virginia Polytechnic Institute

in candidacy for the degree of

MASTER OF SCIENCE

in

AEROSPACE ENGINEERING

May 1964

Blacksburg, Virginia

II. TABLE OF CONTENTS

III. LIST OF FIGURES AND TABLE

FIGURE PAGE

TABLE

TABLE

IV. INTRODUCTION

In modern space age travels, animals and mechanical and electrical apparatus will traverse long distances through an endless hostile environment of space. One of the more important aspects of the environment, which must be provided for the space traveler, is temperature control.

Basically, temperature controls have been developed along two lines, the passive and/or the active thermal control. Of course, the methods of passive thermal design may be incorporated into an active thermal design scheme. It is quite evident that passive temperature control is achieved at the time of construction of the spacecraft, as by the application of proper optical coatings, selection of spacecraft geometry and judicious selection of construction materials. On the other hand, active thermal control employs heat generating devices, refrigeration devices, and other similar systems. The role of passive thermal control is to provide, as nearly as possible, a suitable temperature environment, while the active method should be used only when necessary.

At present the near-earth spacecraft is a reality and its environmental situations include all those encountered by most spacecraft. In support of this premise the present thesis will consider only passive thermal design for near-earth satellites.

The two celestial bodies which dominate the heat transferred to a near-earth spacecraft are the earth and sun. The dominant mode of heat transfer to a spacecraft is by thermal radiation. The spacecraft

receives heat directly from the sun and/or earth; and is heated by the sun's rays which are reflected by the earth onto the vehicle.

There are many papers available in the literature written on the thermal design of spacecraft. Unfortunately, even though the subject is straightforward, the problems encountered in thermal design do not lend themselves well to closed form solutions. Consequently, solutions found in the literature are usually numerical and specialized, or they are analytical and solved under assumptions too rigid to be of general interest or to permit an insight into the problem itself.

The following analysis is intended to obtain analytical solutions of thermal control problems which are general in nature whenever this is possible. When the problems encountered do not permit general solutions to be obtained their methods of solution are presented in sufficient detail to provide the reader with enough "tools" to solve related types of problems. A parametric study of orbital heating which requires only a minimum knowledge of orbital variables is given. This clearly shows the nature and sources of orbital heating.

V. SYMBOLS

A	surface area, $in.^2$
$A_{i,j}$	area of body (i) projected to body (j), $in.^2$
A_i	area of general body projected to body (i), $in.^2$
a_i	coefficient in a Fourier expansion
$a_{i,j}$	absorption of radiation from body i by body j
a_i	absorption of radiation from body i by a general body
B_s	angle between ($\tilde{sun}$) and $-e_{Z_b}$, deg
b_i	coefficient from expansion of G_3
c	specific heat, Btu/lb $^\circ R$
c_i	coefficient in a Fourier expansion
c_{rn}	complex constant, $\bar{c}_{rn} + i\hat{c}_{rn}$ where $i = \sqrt{-1}$
C_i	coefficient from expansion of G_3
d_{rn}	complex constant
$\tilde{e}_H$	unit vector alined with spacecraft momentum vector
$\tilde{e}_{X_i}, \tilde{e}_{Y_i}, \tilde{e}_{Z_i}$	unit vectors which form a right-hand orthogonal cartesian coordinate frame associated with the ith coordinate system
$\tilde{e}$	unit vector at the center of the spacecraft pointing toward the center of the earth
$\hat{e}_{rn}, \bar{e}_{rn}$	coefficient in the expansion of $q(t)$
E	angle measured from orbital ascending node to spacecraft, deg
f_i	a function of orbit angle in the expansion of heat flux falling onto a spacecraft

f_{rn}, ε_{rn}	a function of the X coordinate in the temperature solution of a body with nonlinear radiation on its front face
F_{ik}	integral value in the calculation of albedo heating on a spacecraft
G_i	function appearing in the calculation of earth thermal and albedo heating
G_i	function appearing in the solution of time-dependent temperature distributions
$\bar{G}_i$	function appearing in the solution of time-dependent temperature distributions
h_i	function appearing in the solution of time-dependent temperature distributions
$h_{i,j}$	conductive heat-transfer coefficient for heat flow body i to body j, Btu/^{o}R
H	heavieside step function
i	angle between ecliptic plane and equatorial plane, deg
i	square root of (-1)
i,n,k,r	summation indices
I	angle between the equatorial plane and orbit plane, deg
J_i	intensity of radiant heat leaving body i, Btu/in.^{2} · min
K	thermal conductivity, Btu/min in. ^{o}R
L	orbit period, min
L_1	time in sunlight per orbit period, min

m	mass, lb
$\bar{M}_i$	coefficient in the expansion of solar heat on a spacecraft with cylindrical walls
M_n, N_n	function of x in the temperature solution of a body with nonlinear radiation on its front face
$\tilde{n}$	unit vector normal to a surface
p	power per unit volume generated in a body, Btu/min · in.^{3}
P	total power generated in a body, Btu/min
q	intensity of heat falling on a body, Btu/in.^{2} · min
$\tilde{q}_n$	normal component of heat intensity, Btu/in.^{2} · min
$\tilde{q}_T$	tangential component of heat flow in a body, Btu/min · in.^{2}
Q	rotation matrix
Q_{ij}	components of a rotation matrix
$\hat{Q}$	heat content of a body, Btu
$\hat{q}_R$	mean radiation intensity from a body, Btu/min · in.^{2}
$\hat{q}_k$	mean conduction intensity in a body, Btu/in.^{2} · min
R_T	distance of spacecraft from earth's center, miles
R_1	distance between radiating bodies, miles
r_e	earth albedo (0.4)
r	radial coordinate in cylindrical polar coordinates, in.
R_e	radius of earth, miles
R	distance between radiating bodies, miles
R_{ji}	radiative heat transfer from body j to body i, Btu/$^\circ R^4$

S	solar radiation constant, Btu/in.^{2} • min
T	temperature, $^\circ$R
t	time, min
T_A	volume averaged temperature, $^\circ$R
T_r	the rth temperature perturbation, $^\circ$R
t_1	dummy time variable, min
v	variation of surface temperature from its mean value, $^\circ$R
X,Y,Z	inertial coordinate frame where the Z axis coincides with the north pole and the Y axis is perpendicularly to the earth-sun line at the time of the summer solstice
X',Y',Z'	rectangular coordinate frame with the Z' axis normal to the orbit plane and the X' axis coinciding with the satellite-earth line
X'',Y'',Z''	rectangular cartesian coordinate frame with the X'' axis coincident to the earth-sun line and the Z'' axis perpendicular to the ecliptic plane
X_b,Y_b,Z_b	rectangular cartesian coordinate frame with the Z_b axis coinciding with the spacecraft axis of rotational symmetry
X_b^-,Y_b^-,Z_b^-	rectangular cartesian coordinate frame with the Z_b^- axis coincident to the satellite-earth line and the X_b^- axis lying in the plane formed by the Z_b^- axis and the satellite's spin vector $\tilde{\omega}$
α^2	thermal diffusivity, in.^{2}/min
β	angle specifying the position of a radiating element on the earth's surface relative to the satellite subpoint, deg

β_s angle specifying the position of a reflecting element on the earth's surface relative to the sun's subpoint, deg

γ azimuth angle in spherical coordinates, deg

δ orbit angle, deg

δ cone half angle, deg

$\dot{\delta}$ time derivative of orbit angle, radian/min

Δ factor measuring perturbation strength

∇ del operator from vector calculus, $in.^{-1}$

∇^2 Laplacian operator from vector calculus, $in.^{-2}$

ϵ sun's latitude relative to orbit plane coordinate system, deg

ζ sun's longitude relative to orbit plane coordinate system with the perigee taken as 0^o, deg

η angle measuring viewer's misalinement with a body's axis of rotational symmetry, deg

η_c angle between spacecraft's spin axis and satellite-earth line, deg

η_s angle between spacecraft's spin axis and the satellite-sun line, deg

θ_1 dummy variable, deg

θ polar angle in spacecraft's spherical coordinate system, deg

θ_0 limit of integration of polar angle in spacecraft's spherical coordinate system, deg

λ_0 initial angle between orbit perigee and ascending node, deg

$\dot{\lambda}$ time derivative of λ, deg/min

λ angle between orbital ascending node and perigee, deg

$(\lambda_T, \lambda_{Tn}, \hat{\lambda}_{Tn})$ heat rate ratios

Λ volume, $in.^3$

Λ azimuth angle in cylindrical polar coordinates alined with the (X_b, Y_b, Z_b) coordinate frame, deg

μ projected area of body with unit surface area in short-term spin mode, dimensionless

$\hat{\mu}$ projected area of body with unit surface area in long-term spin mode, dimensionless

$\langle\hat{\mu}\rangle$ expectation value of μ in random motion, dimensionless

$\tilde{\nu}$ unit vector from spacecraft's center pointing to viewer

$\hat{\nu}$ latitude of spacecraft's spin axis $(\tilde{\omega})$ relative to orbit plane coordinate system, deg

ρ density, $lb/in.^3$

ξ spin angle of spacecraft's axis of rotational symmetry about spin vector $(\tilde{\omega})$, deg

ε_n dimensionless temperature perturbation

σ Stephan-Boltzmann constant, 2×10^{-13} $Btu/in.^2 \cdot min \cdot {}^\circ R^4$

τ shell thickness, in.

Γ_n nth term of the modified forcing function, $Btu/in.^2 \cdot min$

ϕ_Λ volumetric radiation intensity, $Btu/in.^3 \cdot min$

$\Phi_{i,j}$ total heat flux on body j from body i, Btu/min

$\phi_{i,j}$ total heat intensity on body j from body i, $Btu/in.^2 \cdot min$

ϕ_0 initial angle between X axis and ascending node of orbit, deg

ϕ_{AN} angle between X axis and ascending node of orbit, deg

$\dot{\phi}$ time derivative of ϕ_{AN}, rad/min

ψ longitude of spacecraft's spin vector $(\tilde{\omega})$ in orbit plane coordinate system with perigee taken as $+\pi/2$, deg

$\bar{\psi}$ largest difference between $\langle\hat{\mu}\rangle$ and $\hat{\mu}$

ψ_{rn} complex function of X in the solution of temperature variations in body with nonlinear radiation on front face

ω_n argument rate in ψ_{rn}, rad/in.

ω argument rate in the expansion of heat rates on a spacecraft's surface, rad/min

ϵ total hemispherical emissivity

$\tilde{\omega}$ unit vector coinciding with the spin axis of the spacecraft

$(\tilde{PA})$ unit vector coinciding with the axis of rotational symmetry of the spacecraft

$(\tilde{SUN})$ unit vector coinciding with the satellite-sun line

$(\tilde{e})$ unit vector coinciding with the satellite-earth line

Subscripts:

$( )_m$ mean value with respect to time

$( )_{surf,mean}$ mean surface value

$( )_{surf,max}$ maximum surface value

$( )_{eq}$ equilibrium condition

VI. ANALYSIS

A. Problem Definition

The study of the thermal control of spacecraft is a study of heat transfer, where the governing equation, expressed in vector notation is (see ref. 3)

$$\nabla \cdot \tilde{q} + p = \rho c \frac{\partial T}{\partial t} \tag{1}$$

Here

∇ is the vector del operator

p is the heat created in the material acting as a heat conductor

ρ is the density of the material acting as a heat conductor

c is the density of the material acting as a heat conductor

T is the temperature of the material acting as a heat conductor

and

t is time

$\tilde{q}$ is the heat flow vector

whose ith component is expressed as

$$q_i = -K_i \frac{\partial T}{\partial X_i}$$

where

K_i is the thermal conductivity in the ith direction

X_i is the coordinate assigned to the ith direction

In many cases equation (1) cannot be solved without recourse to numerical techniques. Even when exact solutions to the equation are available,

many times the approximate solution will provide a more meaningful result. Thus as a beginning equation (1) will be specialized for several cases of particular interest.

A first important specialization will be to find an expression governing the space mean temperature for some segment of a spacecraft. This can be accomplished by integrating equation (1) over the body in question, or

$$\int_{\Lambda} \nabla \cdot \tilde{\mathbf{q}} \, d\Lambda + \int_{\Lambda} p \, d\Lambda = \rho c \int_{\Lambda} \frac{\partial T}{\partial t} \, d\Lambda$$

where Λ represents the volume of the segment under study.

However, by use of the divergence theorem it is recognized that

$$\int_{\Lambda} \nabla \cdot \tilde{\mathbf{q}} \, d\Lambda = \int_{S} \tilde{\mathbf{q}} \cdot \tilde{\mathbf{n}} \, dS = \Phi \quad \text{(net heat absorbed per unit time)}$$

$$\int_{\Lambda} p \, d\Lambda = P \quad \text{(net heat created internally)}$$

and

$$\rho c \int_{\Lambda} \frac{\partial T}{\partial t} \, d\Lambda = \rho c \frac{\partial}{\partial t} \int_{\Lambda} T \, d\Lambda = \rho c \frac{\partial}{\partial t} (T_{\Lambda} \Lambda)$$

$$= (\rho \Lambda) c \frac{\partial T_{\Lambda}}{\partial t} = mc \frac{\partial T_{\Lambda}}{\partial t}$$

where $\tilde{\mathbf{n}}$ is the surface unit normal vector and the script T is

employed for

$$\frac{1}{A}\int_A T\,dA = T_A$$

Thus the differential equation for T_A is

$$mc\frac{\partial T_A}{\partial t} = p + \Phi \tag{2}$$

A second specialization to be considered is for the case of heat flow in a thin-walled body. In this case the heat flow vector ($\tilde{q}$) can be separated into two components; one normal to the shell surface ($\tilde{q}_n$) and the other tangent to the shell surface ($\tilde{q}_\tau$), that is

$$\tilde{q} = \tilde{q}_n + \tilde{q}_\tau$$

Hence, equation (1) can be written as

$$\nabla \cdot \tilde{q}_n + \nabla \cdot \tilde{q}_\tau + p = \rho c\frac{\partial T}{\partial t}$$

But, for thin shells

$$\nabla \cdot \tilde{q}_n \simeq \left(\frac{\text{net } q_n}{\tau}\right) = \frac{q_n}{\tau}$$

where τ is the shell wall thickness. Thus there follows

$$\nabla \cdot \tilde{q}_\tau + \frac{q_n}{\tau} + p = \rho c\frac{\partial T}{\partial t} \tag{3}$$

Equation (3) is of particular importance since it approximates a three-dimensional problem by a much simpler two-dimensional problem. The power term, p, is present only for those bodies where electrical currents are used; q_n is the power received per unit area on the body's external surfaces.

For a spacecraft in a near-earth orbit q_n is predominately due to the radiant power received from the sun; radiant power indirectly received from the sun (reflected by the earth onto the spacecraft (albedo)), and radiant power emitted by the earth. The calculation of q_n is straightforward and presents no theoretical difficulty; however, when conventional methods are applied to the problems encountered in thermal design of spacecraft, they become awkward.

Approximate methods of calculating q_n are presented in the next section.

B. Derivation of the Radiation Transfer Equation

The development of realistic techniques for calculating the heat flux on a spacecraft must begin with the well-known expression for the radiant power exchanged between two elemental areas radiating to each other. Text books on heat transfer are sometimes guilty of leading the reader to believe that thermal radiation is a surface property, thus an oversimplified model is presented to the reader. Consequently, the terms "diffuse" and "specular" radiation sometimes are only vaguely understood.

For these reasons a simplified derivation of the classical radiation heat-transfer equation is presented. Too, this derivation can

serve to define the terms appearing in the radiation heat-transfer equation. The pertinent geometry is shown in figure 1.

In figure 1, plane P is considered to be an infinite plane containing the elemental area (dA_1), which classically radiates heat to (dA_2). The radiating material is bounded on its upper surface by plane P but is considered to be infinite in extent on the lower bound. The radiated heat originates from $(dAdY_\alpha)$, the elemental volume immersed in the semi-infinite material.

The area (dA_1) passes radiant heat from the elemental volume $(d\Lambda = dAdY_\alpha)$ to the elemental area (dA_2). The area (dA_2) is chosen as perpendicular to the center line joining $d\Lambda$ to dA_2.

The radiating material itself radiates heat uniformly in all directions, from all self-contained points. However, $d\Lambda$ is so small it does not appreciably reabsorb its own radiated energy.

Let the power emitted (per unit volume) by $d\Lambda$ be ϕ_Λ. This must be partially reabsorbed as the heat travels away from $(d\Lambda)$, otherwise the media could not radiate. Hence ϕ_Λ is not a constant, but

$$\phi_\Lambda = \phi_\Lambda(r) = 4\pi r^2 q_\Lambda(r)$$

where $q_\Lambda(r)$ is the heat flux per unit area at a distance r from its source.

There is no absorbing media between dA_1 and dA_2, hence all the heat from $d\Lambda$, flowing through dA_1, will reach dA_2. As a direct consequence of this statement

$$(R - R_1)^2 q_\Lambda(r = R - R_1) = (R)^2 q_\Lambda(r = R)$$

or

$$q_\Lambda(r = R) = \frac{(R - R_1)^2}{R^2} q_\Lambda(r = R - R_1)$$

By applying the previous definitions

$$d\phi_2 = \left(\frac{R - R_1}{R}\right)^2 q(R - R_1) d\Lambda$$

Here ϕ_2 is the total radiant power per unit area of dA_2 incident on dA_2 (from Λ) passing through dA_1. Now according to the sketch

$$dA = dA_1 \left(\frac{R}{R_1}\right)^2$$

and

$$dY_a = \cos \theta \, dR$$

Now, defining Φ_2 as

$$\Phi_2 = dA_2 \phi_2$$

then

$$d\Phi_2 = dA_2 \left(\frac{R - R_1}{R}\right)^2 q_\Lambda(r = R - R_1) dA_1 \left(\frac{R}{R_1}\right)^2 \cos \theta \, dR$$

and

$$\Phi_2 = \frac{dA_2 dA_1 \cos\vartheta}{R_1^2} \int_{R_1}^{\infty} (R - R_1)^2 q_\lambda (r = R - R_1) dR$$

Now set $(R - R_1) = X$, so that

$$\Phi_2 = \frac{dA_1 dA_2 \cos\theta}{R_1^2} \int_0^{\infty} X^2 q_\lambda (X) dX$$

Since this is a definite integral, then

$$\Phi_2 = c \frac{dA_2 dA_1 \cos\theta}{R_1^2}$$

A simple integration shows that if $J_1 dA_1$ is the total heat flowing through dA_1 then c is simply (J_1/π). Letting

$$dA_2 = dA_{2,1}$$

and

$$dA_1 \cos\theta = dA_{1,2}$$

where $dA_{i,j}$ reads: the area that dA_i projects onto dA_j, then

$$\Phi_2 = \frac{J_1}{\pi} \frac{dA_{2,1} dA_{1,2}}{R_1^2}$$

There will be no confusion if the subscript on R is dropped; then, in general, for two bodies (i,j),

$$\Phi_{j,i} = \frac{J_j}{\pi} \frac{dA_{i,j} dA_{j,i}}{R^2} \qquad (4)$$

Provided that

$$R^2 \gg dA_j \quad \text{or} \quad dA_i$$

The above described radiation is said to radiate diffusely from dA_i.

C. Calculation of Area Distributions

When equation (4) is employed for calculating the radiant power transferred from the earth to a spacecraft, the projected area of the spacecraft satisfies the condition that its dimensions are small in comparison to the distance between the earth and spacecraft. This thesis will consider spacecraft with external surfaces approximating simply joined (convexly arranged) cones alined along an axis of rotational symmetry. The following preliminary remarks will clarify some spinning motions encountered by rotating spacecraft.

Near-earth satellites, which have passive temperature control, often spin about an axis of rotation. During last-stage coasting and burning of the booster, the spacecraft and the last-stage motor may be spun to achieve dynamic stability. At burnout the payload is injected into orbit with some residual spin. In the absence of strong external torques the spacecraft's angular momentum vector will approximately maintain a fixed direction relative to inertial space. If the spacecraft is not perfectly rigid some angular kinetic energy may be lost through structural vibrations, particularly if the spin axis is an axis other than that of the largest moment of inertia. Under this condition

the spacecraft's spin axis will transfer, in some finite lapse of time, to the axis having the largest moment of inertia. In this thesis it will be assumed that the initial spin axis is that of rotational geometrical symmetry and not the axis of largest moment of inertia. Initial spin will be referred to as the "short term spin mode;" the final spin mode will be referred to as the "long term spin mode." For this reason the projected areas projections of the cone must be investigated for spin about an axis of geometrical symmetry and also for spin about an axis perpendicular to the axis of geometrical symmetry. It is tacitly assumed that intermediate spin modes are unimportant to the thermal design of a spacecraft.

Most spacecraft, whose external surfaces cannot be physically approximated by a series of cones, may be optically representable by a series of cones (if the spacecraft spins fast enough so that temperature fluctuations over one spin cycle can be neglected) for the purpose of calculating heat flux on the spacecraft.

In figure 2 dA_v is an elemental surface area for a cone of half angle δ. The elemental area, dA_v, is viewed along the unit vector $\tilde{v}$, $\tilde{n}$ is the unit normal vector of dA_v. Thus

$$dA_v = \frac{1}{2} l^2 \sin \delta d\gamma$$

while

$$\tilde{n} = \tilde{e}_{X_b}(\cos \delta \cos \gamma) + \tilde{e}_{Y_b}(\cos \delta \sin \gamma) + \tilde{e}_{Z_b}(\sin \delta)$$

and

$$\tilde{\nu} = \tilde{e}_{X_b}(\sin \eta) + \tilde{e}_{Z_b}(\cos \eta)$$

where the $\tilde{e}_{i_b}$ are unit vectors in the ith directions.

The projection of dA_V along $\tilde{\nu}$ is

$$dA_{V,\nu} = (\tilde{n} \cdot \tilde{\nu})dA_V$$

so that the total area of the cone projected onto $\tilde{\nu}$ is

$$A_{V,\nu} = \oint_{\text{cone } A_V} (\tilde{n} \cdot \tilde{\nu})^* dA_V \tag{5}$$

Here the star superscript signifies that all negative values of $(\tilde{n} \cdot \tilde{\nu})$ are deleted from the integration. Thus, for the cone,

$$A_{V,\nu}(\eta) = 2\left(\frac{l^2 \sin \delta}{2}\right) \int_0^{\gamma_0} \left\{\cos \delta \cos \gamma \sin \eta + \sin \delta \cos \eta\right\} d\gamma$$

where γ_0 is determined from

$$\cos \delta \cos \gamma_0 \sin \eta + \sin \delta \cos \eta = 0$$

which is possible if and only if

$$\left|\cos \delta \sin \eta\right| \geq \left|\sin \delta \cos \eta\right| \tag{6}$$

If this condition does not hold, then

$$\gamma_0 = \pi \quad \text{if} \quad \eta < \frac{\pi}{2}$$

$$\gamma_0 = 0 \quad \text{if} \quad \eta > \frac{\pi}{2}$$

If equation (6) does hold then γ_0 is given by

$$\cos \gamma_0 = -\tan \delta \cot \eta$$

and

$$A_{v,\nu}(\eta) = l^2 \sin \delta \left\{(\cos \delta \sin \gamma_0)\sin \eta + (\gamma_0 \sin \delta)\cos \eta\right\}$$

Now, the total lateral area of the cone is

$$A_v = \pi l^2 \sin \delta$$

and hence the normalized area distribution for the cone is simply

$$\mu_v(\eta) = \frac{A_{v,\nu}}{A_v}(\eta) = \frac{1}{\pi}\left\{(\cos \delta \sin \gamma_0)\sin \eta + (\gamma_0 \sin \delta)\cos \eta\right\} \qquad (7)$$

providing for the well-known special cases of

$$\mu_v(\eta) = \frac{1}{\pi} \sin \eta \qquad \text{(cylinder, } \delta = 0\text{)}$$

and

$$\mu_v(\eta) = \cos^* \eta \qquad \text{(flat plate, } \delta = \pi/2\text{)}$$

The other case of interest is the average area projected to the viewer along $\tilde{\nu}$, by the cone, as it rotates (one revolution) about an axis perpendicular to the axis of symmetry. If this projection is denoted by $\hat{\mu}(\eta)$, then

$$\hat{a}_v(\eta) = \left(\frac{1}{2\pi}\right) \int_0^{2\pi} a_v(\eta, \xi) d\xi \qquad (8)$$

where η locates the viewer relative to the spin axis; ξ is the angle of rotation, and η_1 is the angle from $\tilde{\nu}$ to $(\tilde{PA})$. Figure 3 shows the relation between η, η_1, and ξ.

Example of conical projected areas.- A right circular cone of half angle δ, and having a unit surface area, has been chosen to demonstrate these solutions. The projected area of the cone in both spin modes, spinning about its axis of symmetry and about an axis perpendicular to the axis of symmetry, has been calculated for cone half angles of 0°, $22\text{-}1/2^\circ$, 45°, $67\text{-}1/2^\circ$, and 90°. The results, $a(\eta)$ and $\hat{a}(\eta)$, are plotted in figures 13(a) and 13(b).

D. Calculation of Albedo and Earth Thermal Heating

Although the calculation of earth thermal and reflected solar (albedo) power is straightforward, the complete compilation of such data for arbitrarily shaped bodies would be a gigantic task even for modern digital computers. For this reason several series solutions will be developed. These can be truncated to produce simple and accurate approximations for both earth thermal and albedo heating, of an arbitrary shaped spacecraft, provided the spacecraft sees no shaded area on the earth.

In figure 4 a spherical coordinate frame is shown which is centered in the spacecraft. The Z_b axis is the polar axis and γ the azimuth angle of $\tilde{\nu}$ (the unit vector that points to that elemental area on the

earth's surface which transmits radiant power to the spacecraft). This angle is measured from the X_b, Z_b plane which (also) contains the spin vector $\tilde{\omega}$. It should be noted at this point that the projected area of the spacecraft is always referenced to the unit vector $\tilde{s}$. The polar angle of $\tilde{\omega}$, that is, γ_c is the angle between the earth-satellite line and $\tilde{\omega}$; here the Z_b axis coincides with the earth-satellite line. In this coordinate frame equation (4), after integration, yields

$$\Phi_{i,v} = \left(\frac{A_v}{\pi}\right) \iint_{\omega S} J_{i,v}(\ ) \sin\vartheta \, d\vartheta d\gamma \qquad (9)$$

The subscript i denotes the origin of the radiation and v denotes the receiver of the radiation.

For the case of earth thermal radiation J_e is commonly assumed to be constant. For the albedo J_a is, from reference 1,

$$J_a = Sr_e \cos^* \beta_s$$

where

r_e is the percent of the thermal energy (from the sun and incident on the earth) which is reflected by the earth

S is the solar constant

β_s is the incidence angle of the sun's light on the earth's local surface

Under the restrictions for which $\mu(\eta)$ and $\hat{\mu}(\eta)$ were developed both are even functions of η and may be represented by a cosine series, or

$$\mu(\eta) = \sum_{i} C_i \cos i\eta$$

$$\hat{\mu}(\eta) = \sum_{i} \hat{C}_i \cos i\eta$$

With these conventions equation (9) becomes, after interchanging order of summation with integration,

$$\phi_{i,v} = \frac{\Phi_{i,v}}{A_v} = \frac{1}{\pi} \sum_{k} C_k \underset{\omega_S}{\bigcirc} J_i \cos k\eta \sin \theta d\theta d\gamma \qquad (10)$$

From figure (4) it is evident that

$$\tilde{\omega} = \tilde{e}_{X_b}(\sin \eta_e) + e_{Z_b}(\cos \eta_e)$$

and

$$\tilde{\nu} = \tilde{e}_{X_b}(\sin \theta \cos \gamma) + \tilde{e}_{Y_b}(\sin \theta \sin \gamma) + e_{Z_b}(\cos \theta)$$

hence

$$\cos \eta = \tilde{\omega} \cdot \tilde{\nu} = \cos \eta_e \cos \theta + \sin \eta_e \sin \theta \cos \gamma \qquad (11)$$

The geometry defining J_a is shown in figure 5. In the sketch the (X_b, Y_b, Z_b) coordinate frame has been translated along Z_b a distance R_T (the distance from the satellite's center to the earth's center) to facilitate definition of the angles shown in the sketch.

The X_b^-, Y_b^-, Z_b^- reference frame in this sketch is the same as the X_b^-, Y_b^-, Z_b^- coordinate frame described previously. The angles shown are defined from the sketch proper. The law of cosines, from spherical trigonometry, expresses the angle β_s as

$$\cos \beta_s = \cos B_s \cos \beta + \sin B_s \sin \beta \cos(\gamma + \gamma_0)$$

and the angle (γ) is the γ in equation (9). An expression relating θ and β can be written from the geometry of figure 5; namely,

$$R_T = R_e \cos \beta + R \cos \theta \tag{12}$$

But according to the law of sines

$$\frac{R}{\sin \beta} = \frac{R_e}{\sin \theta} \quad \text{and} \quad \sin \theta_0 = \left(\frac{R_e}{R_T}\right)$$

These relations can be combined to yield

$$\sin \theta = \sin \theta_0 \sin(\theta + \beta)$$

which reduces to

$$\sin \beta = \left(\frac{\sin \theta}{\sin \vartheta_0}\right)\left\{\cos \theta - \left[\sin^2\theta_0 - \sin^2\theta\right]^{1/2}\right\} \tag{13}$$

and

$$\cos \beta = \left(\frac{\sin \theta}{\sin \vartheta_0}\right)\left\{\sin \theta + \cot \theta\left[\sin^2\theta_0 - \sin^2\theta\right]^{1/2}\right\} \tag{14}$$

Equations (11), (13), and (14) express all the variables in equation (10) in terms of the variables of integration, θ and γ.

Thus for the albedo heat, through an accuracy of $\cos 4\eta$, is

$$\phi_{a,v} \simeq \left(\frac{Sr_e}{\pi}\right) c_0 \iint_{\omega_S} \{\cos \beta_s\} \sin \theta d\theta\gamma$$

$$+ \left(\frac{Sr_e}{\pi}\right) c_1 \iint_{\omega_S} \{\cos \beta_s \cos \eta\} \sin \theta d\theta d\gamma$$

$$+ \left(\frac{Sr_e}{\pi}\right) c_2 \iint_{\omega_S} \{\cos \beta_s \cos 2\eta\} \sin \theta d\theta d\gamma$$

$$+ \left(\frac{Sr_e}{\pi}\right) c_3 \iint_{\omega_S} \{\cos \beta_s \cos 3\eta\} \sin \theta d\theta d\gamma$$

$$+ \left(\frac{Sr_e}{\pi}\right) c_4 \iint_{\omega_S} \{\cos \beta_s \cos 4\eta\} \sin \theta d\theta d\gamma$$

The integration for γ may be carried out immediately, leaving only the integration with respect to θ to be provided. The resulting expression may be divided into even and odd functions of B_s, or

$$\phi_{a,v} \simeq Sr \{G_1(\theta_0, \eta_e)\cos \gamma_0 \sin B_s$$

$$+ G_2(\theta_0, \eta_e)\cos B_s\} \qquad (15)$$

where

$$G_1(\theta_0, \eta_e) = \left\{c_1\left[\sin \eta_e\right]F_{11}(\theta_0)\right\} + c_2\left\{4\left[\cos \eta_e \sin \eta_e\right]F_{23}(\theta_0)\right\}$$

$$+ c_3\left\{12\left[\cos^2\eta_e \sin \eta_e\right]F_{32}(\theta_0) + 3\left[\sin^3\eta_e\right]F_{33}(\theta_0)\right.$$

$$\left. - 3\left[\sin \eta_e\right]F_{35}(\theta_0)\right\} + c_4\left\{32\left[\cos^3\eta_e \sin \eta_e\right]F_{46}(\theta_0)\right.$$

$$\left. + 24\left[\cos \eta_e \sin^3\eta_e\right]F_{47}(\theta_0) - 16\left[\cos \eta_e \sin \eta_c\right]F_{48}(\theta_0)\right\}$$

and

$$G_2(\vartheta_0,\eta_e) = c_0\left\{2F_{00}(\vartheta_0)\right\} + c_1\left\{2\left[\cos\eta_e\right]F_{10}(\vartheta_0)\right\}$$

$$+ c_2\left\{4\left[\cos^2\eta_e\right]F_{20}(\vartheta_0) + 2\left[\sin^2\eta_e\right]F_{21}(\vartheta_0) - 2F_{22}(\vartheta_0)\right\}$$

$$+ c_3\left\{8\left[\cos^3\eta_e\right]F_{30}(\vartheta_0) + 12\left[\cos\eta_e\sin^2\eta_e\right]F_{31}(\vartheta_0) - 6\left[\cos\eta_e\right]F_{34}\right\}$$

$$+ c_4\left\{16\left[\cos^4\eta_e\right]F_{40}(\vartheta_0) + 48\left[\cos^2\eta_e\sin^2\eta_e\right]F_{41}(\vartheta_0)\right.$$

$$+ 6\left[\sin^4\eta_e\right]F_{42}(\vartheta_0) - 16\left[\cos^2\eta_e\right]F_{43}(\vartheta_0)$$

$$\left. - 8\left[\sin^2\eta_e\right]F_{44}(\vartheta_0) + 2F_{45}(\vartheta_0)\right\}$$

The F_{ik}'s are expressible in terms of elementary functions; however, for this thesis they have been numerically integrated and are given on table 1. In particular, the F_{ik}'s are given by

$$F_{00}(\vartheta_0) = F_{45}(\vartheta_0) = F_{22}(\vartheta_0) = \int_0^{\vartheta_0}\left\{\cos\beta\right\}\sin\theta d\theta$$

$$F_{10}(\vartheta_0) = F_{34}(\vartheta_0) = \int_0^{\vartheta_0}\left\{\cos\beta\cos\theta\right\}\sin\theta d\theta$$

$$F_{11}(\vartheta_0) = F_{35}(\vartheta_0) = \int_0^{\vartheta_0}\left\{\sin\beta\sin\theta\right\}\sin\theta d\theta$$

$$F_{20}(\theta_0) = F_{43}(\theta_0) = \int_0^{\theta_0} \left\{\cos\beta \cos^2\theta\right\} \sin\theta d\theta$$

$$F_{21}(\theta_0) = F_{44}(\theta_0) = \int_0^{\theta_0} \left\{\cos\beta \sin^2\theta\right\} \sin\theta d\theta$$

$$F_{23}(\theta_0) = F_{48}(\theta_0) = \int_0^{\theta_0} \left\{\sin\beta \cos\theta \sin\theta\right\} \sin\theta d\theta$$

$$F_{30}(\theta_0) = \int_0^{\theta_0} \left\{\cos\beta \cos^3\theta\right\} \sin\theta d\theta$$

$$F_{31}(\theta_0) = \int_0^{\theta_0} \left\{\cos\beta \cos\theta \sin^2\theta\right\} \sin\theta d\theta$$

$$F_{32}(\theta_0) = \int_0^{\theta_0} \left\{\sin\beta \cos^2\theta \sin\theta\right\} \sin\theta d\theta$$

$$F_{33}(\theta_0) = \int_0^{\theta_0} \left\{\sin\beta \sin\theta\right\} \sin\theta d\theta$$

$$F_{40}(\theta_0) = \int_0^{\theta_0} \left\{\cos\beta \cos^4\theta\right\} \sin\theta d\theta$$

$$F_{41}(\vartheta_0) = \int_0^{\vartheta_0} \left\{\cos\beta \cos^2\theta \sin^2\vartheta\right\} \sin\vartheta d\vartheta$$

$$F_{42}(\vartheta_0) = \int_0^{\vartheta_0} \left\{\cos\beta \sin^4\vartheta\right\} \sin\vartheta d\vartheta$$

$$F_{46}(\vartheta_0) = \int_0^{\vartheta_0} \left\{\sin\beta \cos^3\vartheta \sin\theta\right\} \sin\vartheta d\vartheta$$

and

$$F_{47}(\vartheta_0) = \int_0^{\vartheta_0} \left\{\sin\beta \cos\vartheta \sin^3\theta\right\} \sin\vartheta d\vartheta$$

For the case of earth thermal radiation the integration of equation (9) yields

$$\phi_{e,v} \simeq (\sigma T_e^4) G_3(\vartheta_0, \eta_e)$$

where

$$\begin{aligned} G_3(\vartheta_0,\eta_e) = {} & C_0\left\{2(1-\cos\vartheta_0)\right\} + C_1\left\{\left[\cos\eta_e\right]\sin^2\vartheta_0\right\} \\ & + C_2\left\{\frac{2}{3}\left[\cos^2\eta_e\right](1-\cos^3\vartheta_0) + \frac{1}{3}\left[\sin^2\eta_e\right](2-\cos\vartheta_0\sin^2\vartheta_0 \right. \\ & \left. - 2\cos\vartheta_0)\right\} + C_3\left\{\frac{1}{2}\left[\cos^3\eta_e\right](1-\cos^4\eta_e) \right. \\ & \left. + \frac{3}{4}\left[\cos\eta_e\sin^2\eta_e\right](\sin^4\vartheta_0)\right\} + C_4\left\{\frac{2}{5}\left[\cos^4\eta_e\right](1-\cos^5\vartheta_0) \right. \\ & + \frac{1}{20}\left[\sin^4\eta_e\right](8-3\sin^4\vartheta_0\cos\vartheta_0 - 4\cos\vartheta_0\sin^2\vartheta_0 - 8\cos\vartheta_0) \\ & \left. + \frac{6}{5}\left[\sin^2\eta_e\cos^2\eta_e\right]\left(\frac{2}{3} - \cos^3\vartheta_0\sin^2\vartheta_0 - \frac{2}{3}\cos^3\vartheta_0\right)\right\} \end{aligned}$$

and where

$$C_0 = c_0 - c_2 + c_4$$

$$C_1 = c_1 - 3c_3$$

$$C_2 = 2c_2 - 8c_4$$

$$C_3 = 4c_3$$

and

$$C_4 = 8c_4$$

Example of albedo and earth thermal radiation.- As an example of albedo and earth thermal radiation, let a flat plate of unit area be irradiated on one exposed side. The relevant geometry is shown in figure 6.

Through an accuracy of $\cos 4\eta$

$$\mu(\eta) \cong c_0 + c_1 \cos \eta + c_2 \cos 2\eta + c_4 \cos 4\eta$$

where

$$c_0 = \frac{1}{\pi} \simeq 0.3185$$

$$c_1 = \frac{1}{2} = 0.5000$$

$$c_2 = \frac{2}{3\pi} \simeq 0.2122$$

$$c_4 = -\frac{2}{15\pi} \simeq -0.0424$$

The angle θ_0 was chosen as 60°, hence the proper values of the pertinent $F_{1\,k}$, from table 1, are

$F_{11} = 0.0594$	$F_{48} = 0.0381$	$F_{21} = 0.202$	$F_{42} = 0.106$
$F_{23} = 0.03812$	$F_{00} = 0.490$	$F_{22} = 0.490$	$F_{43} = 0.288$
$F_{46} = 0.0172$	$F_{10} = 0.370$	$F_{40} = 0.192$	$F_{44} = 0.202$
$F_{47} = 0.0209$	$F_{20} = 0.288$	$F_{41} = 0.096$	$F_{45} = 0.490$

When these numbers are introduced into the defining equation for G_1, G_2 and G_3 it is found that

$$G_1 = 0.0297 \sin \eta_e + 0.0583 \sin \eta_e \cos \eta_e - 0.0233 \sin \eta_e \cos^3 \eta_e - 0.0213 \cos \eta_e \sin^3 \eta_e$$

$$G_2 = 0.217 + 0.369 \cos \eta_e + 0.285 \cos^2 \eta_e - 0.195 \sin^2 \eta_e \cos^2 \eta_e - 0.130 \cos^4 \eta_e - 0.0270 \sin^4 \eta_e$$

and

$$G_3 = 0.2228 + 0.3749 \cos \eta_e + 0.2863 \cos^2 \eta_e - 0.1993 \cos^2 \eta_e \sin^2 \eta_e - 0.1314 \cos^4 \eta_e - 0.0281 \sin^4 \eta_e$$

The close agreement between G_2 and G_3 is striking, while G_1 is small and an odd function of η_e. These solutions are plotted on figures 14(a) and 14(b).

It is easily understood that as θ_0 increases the close agreement between G_2 and G_3 increases. Thus for the θ_0 value used here, or for larger values the so-called "shape factors" for earth thermal and albedo heating are nearly the same provided the intensity of the albedo (J_a) is taken from the satellite's subpoint and provided the spacecraft does not see past the earth's terminator.

At this point a discussion of the assumptions used in calculating the albedo and earth thermal radiations is in order.

When equation (9) is used to calculate the earth's thermal power, incident on a spacecraft, the assumption is usually made that J_e is constant. When one considers that the earth's surface may easily vary from 570° R, at the earth equatorial regions, to 460° R at the earth's polar region, it is clear that J_e could easily vary by as much as 50 percent of its maximum value. It would be difficult to obtain very accurate results with such an assumption; however, the only alternative is to construct some type of J_e map (for the earth). Unfortunately there are few if any of these in existence. For the present (then) the thermal designer should choose J_e as a constant.

Clearly the representation of $\mu(\eta)$ in a Fourier cosine series, for this case, must be acceptable since a termination of the series after $\cos 4\eta$ will introduce only about a 4-percent error over the maximum amplitude for a flat plate, which is (in a sense) an extreme case.

For illustrative purposes $\cos^*\eta$ versus η through terms of $\cos 4\eta$ is plotted in figure 20(a). In figure 20(b) the resulting $G_3(\eta_e)$ values, for heights above the earth's surface of 0 and 392 nautical miles, are plotted. The values of $G_3(\eta_e)/(G_3)_{max}$ evaluated for an infinite height above the earth's surface, where $\mu(\eta)$ has been terminated after $\cos 4\eta$, is plotted in figure 20(a). The corresponding exact solution for $G_3(\eta_e)/(G_3)_{max}$ is plotted in figure 20(b). It should be noted here that $G_3(\eta_e)$ gives ϕ_e for a body of any shape if multiple

light reflections are negligible and if the body spins about some axis with sufficient speed so that only small changes in temperature occur during one complete revolution. Otherwise, the body shape must conform to a rotational symmetry about one particular axis. Other properties of Φ_c will be discussed later.

The calculation of Φ_a is dependent upon the many factors shown in equation (15). In the development of Φ_a it was assumed that the surface of the earth was a uniform diffusively reflecting sphere. The manner in which the earth, and its atmosphere, scatter and reflect sunlight is quite complex; however, it is suggested in reference 7 that the earth's albedo might vary between 32 percent and 52 percent. A large portion of the albedo is due to cloud cover which may or may not be uniformly distributed over the earth's surface. Thus it is evident that there is some futility in attempting an exact solution for Φ_a. With this difficulty in mind it appears that the series approximation for $\mu(\eta)$, for purposes of calculating Φ_a, is more than sufficient.

The calculation of Φ_a, using equation (15), also has the advantage of simplicity and versatility that was found in the calculation of Φ_c by the same process. There is one big failing attached to equation (15) since in its development the assumption was made that $\cos \beta_s$ was always positive. This assumption fails when the spacecraft approaches the earth's terminator; here $\cos \beta_s$ is zero on the terminator and the portion of the earth's surface which is shielded from the sun has a negative value for $\cos \beta_s$. Since these negative values were not deleted from the integration, Φ_a as described by equation (15), is in error.

The precise size of this error can only be determined by an exact solution of equation (9). However, it is clear that when equation (15) is in error, the albedo heat is considerably decreased from its maximum value (at $B_S = 0$). Also assuming the albedo (r_e) constant can introduce more error into the Φ_a calculation than the error caused by including negative values of $\cos \beta_S$ in the Φ_a calculation. (The latter results in values of Φ_a less than the exact Φ_a solutions.)

As was mentioned, the odd part of Φ_a is small compared to the even part; use of the odd part requires the determination of γ_0 which is no simple matter. If the odd part of Φ_a is neglected, and only the even part used, figure 14(a) shows that G_3 is slightly larger than the even part of Φ_a. Thus if G_3 is used in place of G_2 there is a compensating effect for the error incurred by including negative values of $\cos \beta_S$ in the calculation of Φ_a.

For these reasons $G_3(\eta_e, \vartheta_0)$ is used in place of $G_2(\eta_e, \vartheta_0)$ in this thesis. One should also remember that $G_3(\eta_e, \vartheta_0)$ is much simpler to use in the analytical studies.

E. Calculation of Orientation Angles

The preceding developments can be used to calculate the radiant power incident on a spacecraft's external surface as a function of the angles

$$\eta_e, \eta_s, B_s, \vartheta_0, \text{ and } \gamma_0$$

These angles may be found as follows:

Erect a nonrotating cartesian coordinate frame centered at the earth's center. In figure 7, the Z axis coincides with the earth's north pole and the Y axis is perpendicular to the earth-sun line at the summer solstice. Now rotate the axis system about the Z axis, through angle ϕ_{AN}, until the X axis pierces the ascending node; now the (X,Y,Z) frame coincides with the (X_1,Y_1,Z_1) frame. Next provide a rotation about the X_1 axis, through the angle I, until the Y axis lies in the orbit plane; the (X,Y,Z) frame coincides with the (X_2,Y_2,Z_2) frame. Finally a rotation about the Z_2 axis, through the angle E is provided, so that the X axis passes through the satellite and the (X,Y,Z) frame coincides with the (X',Y',Z') frame. The coordinates of any point P(X',Y',Z') may be calculated from P(X,Y,Z) by the coordinate transformation, or

$$\begin{Bmatrix} X' \\ Y' \\ Z' \end{Bmatrix} = Q(E)Q(I)Q(\phi_{AN}) \begin{Bmatrix} X \\ Y \\ Z \end{Bmatrix}$$

where

$$Q(\phi_{AN}) = \begin{bmatrix} \cos \phi_{AN} & \sin \phi_{AN} & 0 \\ -\sin \phi_{AN} & \cos \phi_{AN} & 0 \\ 0 & 0 & 1 \end{bmatrix}$$

$$Q(I) = \begin{bmatrix} 1 & 0 & 0 \\ 0 & \cos I & \sin I \\ 0 & -\sin I & \cos I \end{bmatrix}$$

and

$$Q(E) = \begin{bmatrix} \cos E & \sin E & 0 \\ -\sin E & \cos E & 0 \\ 0 & 0 & 1 \end{bmatrix}$$

On carrying out the indicated multiplication

$$Q(E)Q(I)Q(\phi_{AN}) = Q$$

is a matrix whose elements are

$$Q_{11} = \cos E \cos \phi_{AN} - \sin E \cos I \sin \phi_{AN}$$

$$Q_{12} = \cos E \sin \phi_{AN} + \sin E \cos I \cos \phi_{AN}$$

$$Q_{13} = \sin E \sin I$$

$$Q_{21} = -\sin E \cos \phi_{AN} - \cos E \cos I \sin \phi_{AN}$$

$$Q_{22} = -\sin E \sin \phi_{AN} + \cos E \cos I \cos \phi_{AN}$$

$$Q_{23} = \cos E \sin I$$

$$Q_{31} = \sin I \sin \phi_{AN}$$

$$Q_{32} = -\sin I \cos \phi_{AN}$$

$$Q_{33} = \cos I$$

Here, the symbol $[\ ]$ denotes a square matrix while $\{\ \}$ denotes a column matrix.

To locate the position of the sun relative to the earth start again with the earth centered (X,Y,Z) coordinate frame. (See fig. 8.)

First the axes are rotated about the Y axis, through angle i until the X axis points to the sun at the summer solstice. In this position the (X,Y,Z) frame coincides with the (X_3,Y_3,Z_3) frame. Next give a rotation about the Z_3 axis, through angle Ω, until the X axis points to the sun and the (X,Y,Z) frame coincides with the (X'',Y'',Z'') frame. Proceeding as in the previous case, then

$$\begin{Bmatrix} X'' \\ Y'' \\ Z'' \end{Bmatrix} = Q(\Omega)Q(i)\begin{Bmatrix} X \\ Y \\ Z \end{Bmatrix}$$

where

$$Q(\Omega) = \begin{bmatrix} \cos\Omega & \sin\Omega & 0 \\ -\sin\Omega & \cos\Omega & 0 \\ 0 & 0 & 1 \end{bmatrix}$$

$$Q(i) = \begin{bmatrix} \cos i & 0 & \sin i \\ 0 & 1 & 0 \\ -\sin i & & \cos i \end{bmatrix}$$

and

$$Q(\Omega)Q(i) = \begin{bmatrix} \cos\Omega\cos i & \sin\Omega & \cos\Omega\sin i \\ -\sin\Omega\cos i & \cos\Omega & -\sin\Omega\sin i \\ -\sin i & 0 & \cos i \end{bmatrix}$$

In this thesis it will be assumed that the spacecraft's angular momentum vector lies in its orbit plane and is tangent to the local horizon at perigee. Too, it is assumed that the spacecraft is initially injected into orbit at its perigee position. It follows, then, that the Y' axis coincides with the satellite's angular momentum vector when the satellite is initially injected into orbit, thus

$$\tilde{e}_H = \tilde{e}_{Y'}(0) \quad \text{where} \quad \tilde{e}_{Y'} = \tilde{e}_{Y'}(t)$$

From this it follows that

$$\cos \eta_e = -\left[\tilde{e}_{Y'}(0)\right] \cdot \left[\tilde{e}_{X'}(t)\right]; \; 0 \leq \eta_e \leq \pi$$

$$\cos \eta_s = \left[\tilde{e}_{Y'}(0)\right] \cdot \left[\tilde{e}_{X''}(t)\right]; \; 0 \leq \eta_s \leq \pi$$

$$\cos B_s = +\left[\tilde{e}_{X'}(t)\right] \cdot \left[\tilde{e}_{X''}(t)\right]; \; 0 < B_s \leq 2\pi$$

Now, by the matrix transformation performed previously these equations may be written explicitly as

$$\begin{aligned} -\cos \eta_e = &\left[(-\sin \lambda_0 \cos \phi_0 - \cos \lambda_0 \cos I \sin \phi_0)(\cos E \cos \phi_{AN}\right. \\ &\left. -\sin E \cos I \sin \phi_{AN})\right] + \left[(-\sin \lambda_0 \sin \phi_0\right. \\ &\left. +\cos \lambda_0 \cos I \cos \phi_0)(\cos E \sin \phi_{AN} + \sin E \cos I \cos \phi_{AN})\right] \\ &+ \left[(\cos \lambda_0 \sin I)(\sin E \sin I)\right] \end{aligned} \tag{16}$$

$$\cos \eta_E = \left[(-\sin \lambda_0 \cos \phi_0 - \cos \lambda_0 \cos I \sin \phi_0)(\cos \Omega \cos i)\right]$$

$$+ \left[(-\sin \lambda_0 \sin \phi_0 + \cos \lambda_0 \cos I \cos \phi_0)(\sin \Omega)\right]$$

$$+ \left[(\cos \lambda_0 \sin I)(\cos \Omega \sin i)\right] \qquad (17)$$

and

$$\cos B_E = \left[(\cos E \cos \phi_{AN} - \sin E \cos I \sin \phi_{AN})(\cos \Omega \cos i)\right]$$

$$+ \left[(\cos E \sin \phi_{AN} + \sin E \cos I \cos \phi_{AN})(\sin \Omega)\right]$$

$$+ \left[(\sin E \sin I)(\cos \Omega \sin i)\right] \qquad (18)$$

where

$$\phi_{AN} = \phi_0 + \dot{\phi}\, \Delta t$$

$$\lambda = \lambda_0 + \dot{\lambda}\, \Delta t; \quad E = \delta + \lambda$$

$$\Omega = \Omega_0 + \Delta\Omega$$

Here the subscript zero denotes initial conditions and the quantities $\dot{\phi}$ and $\dot{\lambda}$ may be calculated from reference 2. $\Delta\Omega$ is the angular displacement of the earth about the sun, with $\Delta\Omega$ equal to zero when Δt is zero. δ is the spacecraft's angular position in orbit measured from the perigee.

The orientation quantities already calculated in this section are expressed in terms of the inertial coordinate frame (X,Y,Z). Such a

coordinate system does not lend itself well to mental visualization; that is to say, equations (16), (17), and (18), in their present form, are just so many confusing expressions. The true character of these relations becomes clearer when the (X'_0,Y'_0,Z'_0) coordinates are used. The (X'_0,Y'_0,Z'_0) coordinates are those which coincide with the (X',Y',Z') coordinates when the X' axis passes through the perigee position. However, it should be noted that this reference frame (the X'_0,Y'_0,Z'_0 coordinates) loses most of its mathematical utility because it (the X'_0,Y'_0,Z'_0 coordinate frame) is not fixed in inertial space. From figure 9 the required unit vectors can be expressed by

$$\tilde{e}_{X'} = \tilde{e}_{X'_0}(\cos \epsilon \cos \zeta) + \tilde{e}_{Y'_0}(\cos \epsilon \sin \zeta) + \tilde{e}_{Z'_0}(\sin \epsilon)$$

$$\tilde{e}_{Y'(0)} = \tilde{e}_{X'_0}(\cos \hat{\nu} \sin \hat{\nu}) + \tilde{e}_{Y'_0}(\cos \hat{\nu} \cos \hat{\nu}) + \tilde{e}_{Z'_0}(\sin \hat{\nu})$$

and

$$\tilde{e}_{X'} = \tilde{e}_{X'_0}(\cos \delta) + \tilde{e}_{Y'_0}(\sin \delta)$$

After applying the definitions for η_e, η_s, and B_s the above expressions yield

$$\cos \eta_e = -\cos \hat{\nu} \sin(\delta + \hat{\nu}) \tag{19}$$

$$\cos \eta_s = \cos \epsilon \cos \hat{\nu} \sin(\zeta + \hat{\nu}) + \sin \epsilon \sin \hat{\nu} \tag{20}$$

and

$$\cos B_s = \cos \epsilon \cos(\delta - \zeta) \tag{21}$$

The angles ζ, $\hat{\nu}$, Ψ, and ϵ can be found by comparing equations (19) through (21) with equations (16) through (18). Here the quantities are defined as

ϵ angle between sun and orbit plane

ζ angle between sun's projection onto orbit plane and perigee radius vector

$\hat{\nu}$ angle between orbit plane and spacecraft's angular momentum vector

Ψ angle between the spacecraft's angular momentum vector projection onto the orbit plane and the local earth horizon as the spacecraft passes through perigee

Now, γ_0, the angle between the (satellite momentum vector-satellite earth line) plane and the (sun earth line-satellite earth line) plane is defined by

$$\cos \gamma_0 = + \frac{\tilde{e}_{Y'}(0) \times \tilde{e}_{X'}}{\left|\tilde{e}_{Y'}(0) \times \tilde{e}_{X'}\right|} \cdot \frac{\tilde{e}_{X''} \times \tilde{e}_{X'}}{\left|\tilde{e}_{X''} \times \tilde{e}_{X'}\right|}$$

which, after inserting the definitions of the unit vectors, and after some reduction, becomes

$$\cos \gamma_0 = + \frac{\sin \hat{\nu} \sin \epsilon + \cos \hat{\nu} \cos \epsilon \cos(\delta + \Psi) \sin(\delta - \zeta)}{\left[\sin^2 \epsilon + \cos^2 \epsilon \sin^2(\delta - \zeta)\right]^{1/2} \left[\sin^2 \hat{\nu} + \cos^2 \hat{\nu} \cos^2(\Psi + \delta)\right]^{1/2}} \tag{22}$$

Thus the angles which determine the heat flux in equations (1), (2), and (3) are calculated.

F. Specialization of the Heat Equation to Spacecraft Problems

Consider a spacecraft in a near-earth orbit receiving direct solar energy, earth thermal energy, and albedo energy. Assume its external surfaces are composed of simply joined cones, cylinders, and flat plates.

It should be recognized that for many spacecraft it is impractical to calculate exact solutions for equation (1). And, when an average temperature over a section of the spacecraft is sufficient, equation (2) might be solved with much less computational effort. Equation (2) is

$$(mc)_i \frac{\partial T_{A_i}}{\partial t} = \Phi_i + P_i$$

here the subscript i denotes the section for which the equation is written; Φ_i is the heat flux absorbed onto the ith surface; and P_i is the power generated internally and applied to the ith section. If some other section j of the spacecraft conducts heat to the ith section this heat transfer can be calculated from

$$\Phi_{j,i} = h_{j,i}(T_{A_j} - T_{A_i})$$

If radiative heat transfer occurs between the jth and ith sections it can be calculated by

$$\Phi_{j,i} = R_{j,i}(\overline{T_j^4} - \overline{T_i^4})$$

where

$$\overline{T_i^4} = \frac{1}{A_i} \int_{A_i} T_i^4 dA_i$$

The power to the ith section, from external sources, is

$$\Phi_i = SA_{i,s}a_{s,i} + A_i \phi_{a,i}\, a_{a,i} + A_i \phi_{e,i}\, a_{e,i} - A_i \Sigma_i \sigma\overline{T_i^4}$$

where

$a_{s,i}$ percentage of solar radiation falling on i and which is absorbed

$a_{a,i}$ percentage of $\phi_{a,i}$ absorbed

$a_{e,i}$ percentage of $\phi_{e,i}$ absorbed

Σ_i total hemispherical emissivity of the ith body section

When equation (2) is fully expanded it is

$$(mc)_i \frac{\partial T_{A_i}}{\partial t} = P_i + SA_{i,s}\, a_{s,i} + A_i \phi_{a,i}\, a_{a,i} + A_i \phi_{e,i}\, a_{e,i} - A_i \Sigma_i \sigma\overline{T_i^4}$$

$$+ \sum_{j=1}^{N} h_{j,i}(T_{A_j} - T_{A_i}) + \sum_{j=1}^{N} R_{j,i}(\overline{T_j^4} - \overline{T_i^4}) \qquad (23)$$

In the literature an assumption commonly made is that the sun's energy spectrum is not significantly altered by the earth's scattering and reflection processes, hence

$$a_{s,i} \simeq a_{a,i}$$

also it is commonly assumed (in the literature) that

$$a_{e,i} \simeq \Sigma_i$$

This follows from the fact that most spacecraft are always near to the earth's surface temperature.

It should be noted that in equation (23)

$$T_i^4 \neq T_{\Lambda_1}^4$$

To see this difference let

$$T = T_\Lambda + v$$

from which

$$T^4 = T_\Lambda^4 + 4T_\Lambda^3 v + 6T_\Lambda^2 v^2 + 4T_\Lambda v^3 + v^4$$

so that

$$\overline{T_i^4} = \frac{1}{\Lambda_1} \int_{\Lambda_1} \left\{ T_{\Lambda_1}^4 + 4T_{\Lambda_1}^3 v + 6T_{\Lambda_1}^2 v^2 + 4T_{\Lambda_1} v^3 + v^4 \right\} d\Lambda_{\Lambda_1} \qquad (23a)$$

But, since

$$T_{\Lambda_1} = \frac{1}{\Lambda_1} \int_{\Lambda_1} T_i \, d\Lambda_1 = \frac{1}{\Lambda_1} \int_{\Lambda_1} \left\{ T_{\Lambda_1} + v_1 \right\} d\Lambda_1 = T_{\Lambda_1} + \frac{1}{\Lambda_1} \int_{\Lambda_1} v_1 \, d\Lambda_1$$

then

$$\int_{\Lambda_1} v_1 \, d\Lambda_1 = 0$$

which implies that

$$\int_{\Lambda_1} (v_1)^3 d\Lambda_1$$

is small.

If v_1 is much less than T_{Λ_1} then the last term in equation (23a) is small compared to

$$\frac{6T_{\Lambda_i}^2}{\Lambda_i} \int_{\Lambda_i} (v_i)^2 d\Lambda_i = 6T_{\Lambda_i}^2 v_i^2$$

then

$$\overline{T_i^4} = \simeq T_{\Lambda_i}^4 + 6T_{\Lambda_i}^2 v_i^2 - T_{\Lambda_i}^4 \left\{ 1 + 6\left(\frac{v_i}{T_{\Lambda_i}}\right)^2 \right\} \tag{24}$$

so by the binomial expansion theorem,

$$\sqrt[4]{\overline{T_i^4}} \simeq T_{\Lambda_i} \left\{ 1 + \frac{6}{4}\left(\frac{v_i}{T_{\Lambda_i}}\right)^2 + \ldots \right.$$

and neglecting higher ordered terms, and solving for T_{Λ_i}, then

$$T_{\Lambda_i} \simeq \sqrt[4]{\overline{T_i^4}} - \frac{3}{2}\left(\frac{v_i}{T_{\Lambda_i}}\right)^2 T_{\Lambda_i} \tag{25}$$

If $(v_i/T_{\Lambda_i})^2$ is small compared to one then

$$\overline{T_i^4} \simeq T_{\Lambda_i}^4 \tag{25a}$$

and equation (23) simplifies to

$$(mc)_i \frac{\partial T_{\Lambda_i}}{\partial t} = P_i + \mathcal{S}A_{i,s}\, a_{s,i} + A_i \phi_{a,i}\, a_{s,i} + A_i \phi_{e,i}\, \Sigma_i$$

$$- A_i \Sigma_i \sigma T_{\Lambda_i}^4 + \sum_{j=1}^{N} h_{j,i}(T_{\Lambda_j} - T_{\Lambda_i})$$

$$+ \sum_{j=1}^{N} R_{j,i}(T_{\Lambda_j}^4 - T_{\Lambda_i}^4) \tag{26}$$

Spacecraft having some spin about the axis of symmetry usually satisfy equation (25a), while spacecraft having no spin about the axis of symmetry may have strong surface temperature differences. In this case each conical section of the spacecraft's surface must be divided into smaller sections until the condition

$$\overline{T_i^4} \simeq T_{A_i}^4$$

is satisfied. For such a situation the required labor may become so great that other methods of solution must be employed.

Techniques will be developed later which will enable one to calculate the magnitude of the circumferential temperature variations.

Example of spacecraft temperature variations.- Explorer XVI is an example of a spacecraft which conforms to the assumptions employed in arriving at equation (26) and can be used as an example to illustrate the use of the system of equations described by equation (26).

For this illustration the Explorer XVI spacecraft is subdivided into 12 sections. An equation for each section is written and all 12 equations are integrated simultaneously for several orbital conditions. For purposes of visual definition, a picture of Explorer XVI is presented as figure 21(a). In figure 21(b) Explorer XVI is shown with each thermal section numbered. The thermal properties for these sections are listed below:

Thermal section 1 (forward solar cells)

$$(mc)_1 = 0.145 \text{ Btu/}^\circ\text{R}$$

$$(A)_1 = 32.2 \text{ in.}^2$$

$$(a_s)_1 = 0.42$$

$$(\Sigma)_1 = 0.89$$

Thermal section 2 (sounding boards)

$$(mc)_2 = 0.217 \text{ Btu/}^\circ\text{R}$$

$$(A)_2 = 222 \text{ in.}^2$$

$$(a_s)_2 = 0.71$$

$$(\Sigma)_2 = 0.42$$

Thermal section 3 (side solar cells and ring)

$$(mc)_3 = 1.451 \text{ Btu/}^\circ\text{R}$$

$$(A)_3 = 337 \text{ in.}^2$$

$$(a_s)_3 = 0.57$$

$$(\Sigma)_3 = 0.79$$

Thermal section 4 (telemeter housing)

$$(mc)_4 = 1.354 \text{ Btu/}^\circ\text{R}$$

$$(A)_4 = 504 \text{ in.}^2$$

$$(a_s)_4 = 0.71$$

$$(\Sigma)_4 = 0.42$$

Thermal section 5 (telemeter modules)

$$(mc)_5 = 0.336 \text{ Btu/}^\circ\text{R}$$

Thermal section 6 (telemeter covers)

$$(mc)_6 = 1.626 \text{ Btu/}^\circ\text{R}$$

Thermal section 7 (telemeter support structure)

$$(mc)_7 = 1.827 \text{ Btu/}^\circ\text{R}$$

Thermal section 8 (inner heat shield)

$$(mc)_8 = 2.00 \text{ Btu/}^\circ\text{R}$$

Thermal section 9 (Langley pressure cells)

$$(mc)_9 = 3.30 \text{ Btu/}^\circ\text{R}$$

$$(A)_9 = 3816 \text{ in.}^2$$

$$(a_s)_9 = 0.19$$

$$(\varepsilon)_9 = 0.16$$

Thermal section 10 (Lewis sensors)

$$(mc)_{10} = 1.677 \text{ Btu/}^\circ\text{R}$$

$$(A)_{10} = 584 \text{ in.}^2$$

$$(a_s)_{10} = 0.32$$

$$(\varepsilon)_{10} = 0.82$$

Thermal section 11 (Goddard sensors)

$$(mc)_{11} = 0.[illegible] \text{ Btu}/^{\circ}\text{R}$$

$$(A)_{11} = 565 \text{ in.}^2$$

$$(\alpha_s)_{11} = 0.66$$

$$(\Sigma)_{11} = 0.69$$

Thermal section 12 (transition section)

$$(mc)_{12} = 0.538 \text{ Btu}/^{\circ}\text{R}$$

$$(A)_{12} = 300 \text{ in.}^2$$

$$(\alpha_s)_{12} = 0.93$$

$$(\Sigma)_{12} = 0.74$$

The radiative heat-transfer coefficients of importance are

$$R_{9,8} = 5.63 \times 10^{-10} \text{ Btu/min} \cdot {}^{\circ}\text{R}^4$$

$$R_{1,4} = 0.06 \times 10^{-10} \text{ Btu/min} \cdot {}^{\circ}\text{R}^4$$

$$R_{6,4} = 0.0269 \times 10^{-10} \text{ Btu/min} \cdot {}^{\circ}\text{R}^4$$

The conductive heat-transfer coefficients of importance are

$$h_{4,7} = 3.14 \times 10^{-4} \text{ Btu/min} \cdot {}^{\circ}\text{R}$$

$$h_{4,1} = 0.3276 \text{ Btu/min} \cdot {}^{\circ}\text{R}$$

$h_{4,2}$ = 0.100 Btu/min · °R

$h_{7,9}$ = 0.3864 Btu/min · °R

$h_{8,9}$ = 2.342 Btu/min · °R

$h_{8,10}$ = 0.1536 Btu/min · °R

$h_{10,11}$ = 0.0187 Btu/min · °R

$h_{11,12}$ = 0.0187 Btu/min · °R

$h_{5,6}$ = 6.682×10^{-4} Btu/min · °R

$h_{9,6}$ = 5.972×10^{-2} Btu/min · °R

$h_{7,6}$ = 1.36×10^{-3} Btu/min · °R

$h_{7,8}$ = 0.1536 Btu/min · °R

$h_{10,12}$ = 0.091 Btu/min · °R

For design purposes and temperature calculation it has been assumed that the internal power dissipated was 0.4 watt in section 5.

The value of the solar constant used in the calculations was 0.04968 Btu/in.^{2} · min; the albedo (r_e) used was 0.4. The radius of the earth is assumed to be approximately 3441 nautical miles, and the nominal orbit had an assumed perigee of 3715 nautical miles and an apogee of 4189 nautical miles.

The system of equations (given by eq. (26)) was integrated simultaneously for all 12 sections, and for the orbital conditions

producing the highest and lowest telemetered temperature levels. These results are plotted in figures 18(a), 18(b), 18(c), 18(d), 18(e), and 18(f).

It should be noted that in these figures the integration has not been carried out over a time long enough for the telemeters to reach equilibrium values. If the integrations were continued indefinitely, the telemeter temperature would tend to 45° F in the coldest case, and 115° F in the hottest case.

Explorer XVI was successfully launched from Wallops Island Station on December 17, 1962; as of this writing the spacecraft is still transmitting data. The (flight) measured temperature data, for some of the more important sections of Explorer XVI, are plotted on figures 19(a), 19(b), 19(c), 19(d), 19(e), and 19(f); also the maximum and minimum temperatures predicted from figures 18(a), 18(b), 18(c), 18(d), 18(e), and 18(f) are shown (see ref. 8 also).

G. A Parametric Study of Orbital Heating

A parametric study of equation (26) is easily the most powerful tool available to the spacecraft thermal designer.

If some section of a spacecraft is free of thermal coupling with other sections of the vehicle, then its heat balance is greatly simplified and the more fundamental characteristics of equation (26) appear. For example, equation (26) becomes

$$(mc)\frac{dT_A}{dt} = P + SA_s\, a_s + A\phi_a\, a_s + A\phi_e\, \Sigma - A\Sigma\sigma T_A^4. \qquad (27)$$

after setting

$$R_{j,i} = h_{j,i} = 0$$

and after dropping the subscript 1. From the previous development of ϕ_c and ϕ_a it is clear that ϕ_a contains a term which is multiplied by

$$\sin B_s \cos \gamma_0$$

However, this term is small and its average over B_s is zero. Too, from figure 14(a) it is evident that

$$G_2(\vartheta_0, \eta_e) \simeq G_3(\vartheta_0, \eta_e) \tag{28}$$

This last approximation will be used in this section since $G_3(\vartheta_0, \eta_e)$ is much more amendable to analytical treatment than $G_2(\vartheta_0, \eta_e)$. An approximate, but more enlightening form, of $\hat{\Phi}_e(\eta_e, \vartheta_0)$ can be derived from the following considerations. From equation (9)

$$\hat{\Phi}_e = \frac{A}{\pi} \underset{\mathcal{S}}{\bigcirc} J_e \hat{\mu}(\eta) \sin \vartheta d\vartheta d\gamma$$

where $\mathcal{S}_e$ signifies that the spacecraft is in the "long-term spin mode." Under the assumptions used to derive $\hat{\mu}(\eta)$ it can be shown that

$$\hat{\mu}\left(\eta - \frac{\pi}{2}\right) \equiv \hat{\mu}\left(\frac{\pi}{2} - \eta\right)$$

and if $(\eta - \pi/2)$ is replaced by α, then

$$\hat{\mu}(\alpha) \equiv \hat{\mu}(-\alpha) \tag{29}$$

The calculation of η as $\eta(\vartheta)$ is troublesome and one should be happy in finding an approximation which would circumvent this difficulty. Accounting for equation (2?)

$$\int_0^{2\pi}\int_0^{\pi} J_e\,\hat{\mu}(\eta)\sin\vartheta\,d\vartheta d\gamma = 2\int_0^{2\pi}\int_0^{\pi/2} J_e\,\hat{\mu}(\eta)\sin\vartheta\,d\vartheta d\gamma$$

From the theory of probability, the expectation value of $\hat{\mu}(\eta)$, for a body which is equally likely to have all possible orientations, is defined by

$$\langle\hat{\mu}(\eta)\rangle = \frac{1}{4\pi}\int_0^{2\pi}\int_0^{\pi}\hat{\mu}(\eta)\sin\vartheta\,d\vartheta d\gamma$$

Now setting

$$\hat{\mu}(\eta) = \left[\hat{\mu} - \langle\hat{\mu}\rangle\right] + \langle\hat{\mu}\rangle\Big\}$$

so $\hat{\Phi}_e$ can be expressed as

$$\hat{\Phi}_e = \frac{J_e A}{\pi}\int_0^{2\pi}\int_0^{\vartheta_0}\left\{\left[\hat{\mu} - \langle\hat{\mu}\rangle\right] + \langle\hat{\mu}\rangle\right\}\sin\vartheta\,d\vartheta d\gamma$$

or

$$= \frac{J_e A}{\pi}\int_0^{2\pi}\int_0^{\pi/2}\left\{\left[\hat{\mu} - \langle\hat{\mu}\rangle\right] + \langle\hat{\mu}\rangle\right\}\sin\vartheta\,d\vartheta d\gamma$$

$$- \frac{J_e A}{\pi}\int_0^{2\pi}\int_0^{\vartheta_0}\left\{\left[\hat{\mu} - \langle\hat{\mu}\rangle\right] + \langle\hat{\mu}\rangle\right\}\sin\vartheta\,d\vartheta d\gamma$$

or

$$\hat{\Phi}_e = 2J_e A\langle\hat{\mu}\rangle(1 - \cos\theta_0) - \left(\frac{J_e A}{\pi}\right)\int_0^{2\pi}\int_{\theta_0}^{\pi/2}\left\{\left[\hat{\mu} - \langle\hat{\mu}\rangle\right]\right\}\sin\theta\, d\theta\, d\gamma$$

It is easy to show the expectation value of the last integral is zero. After neglecting that last small integral, then

$$\hat{\Phi}_e \simeq 2AJ_e(1 - \cos\theta_0)\langle\hat{\mu}\rangle$$

Now a randomly oriented body can be represented by a sphere of equal area (A), thus

$$\langle\hat{\mu}\rangle = \frac{1}{4}$$

and

$$\hat{\Phi}_e \simeq \left(\frac{A}{2}\right)J_e(1 - \cos\theta_0) \tag{30}$$

With this amazingly simple approximation and with equation (28), equation (27) now becomes

$$(mc)\frac{dT_\Lambda}{dt} = P + SA_s\, a_s + \frac{A}{2}Sr_e\, a_s(1 - \cos\theta_0)\cos^4 B_s$$

$$+ \frac{A}{2}(\Sigma\sigma T_e^4)(1 - \cos\theta_0) - A\Sigma\sigma T_\Lambda^4 \tag{31}$$

It should be noted here that the foregoing development is possible if and only if $\hat{\mu}(\alpha) = \hat{\mu}(-\alpha)$; otherwise the spacecraft's motion must be completely random.

An upper bound on the error incurred may be found by replacing $\left[\hat{\mu} - \langle\hat{\mu}\rangle\right]$ with

$$\left[\hat{\mu} - \langle\hat{\mu}\rangle\right]_{max} \equiv \bar{\nu}$$

in the integral just neglected. In this case

$$\left|\text{Error in } \hat{\Phi}_e\right| \leq \left|\left(\frac{J_e A}{\pi}\right) \int_0^{2\pi} \int_{\theta_0}^{\pi/2} \bar{\nu} \sin\vartheta d\vartheta\gamma\right| = 2J_2 A \bar{\nu} \cos\vartheta_0$$

It is interesting to note that the neglected integral is zero for $\vartheta_0 = 0$ or for $\vartheta_0 = \frac{\pi}{2}$; that is, equation (30) is exact for either very high or very low altitudes.

The calculation of $\hat{\Phi}_e$ by this technique requires no prior knowledge of the orientation of the spacecraft.

In equation (31) if the member in question is a thin shell of uniform thickness

$$m = A\tau\rho$$

where τ is shell thickness and ρ is the density of the shell, then equation (31) becomes, after division by A and the substitution of equation (21),

$$\tau\rho c \frac{dT_\Lambda}{dt} = \left(\frac{P}{A}\right) + S\left(\frac{A_s}{A}\right) a_s + Sr_e\, a_s \left(\frac{1 - \cos\vartheta_0}{2}\right) \cos\epsilon \cos^*(\delta - \zeta)$$

$$+ (\Sigma\sigma T_e^4)\left(\frac{1 - \cos\vartheta_0}{2}\right) - \Sigma\sigma T_\Lambda^4 \qquad (32)$$

For a slightly eccentric orbit, the effects of eccentricity on heating rates (of the albedo and earth thermal energy incident on the spacecraft) are of the same order of magnitude as the error introduced into equation (32) by employing equation (30). For this reason, the effects of orbit eccentricity will be neglected in this development. Setting the right-hand side of equation (32) equal to $q(t)$ then

$$\tau\rho c \frac{dT_A}{dt} + \Sigma\sigma T_A^4 = q(t) \tag{33}$$

where

$$q(t) = q(t + L)$$

A basic understanding of orbital heating can be obtained from equation (33). Notice that

$$\int_t^{t+L} \tau\rho c\left(\frac{dT_A}{dt}\right)dt = (\tau\rho c)\int_t^{t+L} dT_A = (\tau\rho c)\left[T_A(t + L) - T_A(t)\right]$$

then since T_A is periodic on L, this integral vanishes. Now set

$$\frac{1}{L}\int_t^{t+L} \Sigma\sigma T_A^4 dt = \Sigma\sigma T_{A_0}^4 = \text{constant}$$

so that

$$T_{A_0}^4 = \frac{1}{L\Sigma\sigma}\int_t^{t+L} q(t)dt$$

or, when the indicated integration has been performed,

$$T_{A_0}^4 = \left(\frac{P}{\Sigma\sigma A}\right) + \left(\frac{S}{\sigma}\right)\left(\frac{a_s}{\Sigma}\right)\left\{\left(\frac{L_1}{L}\right)\left(\frac{A_s}{A}\right) + \frac{r_e \cos\epsilon(1 - \cos\theta_0)}{2\pi}\right\}$$

$$+ \left(\frac{T_c^4}{2}\right)(1 - \cos\theta_0) \qquad (34)$$

Here $T_{A_0}^4$, the mean equilibrium temperature raised to the fourth power, represents the fourth power temperature level which the temperature of the surface in question is attempting to attain.

Some of the more important aspects of orbital heating, as received by a spacecraft, becomes obvious in equation (34). To more clearly illustrate the effects of these contributions consider a spacecraft with the following properties:

$$\left(\frac{a_s}{\Sigma}\right) = 1.2$$

$$\left(\frac{L_1}{L}\right) = 0.65$$

$$\left(\frac{A_s}{A}\right) = \frac{1}{4}$$

$\theta_0 = 60^\circ$; altitude = 550 nautical miles

$P = 0$

L_1 = time in sunlight

These numbers are representative of a near-earth spacecraft in a circular orbit. For this configuration

$$T_{\Lambda_0}{}^4 \simeq \left[484 \times 10^8\right] + \left[99 \times 10^8\right] \cos \epsilon + \left[103 \times 10^8\right]$$

The first term in brackets is the direct solar heating term; the second term in brackets is the albedo contribution; and the last term in brackets is the earth-thermal energy input. For this configuration the largest value of $T_{\Lambda_0}{}^4$ is

$$T_{\Lambda_0}{}^4 = 692 \times 10^8, \quad \text{or} \quad T_{\Lambda_0} \simeq 53^\circ \text{ F}$$

while the least value is

$$T_{\Lambda_0}{}^4 = 587 \times 10^8 \quad \text{or} \quad T_{\Lambda_0} \simeq 32^\circ \text{ F}$$

The temperature variation is due to the coefficient of $\cos \epsilon$.

It has been demonstrated by this example that the earth's thermal and albedo heating alters the spacecraft's temperature; however, the individual contributions are small.

From equation (34) it is clear that the ratio

$$\left(\frac{a_s}{\Sigma}\right)$$

is a design variable important to the determination of the direct solar heating. Also, the albedo heating is a linear function of $\left(\frac{a_\epsilon}{\Sigma}\right)$ and $\cos \epsilon$. Perhaps the most surprising effect is that the contribution from earth thermal heating is dependent solely on $\cos \theta_0$. One should keep in mind the conditions for which equation (34) is valid.

One final word before proceeding to the next problem. The conditions used to derive equation (27) from equation (26) need not always exist since the effects of conduction cannot be propagated over long distances in thin shells when radiation is admitted to the shell's surfaces. These bodies tend toward thermal equilibrium when their radiation environment is at a large distance from those locations where conductive heating is effective. For example, if two long cylinders, with drastically different optical properties, are joined with conductive heat paths, equation (27) is still valid at some distance away from the conducting joint.

H. Solution for the Nonlinear Heat Equation

Before an actual solution of equation (33) can be effected, one must realize that equation (33) is nonlinear and has no known exact solution. Too, the nonlinear term is not small and hence is not amendable to the normal perturbation technique, for nonlinear equations, such as that given in reference 4.

Suppose, however, an approximate solution T_{Λ_0} to equation (27) is known. When T_{Λ_0} is introduced it follows that

$$\tau\rho c \frac{dT_{\Lambda_0}}{dt} + \Sigma\sigma T_{\Lambda_0}^4 = q(t) + \bar{\Gamma}_1(t) \tag{35}$$

where $\bar{\Gamma}(t)$ (the modified $q(t)$) measures the error in using $T_\Lambda = T_{\Lambda_0}$, and T_{Λ_0}, in this case, is a function of time. Also, T_Λ could be written as

$$T_\Lambda = (T_{\Lambda_0} + v_0);\ v_0 \ll T_{\Lambda_0}$$

hence

$$T_\Lambda^4 = T_{\Lambda_0}^4 + 4T_{\Lambda_0}^3 v_0 + 6T_{\Lambda_0}^2 v_0^2 + 4T_{\Lambda_0} v_0^3 + v_0^4 \tag{36}$$

When equations (35) and (36) are combined with equation (33), the result is found to be

$$\tau\rho c\left[\frac{dT_{\Lambda_0}}{dt} + \frac{dv_0}{dt}\right] + \Sigma\sigma\left[T_{\Lambda_0}^4 + 4T_{\Lambda_0}^3 v_0 + 6T_{\Lambda_0}^2 v_0^2 + 4T_{\Lambda_0} v_0^3 + v_0^4\right]$$

$$= q(t) = \rho c \frac{dT_{\Lambda_0}}{dt} + \Sigma\sigma T_{\Lambda_0}^4 - \bar{\Gamma}_1(t)$$

which simplifies to

$$\tau\rho c\left[\frac{dv_0}{dt}\right] + \Sigma\sigma\left[4T_{\Lambda_0}^3 v_0 + 6T_{\Lambda_0}^2 v_0^2 + 4T_{\Lambda_0} v_0^3 + v_0^4\right] = -\bar{\Gamma}_1(t) \tag{37}$$

where

$$4T_\Lambda^3 v_0 \gg 6T_{\Lambda_0}^2 v_0^2 \gg 4T_{\Lambda_0} v_0^3 \gg v_0^4$$

Now setting

$$\bar{\Gamma}_1(t) = \Gamma_1(t) + \bar{\Gamma}_2(t)$$

$$v_0 = T_{\Lambda_1} + v_1;\ T_{\Lambda_1} \gg v_1$$

then if this symbolism is substituted into equation (37), and the smaller nonlinear terms are separated into an equation for v_1, the result is given by

$$\rho c \frac{dT_{\Lambda_1}}{dt} + \Sigma\sigma\left[4T_{\Lambda_0}{}^3 T_{\Lambda_1}\right] = -\bar{\Gamma}_1(t) \tag{38}$$

and the separated part is

$$\rho c \frac{dv_1}{dt} + \Sigma\sigma\, 4T_{\Lambda_0}{}^3 v_1 + 6T_{\Lambda_0}{}^2(T_{\Lambda_1}{}^2 + 2T_{\Lambda_1} v_1 + v_1{}^2)$$

$$+ (\text{smaller nonlinear terms}) = -\bar{\Gamma}_2(t) \tag{39}$$

Next writing

$$v_1 = T_{\Lambda_2} + v_2;\ T_{\Lambda_2} \gg v_2$$

$$\bar{\Gamma}_2 = \bar{\Gamma}_2(t) + \bar{\Gamma}_3(t)$$

this assumption may be substituted into equation (39) and, upon retention of larger terms only,

$$\rho c \frac{dT_{\Lambda_2}}{dt} + \Sigma\sigma\left[4T_{\Lambda_0}{}^3 T_{\Lambda_2} + 6T_{\Lambda_0}{}^2 T_{\Lambda_1}{}^2\right] = -\bar{\Gamma}_2(t) \tag{40}$$

This process can be continued ad infinitum, thus for every $\bar{\Gamma}_n(t)$ there is a corresponding T_{Λ_n} where

$$T_{\Lambda_n} = T_{\Lambda_n}(t, \bar{\Gamma}_n, T_{\Lambda_{n-1}}, T_{\Lambda_{n-2}}, \ldots T_{\Lambda_0})$$

Since the choice of Γ_n is arbitrary it will be assumed that Γ_n can be chosen such that

$$T_{\Lambda_n} \ll T_{\Lambda_{n-1}}$$

or, more specifically,

$$T_{\Lambda_n} = 0\left\{\Delta T_{\Lambda_{n-1}}\right\}$$

where $\Delta \ll 1$ and is fixed by one's choice of

$$\Gamma_n(t)$$

Experience has shown that for equations of the type given in this thesis, the proper choice of Γ_n is

$$\Gamma_2(t) = \Gamma_3(t) = \Gamma_4(t) = \ldots = 0$$

if $\bar{\Gamma}_1(t)$ is selected by equation (35), and if T_{Λ_0} is a 'near solution' to T_Λ. Thus a solution is obtained as

$$T_\Lambda = T_{\Lambda_0} + T_{\Lambda_1} + T_{\Lambda_2} + \ldots$$

where

$$T_{\Lambda_n} = 0\left\{\Delta^n T_{\Lambda_0}\right\}\ ;\ \bar{\Gamma}_1 = \sum_{n=1}^{\infty} \Gamma_n(t) = \text{modified forcing function}$$

The development of a solution for equation (33) has, to this point, been an intuitive argument intended to persuade the reader that such a solution method exists. Actually, there is a much easier method of arriving at the same solution.

The first step in achieving the solution is to assume that the solution exists in the form

$$T_\Lambda = T_{\Lambda_0} + T_{\Lambda_1} + T_{\Lambda_2} + T_{\Lambda_3} + \cdots$$

where T_{Λ_0} is an approximate solution and

$$0\left\{T_{\Lambda_k}\, T_{\Lambda_j}\right\} = 0\left\{T_{\Lambda_{k+j}}\right\}$$

$$0\left\{T_{\Lambda_n}\right\} = 0\left\{\Delta T_{\Lambda_{n-1}}\right\};\ \Delta < 1$$

If the differential equation has a forcing function, its modified forcing function must be rewritten as

$$\bar{F}_1 = F_1 + F_2 + F_3 + \cdots$$

where

$$0\left\{F_n\right\} = 0\left\{T_{\Lambda_n}\right\}$$

and

$$\bar{F}_n = F_n + \bar{F}_{n+1}$$

In every case $\bar{F}_{n+1}$ is that portion of $\bar{F}_n$ which would cause T_{Λ_n} to diverge, and $\bar{F}_1$ is determined by equation (35).

The second step (in finding the solution to eq. (33)) is to substitute the assumed solution form into equation (33) and require that the resulting expression be satisfied at each order of magnitude level.

The third step is to solve the resulting system of linear differential equations with their appropriate boundary conditions.

Hereafter, in this thesis, a direct approach will be used; namely, to find solutions for the nonlinear differential equations which will be encountered in connection with thermal design.

I. Solution of the Heat Equation for Spacecraft Having Uniform Temperatures

The solution of equation (33) can be found by the method related in the previous section.

Assume the solution to be of the form

$$T_\Lambda = T_{\Lambda_0} + T_{\Lambda_1} + T_{\Lambda_2} + T_{\Lambda_3} + \cdots$$

so that

$$T_\Lambda^4 = (T_{\Lambda_0}^4) + (4T_{\Lambda_0}^3 T_{\Lambda_1}) + (4T_{\Lambda_0}^3 T_{\Lambda_2} + 6T_{\Lambda_0}^2 T_{\Lambda_1}^2) + \cdots$$

and

$$\frac{dT_\Lambda}{dt} = \left(\frac{dT_{\Lambda_0}}{dt}\right) + \left(\frac{dT_{\Lambda_1}}{dt}\right) + \left(\frac{dT_{\Lambda_2}}{dt}\right) + \cdots$$

then, when this is substituted into equation (33) it is found that

$$(\tau\rho c)\left\{\left(\frac{dT_{\Lambda_0}}{dt}\right) + \left(\frac{dT_{\Lambda_1}}{dt}\right) + \left(\frac{dT_{\Lambda_2}}{dt}\right) + \cdots\right\} + (\Sigma\sigma)\left\{(T_{\Lambda_0}^4) + (4T_{\Lambda_0}^3 T_{\Lambda_1})\right.$$

$$\left. + (4T_{\Lambda_0}^3 T_{\Lambda_2} + 6T_{\Lambda_0}^2 T_{\Lambda_1}^2) + \cdots\right\} = q(t) = \frac{1}{L}\int_t^{t+L} q\,dt + \left\{q - \frac{1}{L}\int_t^{t+L} q\,dt\right\} \tag{41}$$

From a previous development it is evident that

$$q(t) \equiv q(t + L)$$

and from the previous development, it is also obvious that within certain bounds T_{Λ_0} is arbitrary. It is also evident from equation (38) that the most practical choice of T_{Λ_0} is

$$T_{\Lambda_0} = \text{constant}; \quad \frac{dT_{\Lambda_0}}{dt} = 0 \tag{42}$$

so that

$$\Sigma\sigma T_{\Lambda_0}^{4} = \frac{1}{L} \int_t^{t+L} q\,dt \tag{43}$$

Requiring that the remaining terms be satisfied on apparent order of magnitude levels, the following system of linear differential equations is obtained

$$\tau\rho c \frac{dT_{\Lambda_1}}{dt} + \Sigma\sigma 4T_{\Lambda_0}{}^{3}T_{\Lambda_1} = q - \frac{1}{L} \int_t^{t+L} q\,dt = \bar{r}_1(t)$$

$$\tau\rho c \frac{dT_{\Lambda_2}}{dt} + \Sigma\sigma 4T_{\Lambda_0}{}^{3}T_{\Lambda_2} = -\Sigma\sigma 6T_{\Lambda_0}{}^{2}T_{\Lambda_1}{}^{2}$$

$$\tau\rho c \frac{dT_{\Lambda_3}}{dt} + \Sigma\sigma 4T_{\Lambda_0}{}^{3}T_{\Lambda_3} = -\Sigma\sigma \{\ldots$$

and so forth.

The solution of equation (43) is given by equation (34).

Now, writing

$$q(t) = \Sigma\sigma T_{\Lambda_{eq}}{}^4$$

the differential equation for T_{Λ_1} can be rewritten as

$$(\tau\rho c)\frac{dT_{\Lambda_1}}{dt} + (\Sigma\sigma 4T_{\Lambda_0}{}^3)T_{\Lambda_1} = (\Sigma\sigma)\left[T_{\Lambda_{eq}}{}^4 - T_{\Lambda_0}{}^4\right] = \Sigma\sigma T_{\Lambda_0}{}^4\left[\left(\frac{T_{\Lambda_{eq}}}{T_{\Lambda_0}}\right)^4 - 1\right] \tag{44}$$

(It is often convenient to work with the nondimensionalized temperature (ξ_n) which is equal to $(T_{\Lambda_n}/T_{\Lambda_0})$), after rewriting, the equation for T_{Λ_1} becomes

$$(\tau\rho cT_{\Lambda_0})\frac{d\xi_1}{dt} + 4(\Sigma\sigma T_{\Lambda_0}{}^4)\xi_1 = (\Sigma\sigma T_{\Lambda_0}{}^4)\left[\xi_{eq}{}^4 - 1\right] \tag{45}$$

Now setting

$$\tau\rho cT_{\Lambda_0} = \hat{Q};\ \Sigma\sigma T_{\Lambda_0}{}^4 = \hat{q}_R;\ \frac{\hat{q}_R}{\hat{Q}} = \frac{\lambda_T}{4}$$

the well-known solution of equation (45) is, from reference 5,

$$\xi_1 = \left(\frac{\lambda_T}{4}\right)\exp(-\lambda_T t)\int_0^t \exp(\lambda_T t_1)\left[\xi_{eq}{}^4 - 1\right]dt_1 + c_1 \exp(-\lambda_T t)$$

The only condition placed on this result is that $\xi_1(t) = \xi_1(t + L)$, or

$$c_1\left[1 - \exp(-\lambda_T L)\right] = \frac{\lambda_T}{4}\exp(-\lambda_T L)\int_0^L \exp(\lambda_T t_1)\left[\xi_{eq}^4 - 1\right]dt_1$$

so that

$$\xi_1 = \frac{\lambda_T}{4}\exp(-\lambda_T t)\left\{\int_0^t \exp(\lambda_T t_1)\left[\xi_{eq}^4 - 1\right]dt_1 + \frac{\exp(-\lambda_T L)}{1 - \exp(-\lambda_T L)}\int_0^L \exp(\lambda_T t_1)\left[\xi_{eq}^4 - 1\right]dt_1\right\} \qquad (46)$$

where t_1 is a dummy variable.

The differential equation for T_{Λ_2} may be rewritten as

$$(\tau\rho c T_{\Lambda_0})\frac{d\xi_2}{dt} + 4(\Sigma\sigma T_{\Lambda_0}^4)\xi_2 = -6(\Sigma\sigma T_{\Lambda_0}^4)\xi_1^2$$

Its solution is

$$\xi_2 = -\frac{3}{2}\lambda_T \exp(-\lambda_T t)\left\{\int_0^t \exp(\lambda_T t_1)\left[\xi_1^2\right]dt_1 + \frac{\exp(-\lambda_T L)}{1 - \exp(-\lambda_T L)}\int_0^L \exp(\lambda_T t_1)\left[\xi_1^2\right]dt_1\right\} \qquad (47)$$

An oddity of $T_\Lambda(t)$ can be shown as follows: the average value of the forcing function (right-hand side of eq. (45)) is zero, hence the mean value of ξ_1 is zero. However, ξ_1^2 can be written as

$$\xi_1^2 = \frac{1}{L}\int_0^L \xi_1^2 dt_1 + \left\{\xi_1^2 - \frac{1}{L}\int_0^L \xi_1^2 dt_1\right\}$$

$$= (\xi_1^2)_m + (\xi_1^2)_{var}$$

where the mean value of $(\xi_1^2)_{var}$ is zero. Thus ξ_2 is composed (like all functions) of a mean valued term plus a term which fluctuates about the mean value. Now introducing only the mean value of ξ_1^2 into equation (47), one obtains

$$(\xi_2)_m = -\frac{3}{2}(\xi_1^2)_m \tag{48}$$

Thus the mean value of T_Λ can be approximated by

$$(T_\Lambda)_m \approx T_{\Lambda_0}\left\{1 - \frac{3}{2}(\xi_1^2)_m\right\} = T_{\Lambda_0} - \frac{3}{2}\frac{(T_{\Lambda_1}^2)_m}{T_{\Lambda_0}} \tag{49}$$

(Notice the close similarity to eq. (25).) The importance of $(\lambda_T/4)$, the ratio of the mean radiant heat rate to the mean heat content, is illustrated by equations (44) through (48). In equation (46), as t becomes very large the constant term becomes negligible so that

$$\xi_1 \approx \frac{\lambda_T}{4}\exp(-\lambda_T t)\int_0^t \left[\xi_{eq}^4 - 1\right]\exp(\lambda_T t_1)dt_1$$

and as $\lambda_T \to 0$; $\xi_1 \to 0$ and a large λ_T implies a large ξ_1.

For a given mean heat rate per orbital pass, and for λ_T equal to zero, there is a corresponding mean temperature T_{Λ_0} (as calculated by eq. (34)). As λ_T grows to some finite value, ξ_1 also grows to some finite value; this implies that $(\xi_1^2)_m$ increases and that T_{Λ_0} decreases in agreement with equation (48). It is obvious that the same argument holds for a discussion of the effects of the size of

$$\left[\xi_{eq}^4 - 1\right]$$

It will be demonstrated later how these two facts are of vital importance in the passive thermal design of a spacecraft.

Next, notice that the largest term in the temporal temperature variations is given by equation (46). For a given $\xi_{eq}^4(t)$, the parameter in equation (46) which distinguishes between various spacecrafts, is the parameter (λ_T). An inspection of equation (47) shows that the correction, which contains the nonlinear properties of the temporal temperature fluctuation, is also defined by (λ_T). Thus the temporal temperature fluctuations are a function of (λ_T) for a given ξ_{eq}^4. This property could also be derived from the governing differential equation.

It should be recalled that ξ_{eq}^4 is the ratio of surface averaged heat rate incident on the spacecraft to the surface and time averaged heat rate incident on the spacecraft. The parameter (λ_T) is one-fourth of the ratio of the time and space averaged heat rate incident on the spacecraft to the mean heat stored in that surface. The factor of one quarter has no special significance for this particular interpretation of (λ_T).

Inspection of equation (46) shows that the temperature approaches its periodic value, exponentially as a first approximation.

The technique of solution used in this thesis is nothing more than the well-known method of successive approximations employed so as to resemble a perturbation technique. No attempt at a convergence proof is given since it is doubtful that one exists. Instead, it will be shown, by numerical examples, that this method does yield acceptable results for this type of problem.

It is obvious that through terms like $T_{\Lambda_0} + T_{\Lambda_1}$ the method of solution used here reduces to the often used linearization method where T_{Λ_0} plays the role of a constant. For an example of the linearization scheme see references 6 and 9.

No numerical example is given in this section since it is, in reality, a special case of the following section.

J. Solution of the Heat Equation for a Cylindrical Spacecraft With Time Dependent Temperature Distributions

When atron circumferential temperature differences are present on a spacecraft's external surfaces, the solution of the system of differential equations (described by eq. (23)) may be excessively involved. An alternate method for calculating the surface temperature distributions can be found in the solution of

$$\nabla \cdot \tilde{q}_\tau + \frac{q_n}{\tau} + P \simeq \rho c \frac{\partial T}{\partial t} \tag{3}$$

In general, P is zero unless electric currents flow in the member; thus P is of no interest here. The term q_n is the radiant heat

flux (arriving and leaving) the vehicular shell surface. The q_T term is the heat transferred, in the vehicle's tangent plane, by conduction.

It would be impractical to solve equation (3) for a general cone and then try to join cones together in a manner so as to find the temperature distribution for an arbitrary body of revolution. A situation, more amendable to solution, is that of a cylindrical shell with insulated ends and inner walls.

The solution for this example is straightforward and the results can be used to define bounds, or temperature limits, for the more difficult shapes.

As the 'example cylinder' orbits the earth its surface continually sees changing heat rates. Some surfaces receive more heat than others, thus the temperature along the cylinder's circumference is not uniform. Cylindrical polar coordinates are the natural coordinate system for this problem.

In cylindrical polar coordinates (see fig. 10) let the principal axis be alined with the Z_0 axis. Then, the cylinder's tangent plane is perpendicular to $(\tilde{c}_r)$. If the cylinder in question has no thermal coupling to other bodies, and if its optical properties are uniform, then there is no heat flow in the Z direction; hence equation (3) simplifies to

$$\frac{K}{r^2}\frac{\partial^2 T}{\partial \Lambda^2} + \frac{q_n}{\tau} \approx \rho c \frac{\partial T}{\partial t} \qquad (50)$$

where

r is the radius of the cylinder

K is the thermal conductivity of the surface material

τ is the thickness of the cylinder's walls

The problem of interest here occurs when the spin vector is at right angles to its axis of symmetry (the principal axis). In figure 11

$(\tilde{PA})$ is the principal axis vector

$(\tilde{SUN})$ is a vector pointing toward the sun

$(\tilde{e})$ is the vector pointing toward the earth

γ_1 is the angle between the planes $(\tilde{n},\tilde{\omega})$ and $(\tilde{e},\tilde{\omega})$

γ_2 is the angle measured from plane $(\tilde{n},\tilde{\omega})$ to plane $(\tilde{\omega},\tilde{SUN})$

and

$(\tilde{\omega},\tilde{SUN})$ is the plane common to $\tilde{\omega}$ and $\tilde{SUN}$ (etc.)

From the law of cosines, in spherical trigonometry

$$\left\{\tilde{n} \cdot (\tilde{SUN})\right\}^* = \left\{\cos A \cos \eta_s + \sin A \sin \eta_s \cos \gamma_2\right\}^* \qquad (51)$$

$$\tilde{n} \cdot \tilde{e} = \cos A \cos \eta_e + \sin A \sin \eta_e \cos \gamma_1 \qquad (52)$$

and it is clear that

$$\dot{\gamma}_2 = -\dot{\gamma}_1 = \text{spin rate} = \omega$$

In this section it will be assumed that the spin is fast enough so that no sizeable temperature fluctuations occur over one spin cycle of $(\tilde{PA})$ about $\tilde{\omega}$. If this condition is met (a means of checking

this condition is given in ref. 6), then the heat rates can be averaged over one spin cycle and the rewards of the ensuing simplicity can be achieved.

The solar contribution (q_s) to q_n is calculated as follows: Setting

$$\tilde{n} \cdot (\tilde{SUN}) = \cos \gamma_1$$

$$\tilde{n} \cdot \tilde{e} = \cos \gamma_2$$

and writing the fourier series

$$(\cos \gamma_1)^* = \sum_{n=0}^{\infty} a_n \cos n\gamma_1 \tag{53}$$

then with the aid of this expansion and trigonometric identities, along with equation (51), $\cos \gamma_1^*$ can be averaged over one revolution of γ_2 to yield

$$\frac{1}{2\pi} \int_0^{2\pi} \cos \gamma_1^* d\gamma_1 \cong \bar{M}_0 + \bar{M}_1 \cos \Lambda + \bar{M}_2 \cos 2\Lambda + \bar{M}_4 \cos 4\Lambda \tag{54}$$

where

$$\bar{M}_0 = a_0 - \frac{a_2}{2} \sin^2 \gamma_s + a_4 \left[3 \cos \gamma_s + 3 \cos^2 \gamma_s \sin^2 \gamma_s + \frac{2}{8} \sin^4 \gamma_s \right.$$

$$\left. - 2 \cos^2 \gamma_s - 1 \right]$$

$$\bar{M}_1 = a_1 \cos \eta_s$$

$$\bar{M}_2 = \frac{a_2}{2}\left[2\cos^2\eta_s - \sin^2\eta_s\right] + a_4\left[4\cos\eta_s - \frac{3}{2}\sin^4\eta_s - 4\cos^2\eta_s + 2\sin^2\eta_s\right]$$

$$\bar{M}_4 = a_4\left[\cos\eta_s - 3\sin^2\eta_s\cos^2\eta_s + \frac{3}{8}\sin^4\eta_s\right]$$

Here terms smaller than a_4 have been neglected.

Next set the right-hand side of equation (54) equal to $(\cos\eta_s^*)_m$ so that the heat from the sun per unit area is

$$q_s = Sa_s(\cos\eta_s^*)_m$$

The heat input on the spacecraft due to the presence of the earth ($q_e + q_a$) is calculated next. If the direct solar heat input is used, to an accuracy of a_4, then a compatible place to terminate $G_3(\eta_e)$ is at c_2 (neglecting higher ordered terms). Equation (34a) can be employed to justify this operation. The appropriate approximation for G_3 is now

$$G_3(\vartheta_0,\eta_2) \simeq C_0\left\{2(1-\cos\vartheta_0)\right\} + C_1\left\{\sin^2\vartheta_0\right\}\cos\eta_2 + C_2\left\{\frac{2}{3}(1-\cos^3\vartheta_0) - \frac{1}{3}(2-\cos\vartheta_0\sin^2\vartheta_0 - 2\cos\vartheta_0)\right\}\cos^2\eta_2$$

$$+ C_2\left\{\frac{1}{3}(2-\cos\vartheta_0\sin^2\vartheta_0 - 2\cos\vartheta_0)\right\}$$

or

$$G_3(\vartheta_0, \gamma_2) = b_0 + b_1 \cos \gamma_2 + b_2 \cos^2 \gamma_2$$

where

$$b_0 = C_0 \left\{ \tfrac{1}{2}(1 - \cos \vartheta_0) \right\} + C_2 \left\{ \tfrac{1}{3}(2 - \cos \vartheta_0 \sin^2 \vartheta_0 - 2 \cos \vartheta_0) \right\}$$

$$b_1 = C_1 \sin^2 \vartheta_0$$

$$b_2 = C_2 \left\{ \tfrac{2}{3}(1 - \cos^3 \vartheta_0) - \tfrac{1}{3}(2 - \cos \vartheta_0 \sin^2 \vartheta_0 - 2 \cos \vartheta_0) \right\}$$

after applying equation (52) and integrating G_3 over one cycle of γ_2 and introducing equation (19) it is found that

$$\frac{1}{2\pi} \int_0^{2\pi} G_3(\vartheta_0, \gamma_2) d\gamma \simeq (G_3(\vartheta_0, \gamma_e))_m = \left\{ n_{01} - n_{02} \cos 2(\delta + \psi) \right\}$$

$$- \left\{ n_{11} \sin(\delta + \psi) \right\} \cos \Lambda + \left\{ n_{21} \right.$$

$$\left. - n_{22} \cos 2(\delta + \psi) \right\} \cos 2\Lambda \qquad (55)$$

where

$$n_{01} = \left(b_0 + \frac{b_2}{4} + \frac{b_2}{8} \cos^2 \hat{\nu} \right)$$

$$n_{02} = \left(\frac{b_2}{4} \cos^2 \hat{\nu} \right)$$

$$n_{11} = (b_1 \cos \hat{\nu})$$

$$n_{21} = \left(\frac{3b_2}{8} \cos^2\hat{\nu} - \frac{b_2}{4}\right)$$

$$n_{22} = \left(\frac{3b_2}{8} \cos^2\hat{\nu}\right)$$

Now applying equation (28), then the earth thermal radiation and the reflected solar radiation can be expressed by

$$q_e + q_a = \left\{J_e \Sigma + Sr_e a_s \cos \epsilon \cos^*(\delta - \zeta)\right\}\left[G_3(\theta_0, \eta_e)\right]_m \qquad (56)$$

The total incoming power (by radiation) is

$$q_s + q_a + q_e \simeq Sa_s(\cos \eta_s^*)_m + \left\{J_e \Sigma + Sr_e a_s \cos \epsilon \cos^*(\delta - \zeta)\right\}\left[G_3(\theta_0, \eta_e)\right]_m$$

This expression can be rearranged and replaced by

$$q_s + q_a + q_e \simeq f_0(\delta) + f_1(\delta)\cos \Lambda + f_2(\delta)\cos 2\Lambda + f_4(\delta)\cos 4\Lambda \qquad (57)$$

where

$$f_0(\delta) = \left\{Sa_s\right\}\bar{H}_0 + \left\{J_e \Sigma + Sr_e a_s \cos \epsilon \cos^*(\delta - \zeta)\right\}\left\{n_{01} - n_{02} \cos 2(\delta + \Psi)\right\}$$

$$f_1(\delta) = \left\{Sa_s\right\}\bar{M}_1 - \left\{J_e\,\Sigma + Sr_e\,a_s\cos\epsilon\cos^*(\delta - \zeta)\right\}\left\{n_{11}\sin(\delta + \psi)\right\}$$

$$f_2(\delta) = \left\{Sa_s\right\}\bar{M}_2 + \left\{J_e\,\Sigma + Sr_e\,a_s\cos\epsilon\cos^*(\delta - \zeta)\right\}\left\{n_{21} - n_{22}\cos 2(\delta + \psi)\right\}$$

$$f_4(\delta) = \left\{Sa_s\right\}\bar{M}_4$$

The heat lost from the spacecraft's external surface by radiation is

$$\Sigma\sigma T^4$$

and the net heat on a surface element is, then,

$$q_n = q_s + q_a + q_\Sigma - \Sigma\sigma T^4 \tag{58}$$

With these results, after multiplication by τ, equation (50) becomes

$$-\frac{K\tau}{r^2}\frac{\partial^2 T}{\partial\Lambda^2} + \Sigma\sigma T^4 + \tau\rho c\frac{\partial T}{\partial t} = + f_0(\delta) + f_1(\delta)\cos\Lambda + f_2(\delta)\cos 2\Lambda + f_4(\delta)\cos 4\Lambda \tag{59}$$

Only a few changes are necessary to prepare equation (59) for its solution. First evaluate

$$\left(\frac{1}{2\pi}\right)\left(\frac{1}{2\pi}\right)\int_0^{2\pi}\int_0^{2\pi} q_R \, d\delta d\Lambda = \frac{1}{2\pi}\int_0^{2\pi} f_0(\delta)d\delta = (f_0)_m$$

then set

$$T = T_{\Lambda_0}\left\{1 + \xi_1 + \xi_2 + \cdots\right.$$

$$\Sigma\sigma T_{\Lambda_0}^{\ 4} = \hat{q}_R$$

$$\tau\rho c T_{\Lambda_0} = \hat{Q}$$

and

$$\frac{K\tau T_{\Lambda_0}}{r^2} = \hat{q}_K$$

so that equation (59) becomes

$$-\hat{q}_K\left\{\frac{\partial^2\xi_1}{\partial\Lambda^2} + \frac{\partial^2\xi_2}{\partial\Lambda^2} + \cdots\right.$$

$$+\hat{q}_R\left\{1 + 4\xi_1 + 4\xi_2 + 6\xi_1^{\ 2} + \cdots\right.$$

$$+\hat{Q}\left\{\frac{\partial\xi_1}{\partial t} + \frac{\partial\xi_2}{\partial t} + \cdots\right.$$

$$= (f_0)_m + \left\{f_0(\delta) - (f_0)_m\right\} + f_1(\delta)\cos\Lambda$$

$$+f_2(\delta)\cos 2\Lambda + f_4(\delta)\cos 4\Lambda$$

Proceeding as before, set

$$\hat{q}_R = (f_0)_m \tag{60}$$

then

$$-\hat{q}_K \frac{\partial^2 \xi_1}{\partial \Lambda^2} + \hat{q}_R\, 4\xi_1 + \hat{Q} \frac{\partial \xi_1}{\partial t} = \left\{f_0(\delta) - (f_0)_m\right\} + f_1(\delta)\cos \Lambda$$

$$+f_2(\delta)\cos \Lambda + f_4(\delta)\cos 4\Lambda \tag{61}$$

and

$$-\hat{q}_K \frac{\partial^2 \xi_2}{\partial \Lambda^2} + \hat{q}_R\, 4\xi_2 + \hat{Q} \frac{\partial \xi_2}{\partial t} = -6q_R\, \xi_1^2 \tag{62}$$

The homogeneous solution (for ξ_1) is of no interest since it is not periodic. The particular solution of ξ_1 can be found by assuming

$$\xi_1 = g_0(t) + g_1(t)\cos \Lambda + g_2(t)\cos 2\Lambda + g_4(t)\cos 4\Lambda$$

When this expression is introduced into equation (61) then, after grouping on $\cos n\Lambda$, one obtains

$$\frac{\partial g_0}{\partial t} + \lambda_T\, g_0 = \frac{1}{\hat{Q}} \left\{f_0(\delta) - (f_0)_m\right\}$$

$$\frac{\partial g_1}{\partial t} + (\lambda_T + \lambda_{T1})g_1 = \frac{1}{\hat{Q}} f_1(\delta)$$

$$\frac{\partial g_2}{\partial t} + (\lambda_T + \lambda_{T2})g_2 = \frac{1}{\hat{Q}} f_2(\delta)$$

and

$$\frac{\partial g_4}{\partial t} + (\lambda_T + \lambda_{T4})g_4 = \frac{1}{\hat{Q}} f_4(\delta)$$

where

$$\lambda_{T1} = \frac{\hat{q}_K}{\hat{Q}}; \quad \lambda_{T2} = \frac{4\hat{q}_K}{\hat{Q}}; \quad \lambda_{T4} = \frac{16\hat{q}_K}{\hat{Q}}$$

Now, set $\lambda_T + \lambda_{Tn} = \hat{\lambda}_{Tn}$ then the straightforward solution for this set of linear first-order differential equations is

$$g_0(t) = \frac{1}{\hat{Q}} \exp(-\lambda_T t) \int_0^t \left\{ f_0(\delta_1) - (f_0)_m \right\} \exp(\lambda_T t_1) dt_1$$

$$+ \frac{1}{\hat{Q}} \exp(-\lambda_T t) \frac{\exp(-\lambda_T L)}{1 - \exp(-\lambda_T L)} \int_0^L \left\{ f_0(\delta_1) - (f_0)_m \right\} \exp(\lambda_T t_1) dt$$

and

$$g_n(t) = \frac{1}{\hat{Q}} \exp(-\hat{\lambda}_{Tn} t) \int_0^t f_n(\delta_1) \exp(\hat{\lambda}_{Tn} t_1) dt_1$$

$$+ \frac{1}{\hat{Q}} \exp(-\hat{\lambda}_{Tn} t) \frac{\exp(-\hat{\lambda}_{Tn} L)}{1 - \exp(-\hat{\lambda}_{Tn} L)} \int_0^L f_n(\delta_1) \exp(\hat{\lambda}_{Tn} t_1) dt_1$$

where $g_n(t) = g_n(t + L)$; $n > 0$. When equation (62) is divided by $\hat{Q}$, and with

$$\frac{\hat{q}_K}{\hat{Q}} = \lambda_{T1}; \left(\frac{\hat{q}_R}{\hat{Q}}\right) = \frac{\lambda_T}{4}$$

introduced, then it follows that

$$\frac{\partial \xi_2}{\partial t} + \lambda_T \xi_2 - \lambda_{T1} \frac{\partial^2 \xi_2}{\partial \Lambda^2} = -\frac{3}{2} \lambda_T \xi_1^2$$

When ξ_1 is squared, and terms through $\cos 4\Lambda$ are retained,

$$\xi_1^2 \simeq \bar{G}_0 + \bar{G}_1 \cos \Lambda + \bar{G}_2 \cos 2\Lambda + \bar{G}_3 \cos 3\Lambda + \bar{G}_4 \cos 4\Lambda \qquad (63)$$

where

$$\bar{G}_0 = \left[g_0^2 + \frac{g_1^2}{2} + \frac{g_2^2}{2} + \frac{g_4^2}{2}\right]$$

$$\bar{G}_1 = \left[2g_0 g_1 + g_1 g_2\right]; \bar{G}_2 = \left[\frac{g_1^2}{2} + 2g_0 g_2 + g_2 \frac{g_4}{2}\right]$$

$$\bar{G}_3 = \left[g_1 g_2 + g_1 g_4\right]; \bar{G}_4 = \left[\frac{g_2^2}{2} + 2g_0 g_4\right]$$

Here, again, the homogeneous solution of ξ_2 is not periodic and therefore not of interest in this thesis.

Assuming that

$$\xi_2 = h_0(t) + h_1(t)\cos\Lambda + h_2(t)\cos 2\Lambda + h_3(t)\cos 3\Lambda + h_4(t)\cos 4\Lambda$$

and introducing this into the differential equation for ξ_2, after equating coefficients of $\cos n\Lambda$, note that

$$\frac{\partial h_0}{\partial t} + \lambda_T h_0 = -\frac{3}{2}\lambda_T \bar{G}_0 \tag{64}$$

and

$$\frac{\partial h_n}{\partial t} + \hat{\lambda}_{Tn} h_n = -\frac{3}{2}\lambda_T \bar{G}_n \tag{65}$$

The periodic solution to these expressions is

$$h_n(t) = -\frac{3}{2}\lambda_T \exp(-\hat{\lambda}_{Tn}\, t)\left\{\int_0^t \exp(\hat{\lambda}_{Tn}\, t_1)\bar{G}_n(t_1)dt_1 + \frac{\exp(-\hat{\lambda}_{Tn}\, L)}{1-\exp(-\hat{\lambda}_{Tn}\, L)}\int_0^L \exp(\hat{\lambda}_{Tn}\, t_1)\bar{G}_n(t_1)dt_1\right\};\ n \geq 0 \tag{66}$$

In the general case the integrations, indicated for the solution of $T(\Lambda,t)$, must be performed numerically. This is of no great disadvantage since numerical integration requires fewer operations than would the evaluation of the closed form results.

One immediate application of this problem can be established as follows: The mean value of ξ_1^2 is

$$(\xi_1^2)_m = (\bar{G}_0)_m = \left(\varepsilon_0^2 + \frac{\varepsilon_1^2 + \varepsilon_2^2 + \varepsilon_3^2}{2}\right)_m$$

where $\varepsilon_1 > \varepsilon_2 > \varepsilon_3$. In many cases the approximation can be made that

$$(\bar{G}_0)_m \simeq (\varepsilon_0^2)_m + \tfrac{1}{2}(\varepsilon_1^2)_m$$

where ε_0 is a time variant quantity and ε_1 measures the space variance (surface variance). The pure time variance can be approximated by

$$(\Delta T_t) \simeq T_{\Lambda_0}\, \varepsilon_0$$

and the pure surface variance can be approximated by

$$(\Delta T_{surf,max}) \simeq T_{\Lambda_0}(\varepsilon_1); \text{ for } (\cos \Lambda)_{max} = 1$$

so that

$$(\bar{G}_0)_m \simeq \left(\frac{\Delta T_t^2}{T_{\Lambda_0}}\right) + \frac{1}{2}\left(\frac{\Delta T^2_{surf,max}}{T_{\Lambda_0}}\right)_m$$

It is easy to prove that the mean value of ξ_1 is zero, so that the mean temperature of the section in question is approximated by

$$(T_\Lambda)_m \simeq T_{\Lambda_0} - \frac{3}{2}\left\{\frac{(\Delta T_t^2)_m}{T_{\Lambda_0}} + \frac{1}{2}\,\frac{(\Delta T^2_{surf,max})_m}{T_{\Lambda_0}}\right\}$$

$$= T_{\Lambda_0}(1 + \xi_2)_m \qquad (67)$$

One should notice that $\Delta T_{surf,max}$, as defined in this problem, represents the largest temperature variance on the surface; but it is not equal to $\Delta T_{surf,mean}$, which is defined as

$$\Delta T_{surf,mean} = \left[\frac{1}{2\pi}\int_0^{2\pi} \Delta T_{surf}^2 \, d\Lambda\right]^{1/2}$$

where

$$\Delta T_{surf} \simeq (\Delta T_{surf,max})\cos \Lambda$$

When these two definitions are combined it follows that

$$(\Delta T_{surf,mean}^2)_m \simeq \tfrac{1}{2}(\Delta T_{surf,max}^2)_m$$

and then the final form of equation (67) is

$$(T_\Lambda)_m \simeq T_{\Lambda_0} - \frac{3}{2}\left\{\frac{(\Delta T_t^2)_m}{T_{\Lambda_0}} + \frac{(\Delta T_{surf,mean}^2)_m}{T_{\Lambda_0}}\right\} \qquad (68)$$

The subscript m in every case infers the operation

$$(Z)_m = \frac{1}{L}\int_0^L (Z)dt$$

has been performed on Z.

Equation (68) is in good agreement with equation (25) and shows how the time and space temperature variations combine to decrease $(T_\Lambda)_m$.

In order to show one important aspect of this result consider a body i which has thermal coupling with only one other body (body j). Also, let the $(mc)_i$ term approach infinity so that T_i is approximately a constant. Then equation (23), specialized for body i, can be time integrated to yield

$$\frac{1}{L} R_{i,j} \int_0^L (\bar{T}_j^4 - T_{\Lambda_i}^4)dt + \frac{1}{L} h_{i,j} \int_0^L (T_{\Lambda_j} - T_{\Lambda_i})dt = 0$$

and

$$h_{i,j} = 0 \Longrightarrow T_{\Lambda_i} = \frac{1}{L} \int_0^L T_{\Lambda_j}\, dt \simeq (T_{\Lambda_0})_j - \frac{3}{2}(\xi_1^2)_{j,m}(T_{\Lambda_0})_j$$

with

$$R_{i,j} = 0 \Longrightarrow T_{\Lambda_i} = \left\{ \frac{1}{L} \int_0^L \overline{T_j^4}\, dt \right\}^{1/4} \simeq (T_{\Lambda_0})_j$$

Hence the temperature of body i, for this simple case, is determined by the heat-transfer mode between body i and body j.

In an earlier section (section I) it was shown that λ_T is the parameter governing the nondimensional temporal fluctuations when no space temperature variations exist. In the present section one finds that λ_T and $\hat{\lambda}_T$ are a pair of parameters which, for a given set of $f_n(\delta)/\hat{\delta}$, governs the nondimensional temperature variations when the temperature varies with both time and space.

The terms λ_T and $f_n(\delta)/\hat{Q}$ have already been defined; the quantity $\hat{\lambda}_T$ is a measure of heat conducted (inside the shell) divided by the mean heat content of the shell.

Most electronic equipment used by the aerospace industries is of the high density variety and (usually) quite sensitive to temperature. Often it is desirable to protect the electronic equipment from the severe temperature fluctuations which the spacecraft's external surfaces will see. This implies that (at least) during one orbital pass of the spacecraft around the earth the electronic equipment's temperatures will not have large fluctuations. The electronic gear will usually be housed in a given compartment and the temperature of this equipment may be partially controlled by its surrounding structure. It is evident from the discussion following equation (68) that the temperature of such equipment will be a function of not only the heat flux on the external surfaces of housing, but also the heat-transfer mode between the two sections. If this fact is neglected the resulting temperature error can be of the order of that caused by omitting the albedo heating effect. However, if no conductive heat transfer is present (into the spacecraft) and only radiative transfer used then the temperature fluctuations of the spacecraft's external surface is of no great consequence to the internal temperatures. Indeed for this case the analytical problem is reduced to the simple problem of solving the system of equations defined by equation (26). This task can be simplified by averaging equation (26) over one orbital pass. The result is a set of algebraic equations which are linear in T_i^4 and can be solved by ordinary methods of matrix algebra.

Example of time-dependent temperature distributions.- An example of time-dependent temperature distributions is given below. The properties of the cylinder (the vehicle) chosen to illustrate this example are:

Cylinder thermal conductivity (K) = 0.135 Btu/min in. ^{o}R

Cylinder specific heat (c) = 0.21 Btu/^{o}R lb

Cylinder density (ρ) = 0.0978 lb/in.^{3}

Cylinder thermal diffusivity (α^2) = 6.770 in.^{2}/min

$$\alpha = 2.602 \text{ in./(min)}^{1/2}$$

Radius of cylinder (r) = 15 in.

Thickness of cylinder shell (τ) = 0.0625 in.

Solar absorptivity (a_s) = 0.60

Total hemispherical emissivity (Σ) = 0.50

The orbital properties are:

Spin mode - long term

Solar orientation (η_s) = 0.0^{o}

Orbit period L = 100 min

Time in direct sunlight (L_1) = 60 min

For this example, and for the sake of saving labor, the earth thermal radiation and the albedo heat have been neglected. This is not meant to imply that they are negligible; they are simply neglected in this one example case. Under these conditions equation (60) reduces to

$$\hat{q}_R = \left(\frac{L_1}{L}\right)\left\{Sa_s\right\}\bar{M}_0$$

where $\bar{M}_0 = a_0 = \frac{1}{\pi}$. It should be noted here that, in general, $\bar{M}_0$ is usually an approximation to (A_s/A); however, in this case it is the exact value.

Now

$$S \cong 0.04968 \text{ Btu/in.}^2 \text{ min}$$

thus

$$T_{\Lambda_0}^4 = \left(\frac{L_1}{L}\right)\left(\frac{a_0}{\Sigma}\right)\left(\frac{A_s}{A}\right)\frac{S}{\sigma}$$

$$= \frac{1}{\pi}\left(\frac{0.6}{0.5}\right)(0.60)\left(\frac{0.04968}{2 \times 10^{-13}}\right) = 569.3 \times 10^8$$

or

$$T_{\Lambda_0} = 488.5^\circ \text{ R}$$

Hence,

$$\hat{Q} = \tau\rho c T_{\Lambda_0} = 0.0625(0.0978)(0.21)(488.5) \text{ Btu/in.}^2$$

$$= 0.627 \text{ Btu/in.}^2$$

and

$$\hat{q}_R = \Sigma\sigma T_{\Lambda_0}^4 = 0.5 \times 2 \times 10^{-13} \times 569.3 \times 10^8 = 0.00569 \text{ Btu/in.}^2 \text{ min}$$

also

$$\bar{M}_1 = a_1 = 0.500$$

$$\bar{M}_2 = a_2 = \frac{2}{3\pi} \cong 0.2122$$

$$\bar{M}_4 = a_4 = -\frac{2}{\pi 15} \simeq -0.0424$$

In the following $\bar{M}_4$ can be safely neglected. Now

$$\lambda_T = 4\left(\frac{\hat{q}_R}{\hat{Q}}\right) = 0.0362(\text{min})^{-1}$$

and

$$\hat{q}_K = \frac{K_T T_{10}}{r^2} = \frac{0.135 \times 0.0625 \times 488.5}{225} = 0.01886 \text{ Btu/in.}^2 \text{ min}$$

thus

$$\lambda_{T1} = \frac{0.01886}{0.627}(\text{min})^{-1} = 0.0301(\text{min})^{-1}$$

and so

$$\hat{\lambda}_{T1} = 0.0362 + 0.0301 = 0.0663(\text{min})^{-1}$$

$$\hat{\lambda}_{T2} = 0.0362 + 0.1204 = 0.1566(\text{min})^{-1}$$

The time-dependent functions in equation (57) are given below

$$\left\{f_0(\delta_1) - (f_0)_m\right\} = Sa_s \bar{M}_0 \left\{H - \frac{L_1}{L}\right\}$$

Where H is one in the sunlight and zero when the spacecraft is in darkness. The coefficients of $\cos A$ and $\cos 2A$ in equation (57) simplify to

$$f_1(\delta) = Sa_s \bar{M}_1 H$$

$$f_2(\delta) = Sa_s \bar{M}_2 H$$

Thus

$$\left\{f_0(\delta_1) - (f_0)_m\right\} = 0.0948 \left\{H - 0.60\right\} \text{ Btu/in.}^2 \text{ min}$$

$$f_1(\delta_1) = 0.1488 \text{ H Btu/in.}^2 \text{ min}$$

$$f_2(\delta_1) = 0.0632 \text{ H Btu/in.}^2 \text{ min}$$

This completes all the necessary inputs to integrate the equation for dg_n/dt. The results of this integration are plotted as figures 15(a), 15(b), and 15(c).

Next, the $\bar{G}_n(t)$ can be calculated from equation (63), then equation (66) can be integrated. The values $h_n(t)$ are plotted as figures 15(d), 15(e), and 15(f). These results can be used directly to calculate $T(t,\Lambda)$, which, in turn, is plotted as figure 15(g) for the cases of

$$\Lambda = 0^\circ$$

$$\Lambda = 90^\circ$$

$$\Lambda = 180^\circ$$

where Λ is the azimuth angle from a cylindrical polar coordinate system (measured zero when η_s assumes its minimum value).

The values $g_n(t)$ were obtained by analytical integration while the $h_n(t)$ values were obtained by numerical integration.

This example is of particular interest since the properties are realistic and might be thought of as "typical of near-earth spacecraft." From figure 16(d) it can be seen that

$$\frac{1}{L}\int_0^L h_0(t)dt \approx 0.058$$

so that

$$(T_A)_m \simeq 488.5 - 0.058 \times 488.5 = 488.5 - 28.3 = 460.2^\circ \text{ R}$$

Now, if an electronic package was housed in this particular cylinder, and if the only heat which the package exchanged was with the cylinder (in this problem), then the temperature of the electronics package could seek one of two levels. If the heat exchanged to the electronic package was purely by radiation then the package would seek a temperature of 488.5° R. However, if the heat was transferred purely by conduction, the package would seek a temperature of 460.2° R. It is obvious then, why temperature variations must be investigated in cases such as this. Of the 28° R temperature drop about 7° is due to the time temperature variation; thus, in this case the circumferential variation is predominant.

In figure 15(g) it can be seen that when the spacecraft enters the sunlight the circumferential temperature variations grow rapidly. When the spacecraft enters the earth's shadow the temperature differences decrease rapidly.

In the literature problems of this type are commonly solved by employing a linear approximation for T^4. This corresponds exactly to the accuracy achieved through $T_{\Lambda_0}(1 + \xi_1)$. From the plots in figures 15(d), 15(e), and 15(f) it is clear that $T_{\Lambda_0}\,\xi_2$ can be appreciable. Also from the plot of $h_0(t)$ in figure 15(d) it can be seen that the largest contribution from $(T_{\Lambda_0}\,\xi_2)$ is simply a negative constant.

It must be pointed out (here) that temperature fluctuations, as predicted by the linear approximation to T^4, are generally good. The largest part of the temperature error comes from the fact that the mean value of the temperatures, found by this technique, is too high. It can be easily verified, by numerical integration, that solutions through an accuracy of $T_0 + T_1$ are not in equilibrium with their environment. That is to say, solutions of the linearized variety radiate more heat away than is received. Solutions through an accuracy of $T_0 + T_1 + T_2$ are in closer equilibrium with the surrounding environment.

Time-dependent temperature distribution solutions can be employed to show how a spacecraft might be divided into the minimum number of sections which permits the use of equation (26).

K. Solution of the Linear Heat Equation With Nonlinear Boundary Conditions

One-dimensional, time-dependent heat flow with a nonlinear radiation boundary is solved in this section.

Consider the heat conduction equation (eq. (1)). If p (power per unit volume of the conductor) is zero then

$$\nabla^2 T = \left(\frac{\rho c}{K}\right)\frac{\partial T}{\partial t} = \frac{1}{a^2}\frac{\partial T}{\partial t}$$

where

ρ density of the body shell

c specific heat of the shell

K thermal conductivity of the shell

In the present problem it will be assumed that the heat conducted in a direction normal to the surface is very large compared to the heat conducted in the direction of the shell's tangent plane. Thus predominantly $\nabla^2 T$ is expressed as

$$\nabla^2 T \simeq \frac{\partial^2 T}{\partial X^2}$$

where X is measured in the surface normal direction and is zero at the back insulated face. When this approximation is applied, equation (1) simplifies to the well-known diffusion equation in one space variable

$$\frac{\partial^2 T}{\partial X^2} = \frac{1}{a^2}\frac{\partial T}{\partial t}$$

the back face (X = 0) is insulated, hence

$$\frac{\partial T}{\partial X} = 0, \quad X = 0$$

on the front face (X = τ)

$$-K\frac{\partial T}{\partial X} = \Sigma\sigma T^4 - q(t), \quad X = \tau$$

It has been shown, in several examples, that $q(t)$ is a periodic function. Guided by the previous analysis, it is assumed that

$$T(X,t) = T_0(X,t) + T_1(X,t) + T_2(X,t) + \ldots + \ldots$$

where the $T_r(X,t)$ are the modes of a perturbation solution to the governing differential equation.

Assuming the quantity $q(t)$ may be written as

$$q(t) = (q)_m + \left\{q(t) - (q)_m\right\}$$

then the boundary condition can be expressed by

$$\begin{aligned} -K\left[\frac{\partial T_0(t,\tau)}{\partial X} + \frac{\partial T_1(t,\tau)}{\partial X} + \frac{\partial T_2(t,\tau)}{\partial X} + \ldots\right] = \Sigma\sigma\Big[&T_0^4(t,\tau) \\ &+ 4T_0^3(t,\tau)T_1(t,\tau) \\ &+ 4T_0^3(t,\tau)T_2(t,\tau) \\ &+ 6T_0^2(t,\tau)T_1^2(t,\tau) \\ &+ \ldots\Big] - (q)_m - \left\{q(t)\right. \\ &\left. - (q)_m\right\} \end{aligned} \tag{69}$$

This expression will be satisfied at each order of magnitude if

$$T_0(t,X) = \text{const}$$

and

$$\Sigma\sigma T_0^4 = (q)_m$$

hence

$$-K\frac{\partial T_1(t,\tau)}{\partial X} - \Sigma\sigma^4 T_0^3(t,\tau)T_1(t,\tau) = -q(t) + (q)_m \qquad (70)$$

and

$$-K\frac{\partial T_2(t,\tau)}{\partial X} - \Sigma\sigma^4 T_0^3(t,\tau)T_2(t,\tau) = +6\Sigma\sigma T_0^2(t,\tau)T_1^2(t,\tau) \qquad (71)$$

Thus the nonlinear boundary condition can be satisfied by a system of linear relations. If the assumed solution is introduced into the diffusion equation it is apparent that

$$\frac{\partial^2 T_1(t,X)}{\partial X^2} = \frac{1}{\alpha^2}\frac{\partial T_1(t,X)}{\partial t}$$

$$\frac{\partial^2 T_2(t,X)}{\partial X^2} = \frac{1}{\alpha^2}\frac{\partial T_2(t,X)}{\partial t}$$

.

.

.

and so on.

If the initial transient solution is of no interest then $T_r(t,X)$ may be expressed as

$$T_r(t,X) = \sum_{n=0}^{\infty} \left\{ f_{rn}(X)\sin n\Omega t + g_{rn}(X)\cos n\Omega t \right\} \qquad (72)$$

where T_r is the rth mode of a perturbation solution to equation (1). This assumed solution, when introduced into the governing differential equation, becomes

$$f''_{rn}(X)\sin n\Omega t + g''_{rn}(X)\cos n\Omega t = \left(\frac{n\Omega}{a^2}\right) f_{rn}(X)\cos n\Omega t - \left(\frac{n\Omega}{a^2}\right) g_{rn}(X)\sin n\Omega t$$

and since this expression must hold for all t, then

$$f''_{rn}(X) + \left(\frac{n\Omega}{a^2}\right) g_{rn}(X) = 0$$

and

$$g''_{rn}(X) - \left(\frac{n\Omega}{a^2}\right) f_{rn}(X) = 0$$

where

$$g''_{rn}(X) = \frac{d^2}{dX^2}\, g_{rn}(X)$$

and so on. Multiplying this last equation by $i = \sqrt{-1}$ and adding to the former equation, then after some rearrangement, and setting

$$\psi_{rn}(X) = (f_{rn} + ig_{rn})$$

one finds that

$$\psi''_{rn} - i\left(\frac{n\Omega}{a^2}\right)\psi_{rn} = 0 \qquad (73)$$

Now, let

$$\omega_n = \frac{1}{c}\sqrt{\frac{n\Omega}{2}}$$

then the solution to equation (73) is found to be

$$\gamma_{rn}(X) = c_{rn} \cosh \omega_n(1 + i)X + d_{rn} \sinh \omega_n(1 + i)X$$

However, since no heat is to flow through the plane $X = 0$, $d_{rn} = 0$,

$$\gamma_{rn}(X) = c_{rn} \cosh \omega_n(1 + i)X = (\bar{c}_{rn} + i\hat{c}_{rn})\Big\{\cosh \omega_n X \cos \omega_n X + i \sinh \omega_n X \sin \omega_n X\Big\}$$

Upon separating $\gamma_{rn}(X)$ into its real and imaginary parts it follows that

$$f_{rn}(X) = \bar{c}_{rn} \cosh \omega_n X \cos \omega_n X - \hat{c}_{rn} \sinh \omega_n X \sin \omega_n X \qquad (74)$$

and

$$g_{rn}(X) = \hat{c}_{rn} \cosh \omega_n X \cos \omega_n X + \bar{c}_{rn} \sinh \omega_n X \sin \omega_n X \qquad (75)$$

Setting

$$M_n(X) = \cosh \omega_n X \cos \omega_n X$$

$$N_n(X) = \sinh \omega_n X \sin \omega_n X$$

it follows that if $r \neq 0$ then

$$T_r(t,X) = \sum_{n=0}^{\infty} \left\{ \left[\bar{c}_{rn} M_n(X) - \hat{c}_{rn} N_n(X) \right] \sin n\Omega t + \left[\hat{c}_{rn} M_n(X) + \bar{c}_{rn} N_n(X) \right] \cos n\Omega t \right\} \tag{76}$$

The constants $\bar{c}_{rn}$ and $\hat{c}_{rn}$ will be found from the boundary conditions.

Expanding

$$q(t) - q_m$$

in a complete fourier series, that is

$$q(t) - q_m = \sum_{n=0}^{\infty} \left\{ \hat{e}_{1n} \cos n\Omega t + \bar{e}_{1n} \sin n\Omega t \right\} \tag{77}$$

and introducing this and equation (76) into equation (70), it follows that for each value of n,

$$K\left[\bar{c}_{1n} M_n'(\tau) - \hat{c}_{1n} N_n'(\tau)\right] \sin n\Omega t + K\left[\hat{c}_{1n} M_n'(\tau) + \bar{c}_{1n} N_n'(\tau)\right] \cos n\Omega t$$

$$+ (4\Sigma\sigma T_0^3)\left[\bar{c}_{1n} M_n(\tau) - \hat{c}_{1n} N_n(\tau)\right] \sin n\Omega t + (4\Sigma\sigma T_0^3)\left[\hat{c}_{1n} M_n(\tau)\right.$$

$$\left. + \bar{c}_{1n} N_n(\tau)\right] \cos n\Omega t = \hat{e}_{1n} \cos n\Omega t + \bar{e}_{1n} \sin n\Omega t \tag{78}$$

If this expression is separated into two parts (the coefficients of $\sin n\Omega t$ and $\cos n\Omega t$, respectively) the results can be written, in matrix form, as

$$\begin{bmatrix} \left[KM_n' + 4\Sigma\sigma T_0^3 M_n\right] & -\left[KN_n' + 4\Sigma\sigma T_0^3 N_n\right] \\ \left[KN_n' + 4\Sigma\sigma T_0^3 N_n\right] & \left[KM_n' + 4\Sigma\sigma T_0^3 M_n\right] \end{bmatrix} \begin{Bmatrix} \bar{c}_{1n} \\ \hat{c}_{1n} \end{Bmatrix} = \begin{Bmatrix} \bar{e}_{1n} \\ \hat{e}_{1n} \end{Bmatrix} \qquad (79)$$

where M_n, N_n, M_n', N_n' are evaluated at $X = \tau$. This expression determines $\hat{c}_{1n}$ and $\bar{c}_{1n}$.

To determine $T_2(t,X)$, set $X = \tau$ in $T_1(t,X)$ and form $T_1^2(t,\tau)$. Making the proper use of certain trigonometric identities $T_1^2(t,\tau)$ can be expressed as

$$+6\Sigma\sigma T_0^2 T_1^2(t,\tau) = + \sum_{n=0}^{\infty} \left\{ \hat{e}_{2n} \cos n\Omega t + \bar{e}_{2n} \sin n\Omega t \right\} \qquad (80)$$

Now noting that the equations expressing $T_2(t,X)$ and its boundary conditions have the identical form of $T_1(t,X)$, it is obvious that the equation for the unknown constants in $T_2(t,X)$ will be equation (79) with the subscript (1) changed to (2), hence

$$\begin{bmatrix} \left(KM_n' + 4\Sigma\sigma T_0^3 M_n\right) & -\left(KN_n' + 4\Sigma\sigma T_0^3 N_n\right) \\ \left(KN_n' + 4\Sigma\sigma T_0^3 N_n\right) & \left(KM_n' + 4\Sigma\sigma T_0^3 M_n\right) \end{bmatrix} \begin{Bmatrix} \bar{c}_{2n} \\ \hat{c}_{2n} \end{Bmatrix} = - \begin{Bmatrix} \bar{e}_{2n} \\ \hat{e}_{2n} \end{Bmatrix}$$

The unknown constants for all the $T_r(t,X)$ may be found in a similar manner, thus finally the solution of $T(t,X)$ is formed by

$$T(t,X) = T_0(t,X) + T_1(t,X) + T_2(t,X) + \ldots$$

One important feature of this solution lies in the fact that it can predict the temperature fluctuations of a thick wall structure which is exposed to radiative heat transfer on its front face. Therefore, it can also be used to justify the assumption necessary in arriving at equation (3).

Another interesting property can be found in the boundary conditions. From the boundary conditions for $T_1(t,X)$ it can be shown that

$$(T_1(t,X))_m = 0 \quad \begin{matrix}(\text{The subscript } m \text{ denotes} \\ \text{time average})\end{matrix}$$

Also since the back face is insulated

$$\int_t^{t+L} \frac{\partial T_2(t,X)}{\partial X}\, dt = 0 \quad (\text{for all } X) \qquad (82)$$

hence, the boundary condition on the front face becomes

$$-K \int_t^{t+L} \frac{\partial T_2(t,\tau)}{\partial X}\, dt - \Sigma\sigma(4T_0^3) \int_t^{t+L} T_2(t,\tau)dt$$

$$= 6\Sigma\sigma T_0^2 \int_t^{t+L} T_1^2(t,\tau)dt$$

or

$$(T_2)_m = -\frac{3}{2}\left(\frac{T_1^2}{T_0}\right)_m$$

Thus from the assumed solution it is clear that

$$(T(t,X))_m \cong T_0 - \frac{3}{2}\left(\frac{T_1^2(t,\tau)}{T_0}\right)_m \qquad (83)$$

which is the usual temperature drop due to temporal fluctuations.

Example of diffusion equation with nonlinear boundary condition.- The numerical example given here illustrates temperature fluctuations on the face of a spacecraft's external surface, when the shell cannot be assumed to have a constant temperature through its thickness.

Suppose the shell in question is 1 inch thick and made of a foam plastic having the following properties:

Thermal conductivity (K) = 1.25×10^{-5} Btu/min · in. ^{o}R

Density (ρ) = 8.68×10^{-4} lb/in.^{3}

Specific heat (c) = 0.25 Btu/lb ^{o}R

Thermal diffusivity (α^2) = 0.0576 in.^{2}/min

Solar absorbtivity (a_S) = 0.3

Emissivity (Σ) = 0.9

Thickness (τ) = 1 inch

$$q(t) = 0.3 \times 0.04968 + 0.3 \times 0.04968 \cos \Omega t \text{ Btu/in.}^2 \cdot \text{min}$$

Circular frequency of heat cycle (Ω) = 0.1256 radian/min

Period (L) = 50 minutes. Now, from equation (77)

$$\hat{e}_{10} = 14.90 \times 10^{-3} \text{ Btu/min} \cdot \text{in.}^2$$

$$\hat{e}_{11} = 14.90 \times 10^{-3} \text{ Btu/min} \cdot \text{in.}^2$$

and

$$\omega_1 = \frac{1}{\alpha}\sqrt{\frac{\Omega}{2}} = \left(\frac{1}{0.2399}\right)\left(\sqrt{\frac{0.1256}{2}}\right) = 1.0446 \text{ radians/in.}$$

From equation (69)

$$T_0^4 = \frac{(q)_m}{\Sigma\sigma} = 827.7 \times 10^8$$

so that

$$T_0 = 536.3^\circ \text{ R}$$

Also

$$4\Sigma\sigma T_0^3 = 4 \times 0.9 \times 2 \times 10^{-13}\, T_0^3$$

$$= 11.105 \times 10^{-5} \text{ Btu/in.}^2 \,^\circ\text{R min}$$

and

$$\omega_1 \tau = 1.0446 \times 1 = 1.0446 \text{ radians}$$

so that

$$\cosh \omega_1 \tau = 1.5970$$

$$\sinh \omega_1 \tau = 1.2452$$

$$\cos \omega_1 \tau = 0.50227$$

$$\sin \omega_1 \tau = 0.86471$$

thus

$$M_1(\tau) = 1.5970$$

$$M_1'(\tau) = \frac{d}{dX}(M_1)_{X=\tau} = -0.7892$$

$$N_1(\tau) = 1.0767$$

$$N_1'(\tau) = \frac{d}{dX}(N_1)_{X=\tau} = 2.0958$$

Now equation (79) gives

$$\bar{c}_{11} = 102.22$$

$$\hat{c}_{11} = 56.23$$

From equations (74) and (75) it follows that

$$f_{11}(\tau) = 21.4;\ f_{11}(0) = 102.22$$
$$g_{11}(\tau) = 151.7;\ g_{11}(0) = 56.23$$

and from an application of equation (72)

$$T_1(t,\tau) = 21.4 \sin \Omega t + 151.2 \cos \Omega t$$
$$T_1(t,0) = 102.2 \sin \Omega t + 56.2 \cos \Omega t$$
$$T_1^2(t,\tau) = 11{,}659.6 + 1{,}617.8 \sin 2\Omega t + 11{,}201.7 \cos 2\Omega t$$

so that

$$-6\Sigma\sigma T_0^2 T_1^2(t,\tau) = -34.8 \times 10^{-4} - 4.8 \times 10^{-4} \sin 2\Omega t$$
$$-33.5 \times 10^{-4} \cos 2\Omega t$$

It is easy to see that the constant part of $-6\Sigma\sigma T_0^2 T_1(t,\tau)$ produces a constant solution equal to

$$\frac{-34.8 \times 10^{-4}}{4\Sigma\sigma T_0^3} = -33.3^\circ \text{ R}$$

The remainder of the solution gives

$$\hat{e}_{22} = -33.5 \times 10^{-4}$$

$$\tilde{e}_{22} = -4.8 \times 10^{-4}$$

This completes the calculations for all the unknowns necessary to determine $T_2(t,X)$; the procedure is identical to the calculation of $T_1(t,X)$, so without further ado

$$T_2(t,\tau) = -33.3 - 0.5 \sin 2\Omega t - 28.2 \cos 2\Omega t$$

$$T_2(t,0) = -33.3 - 12.4 \sin 2\Omega t - 1.1 \cos 2\Omega t$$

and the complete solution is, approximately, given by

$$T(t,X) \simeq T_0 + T_1(t,t) + T_2(t,X)$$

The solutions

$$T_0 + T_1(t,\tau) \quad \text{and} \quad T_0 + T_1(t,\tau) + T_2(t,\tau)$$

are plotted in figure 16(b). The solutions

$$T_0 + T_1(t,0) \quad \text{and} \quad T_0 + T_1(t,0) + T_2(t,0)$$

are plotted in figure 16(a). In these figures it can be observed that the temperature on the insulated face has slightly lower temperature fluctuation, and lags the temperature on the surface ($X = \tau$) by a few minutes. It is clear that this structure would not satisfy an assumption of constant temperature throughout the shell's thickness.

On figure 16(b) the upper equilibrium temperature is plotted. The solution $T_0 + T_1$ rises well above this value and is therefore clearly in error. The solution $T_0 + T_1 + T_2$ falls just short of the upper limit and so in this sense $(T_0 + T_1 + T_2)$ is a better solution than $(T_0 + T_1)$.

L. Comparison of Exact and Approximate Solutions

The problem remaining is to compare the approximate solution with the exact solution. One of the few problems which possesses a closed form solution is that of a body with no spatial temperature gradient and heated by a constant heat flux. As an example of such a problem consider a small flat plate heated solely by the sun. For this case equation (2) becomes

$$mc \frac{dT_A}{dt} = SA_s a_s - A\Sigma\sigma T_A^4 \tag{84}$$

Letting

$$m = \rho\tau A; \quad SA_s a_s = A\Sigma\sigma T_{A_0}^4$$

then

$$\frac{dT_A}{dt} = \left(\frac{\Sigma\sigma}{\rho\tau c}\right)(T_{A_0}^4 - T_A^4) \tag{85}$$

and

$$\frac{dT_A}{T_{A_0}^4 - T_A^4} = \left(\frac{\Sigma\sigma}{\rho\tau c}\right)dt$$

which integrates to

$$\ln\left(\frac{T_{A_0} + T_A(t)}{T_{A_0} - T_A(t)}\right)\left(\frac{T_{A_0} - T_A(0)}{T_{A_0} + T_A(0)}\right) + 2\left[\tan^{-1}\left(\frac{T_A(t)}{T_{A_0}}\right) - \tan^{-1}\left(\frac{T_A(0)}{T_{A_0}}\right)\right]$$

$$= \left(\frac{4\Sigma\sigma T_{A_0}^{3}}{\rho\tau c}\right)t \qquad (86)$$

where $T_A(0) = T_A(t)$ for $t = 0$.

If the sun does not heat the plate then the equation which governs its cooling is

$$-\frac{dT_A}{T_A^4} = \left(\frac{\Sigma\sigma}{\rho\tau c}\right)dt$$

This can be integrated to provide

$$\left(\frac{1}{T_A^3(t)} - \frac{1}{T_A^3(0)}\right) = 3\left(\frac{\Sigma\sigma}{\rho\tau c}\right)t \qquad (87)$$

For the perturbation solution of equation (84), it is assumed that

$$T_A = T_{A_0} + T_{A_1} + T_{A_2} + \ldots$$

hence

$$T_A^4 = T_{A_0}^4 + 4T_{A_0}^3T_{A_1} + 4T_{A_0}^3T_{A_2} + 6T_{A_0}^2T_{A_1}^2 + \ldots$$

When this assumption is introduced into equation (85) it is found that

$$\overset{\circ}{T}_{\Lambda_1} + \overset{\circ}{T}_{\Lambda_2} + \ldots + \left(\frac{\Sigma\sigma}{\rho\tau c}\right)\left[T_{\Lambda_0}^{\ 4} + 4T_{\Lambda_0}^{\ 3}T_{\Lambda_1} + 4T_{\Lambda_0}^{\ 3}T_{\Lambda_2} + 6T_{\Lambda_0}^{\ 2}T_{\Lambda_1}^{\ 2} + \ldots\right.$$

$$= \left(\frac{\Sigma\sigma}{\rho\tau c}\right)T_{\Lambda_0}^{\ 4}$$

and, as usual, this can be separated into

$$\overset{\circ}{T}_{\Lambda_1} + 4T_{\Lambda_0}^{\ 3}\left(\frac{\Sigma\sigma}{\rho\tau c}\right)T_{\Lambda_1} = 0;\ T_{\Lambda_1}(0) = \text{initial condition}$$

and

$$\overset{\circ}{T}_{\Lambda_2} + 4T_{\Lambda_0}^{\ 3}\left(\frac{\Sigma\sigma}{\rho\tau c}\right)T_{\Lambda_2} = -6T_{\Lambda_0}^{\ 2}\left(\frac{\Sigma\sigma}{\rho\tau c}\right)T_{\Lambda_1}^{\ 2};\ T_{\Lambda_2}(0) = 0$$

whose solutions are

$$T_{\Lambda_1}(t) = T_{\Lambda_1}(0)\exp(-\lambda_T\, t);\ \lambda_T = \left(\frac{4T_{\Lambda_0}^{\ 3}\Sigma\sigma}{\rho\tau c}\right)$$

and

$$T_{\Lambda_2}(t) = \frac{3}{2}\left(\frac{T_{\Lambda_1}(0)}{T_{\Lambda_0}}\right)T_{\Lambda_1}(0)\left[\exp(-2\lambda_T\, t) - \exp(-\lambda_T\, t)\right]$$

Finally, it is apparent that

$$T_\Lambda(t) \simeq T_{\Lambda_0} + T_{\Lambda_1}(0)\exp(-\lambda_T\, t) + \frac{3}{2}\left(\frac{T_{\Lambda_1}(0)}{T_{\Lambda_0}}\right)T_{\Lambda_1}(0)\left[\exp(-2\lambda t) - \exp(-\lambda t)\right] \tag{88}$$

The approximation to equation (87) is obtained as follows:

Assume that

$$T_\Lambda = T_{\Lambda_0} + T_{\Lambda_1} + T_{\Lambda_2} + \cdots$$

then

$$\overset{\circ}{T}_{\Lambda_0} + \overset{\circ}{T}_{\Lambda_1} + \overset{\circ}{T}_{\Lambda_2} + \cdots + \left(\frac{\Sigma\sigma}{\rho\tau c}\right)\Big[T_{\Lambda_0}{}^4 + 4T_{\Lambda_0}{}^3 T_{\Lambda_1} + 4T_{\Lambda_0}{}^3 T_{\Lambda_2}$$

$$+ 6T_{\Lambda_0}{}^2 T_{\Lambda_1}{}^2 + \cdots\Big] = 0$$

Now, let $T_{\Lambda_0} = T_\Lambda(0)$ so that

$$\overset{\circ}{T}_{\Lambda_1} + 4T_{\Lambda_0}{}^3\left(\frac{\Sigma\sigma}{\rho\tau c}\right)T_{\Lambda_1} = -\left(\frac{\Sigma\sigma}{\rho\tau c}\right)T_{\Lambda_0}{}^4;\ T_{\Lambda_1}(0) = 0$$

and

$$\overset{\circ}{T}_{\Lambda_2} + 4T_{\Lambda_0}{}^3\left(\frac{\Sigma\sigma}{\rho\tau c}\right)T_{\Lambda_2} = -6T_{\Lambda_0}{}^2\left(\frac{\Sigma\sigma}{\rho\tau c}\right)T_{\Lambda_1}{}^2;\ T_{\Lambda_2}(0) = 0$$

With the accompanying solutions

$$T_{\Lambda_1} = \frac{T_{\Lambda_0}}{4}\Big[\exp(-\lambda t) - 1\Big]$$

$$T_{\Lambda_2} = \frac{3}{32}T_{\Lambda_0}\Big[\exp(-\lambda t) - 1\Big] + \frac{3}{32}T_{\Lambda_0}\Big[\exp(-\lambda t) - 1\Big]\exp(-\lambda t)$$

$$+ \frac{3\lambda}{16}T_{\Lambda_0}\, t\exp(-\lambda t)$$

Thus it is evident that an approximate solution of the cooling curve is given by

$$T_\Lambda(t) \simeq T_{\Lambda_0} + T_{\Lambda_1} + T_{\Lambda_2} \qquad (89)$$

This example provides for a comparison between the exact solutions, equations (86) and (87), and the approximate solution, equations (88) and (89). The properties of the vehicle used in this example are the same as those for the body used in the example on time-dependent temperature distributions. The calculations are straightforward so that only the results are given here.

In figure 17(b) the heating curve, from 355° R to the equilibrium temperature, 555° R, is presented. This represents the case of a thin walled cylinder spinning about its axis of symmetry. The heating source is the sun which sees the cylinder broadside. Initially, the cylinder has been cooled to 355° R and then subjected to direct sunlight.

The curve marked $(T_{\Lambda_0} + T_{\Lambda_1} + T_{\Lambda_2})$ is seen to be in good agreement with the exact solution. The curve marked $(T_{\Lambda_0} + T_{\Lambda_1})$ corresponds to the linearized solution and does not provide a very good comparison. In figure 17(a) the cylinder has been suddenly hidden from the sun, and the cooling curves (from 555° R) are shown. As before, the curve marked $(T_{\Lambda_0} + T_{\Lambda_1} + T_{\Lambda_2})$ is in much better agreement with the exact solution than is the curve marked $(T_{\Lambda_0} + T_{\Lambda_1})$. In fact, adding the term T_2 almost doubles the range of applicability. Although no positive statement should be made from these results, figure 17(a) suggests that $(T_{\Lambda_0} + T_{\Lambda_1} + T_{\Lambda_2})$ might be valid for variations of T_Λ up to about 25 percent of T_{Λ_0}.

For periodic solutions this variance is above and below T_0; and for this case, the 25-percent variation now represents a 50-percent variation. This range of variance is usually sufficient for the thermal design of spacecraft.

It should be noted that the addition of more terms is not usually practical since the labor or calculating the higher modes increases rapidly. Even the inclusion of T_{Λ_3} is usually too involved for practical purposes.

If the fluctuations of temperature are not too large, as compared to (T_{Λ_0}), then the series $T_{\Lambda_0} + T_{\Lambda_1} + T_{\Lambda_2} + \ldots$ converges to T_Λ. However, if the temperature fluctuations become large, as compared to T_{Λ_0}, then the sequence may not converge rapidly enough to be of any real use for thermal design purposes.

M. An Approach to the Passive Thermal Design of a Spacecraft

The purpose of this section is to bring together all the previously presented problems by means of a short discussion of one possible approach to achieve temperature control by a passive thermal design.

The thermal design of a typical spacecraft might be accomplished in the following manner. First one investigates the spin characteristics of the spacecraft. If the vehicle has two spin modes, as previously mentioned, then it is quite probable that only the "long term spin mode" needs to be considered at this stage.

The projected area of the spacecraft, referenced to the long term spin axis, should be averaged over one cycle of spin.

The functions $\mu(\eta)$ and $\hat{\mu}(\eta)$ can be calculated for every external section of the spacecraft. This allows for the calculation of $\hat{\mu}(\eta)_{max}$ and $\hat{\mu}(\eta)_{min}$.

If the spacecraft's orbital elements are known then the quantity ($\cos \theta_0$) can be calculated.

Now, there could be three different temperature conditions to be designed for: mean temperatures, maximum temperatures, and minimum temperatures. The mean temperatures (of the external surfaces) generally govern the temperature of the spacecraft's internal components, such as electrical equipment and structure. The mean temperature, of at least one of the external surfaces, will be governed by the requirements of the spacecraft's electronics.

Equation (34) can be used to determine the orbital conditions which lead to the highest and lowest temperature levels in the internal structure and for the electronics section. If the mission demands that the spacecraft remains in operation for long periods of time it will in general be impossible to predict, before launch, what orientations (with respect to the sun) the spacecraft will encounter. Then, the designer must assume that every possible orientation might be realized. Here, equation (34) immediately leads the thermal designer to conditions which produce the highest and lowest temperatures for the internal structures and electronics package. For the highest mean temperatures the conditions are:

$$\bar{a}(\eta) = \bar{a}(\eta)_{max}$$

$$\frac{L_1}{L} = 1.00$$

$$\zeta = 0.0$$

At first glance it appears that ϵ should be zero; but, under this condition it is impossible to achieve 100 percent time in sunlight ($L_1/L = 1$). Hence ϵ is chosen to be the smallest value which still permits (L_1/L) to equal unity.

For the lowest mean temperatures, the conditions are

$$\hat{\mu}(\eta) = \hat{\mu}(\eta)_{min}$$

$$(L_1/L) = (L_1/L)_{min}$$

$$\zeta = \pi; \epsilon = 0$$

These two sets of conditions will roughly determine the quantity (a_{s_1}/Σ_1) for the ith section. In general there is no requirement which governs the values of a_s and Σ except the following considerations:

If a_s and Σ are large, then temperature fluctuations on the external surfaces are large. If a_s and Σ are very small, then the possible error in (a_s/Σ) becomes large (because small values of a_s and Σ cannot be measured accurately) so absolute values of a_s and Σ are determined by a trade-off, values from 0.2 to 0.3 are usually acceptable. It should be remembered here that the individual case (heat radiators for example) can alter these requirements.

When the selection of a_s and Σ is made it will be clear whether or not a passive thermal control scheme is possible. If it is not possible to achieve the proper temperatures by a passive scheme, it should still be developed as far as possible since this will lessen the demands made on the active thermal control apparatus.

Once the $a_{s,i}$ and Σ_1 values have been chosen, tentatively, then solutions for the temperature distributions on the external surfaces can be found. These distributions refer to the case when each section is assumed to be isolated from its neighbors and can be calculated by the methods presented in this thesis. An exception, of course, is for the case of multiple reflections of light between adjacent surfaces. The previously mentioned solutions may not yield accurate temperature values where the assumption of isolated parts is in error. Therefore these procured can only be used to decide how sections of the spacecraft should be divided when solving the system of equations introduced by equation (26). This approach makes it possible to idealize the spacecraft into the minimum number of sections necessary to fulfill the assumptions made in arriving at equation (26).

The earlier selection of $a_{s,i}$ and Σ_1 values was made on the assumption that the spacecraft was spinning in its long-term spin mode. Should the spacecraft have two spin modes, then the desirable temperatures can be achieved during the short-time spin mode by restricting the allowable launch times.

VII. DISCUSSION AND RESULTS

A few of the problems which arise in the thermal design of spacecraft have been presented. In the literature it is commonly assumed that the nonlinear heat-transfer term (T^4) can be replaced by a linear approximation. This, unfortunately, omits the nonlinear characteristics of the solution and offers no method by which more accurate solutions can be obtained. For the problems studied in this thesis $T_0 + T_1$ corresponds exactly to the linearized solutions so often found in the literature.

The approach used in this thesis is, in reality, a method of successive approximations. Although T_0 has been chosen as a constant, this is not a necessary condition; in fact, the more closely T_0 approaches to T the quicker the sequence (T_0), $(T_0 + T_1)$, $(T_0 + T_1 + T_2) + (\ldots)$ converges. In most cases, however, when T_0 is a variable, the calculation of the higher modes is extremely difficult and the author feels that a realistic compromise between complexity and the rapidity of convergence is afforded by taking T_0 to be a constant.

The numerical examples presented in this thesis were chosen because they primarily emphasize properties peculiar to the different problems.

In the discussion that follows, the more important ideas from each example are summarized, the discussion begins with section A.

In section A the classical heat-transfer equation is presented for three cases commonly confronted in the thermal design of

spacecraft. The first case occurs when the "space mean temperatures," of different sections of a spacecraft, are needed. The equation governing space mean temperatures, for any section of a spacecraft, is found to be a first-order nonlinear expression in T^4, when T is temperature in degrees Rankine.

The second case investigated is that of a spacecraft with thin external shells which have uniform temperatures throughout the shell thickness. The equation governing this type of heat flow is found to be second order in two space variables, first order in the time variable, and nonlinear in T^4, where T is again the temperature in degrees Rankine.

The third case given is that where no simplifying assumptions can be made. This type of heat flow is governed by the well-known "Diffusion Equation," with nonlinear boundary conditions.

Section B presents a simplified derivation of the radiation transfer equation. It is shown that the model used in section B produces diffuse radiation. All the radiative heat transfer investigated in this thesis is assumed to be diffuse.

The problem of calculating projected areas of spacecraft is attacked in section C. The projected area for a cone, with an arbitrary half angle, is calculated for the cone spinning about its axis of symmetry, and for the cone spinning about an axis normal to the axis of symmetry. It is stated in this section that the cone's area projections can be represented by fourier cosine series.

In section D, the albedo and earth thermal energy, incident on a spacecraft of arbitrary shape, is calculated by the use of a

fourier cosine series. The projected area of the arbitrary body is expressed as a cosine series and the integral governing the radiant heat transfer (between the earth and spacecraft) is integrated. Also, it is shown that heating of a spacecraft from the earth's albedo can be approximated by the equation describing the earth thermal energy incident on the vehicle.

The orientation angles, necessary to describe the different heat fluxes incident on a spacecraft, are calculated in section E by matrix methods. Also, simplified expressions for the orientation angles are given to aid the reader in visualizing a spacecraft's motion relative to the sun and the earth.

In section F, a 'generalized finite difference equation' is given for the spacecraft's heat transfer. It is pointed out that this system of equations usually requires integration by digital computers and, in these cases where large temperature variations occur on the spacecraft's external surfaces, the labor may become prohibitive.

A parametric study of orbital heating is given in section G. This section presents a simplified study of albedo and earth thermal heating, on an arbitrarily shaped spacecraft, which clearly points out the most important variables connected with heat transfer between the earth and the spacecraft. Also, an expression is obtained which can be used to calculate the average equilibrium temperature for any isolated section of the spacecraft.

A method useful for solving nonlinear differential equations is given in section H. This method is introduced by assuming that

an approximate solution is known. The exact solution is then assumed to be the sum of the approximate solution plus a small perturbation value. This approach is pursued until it becomes evident that the exact solution can be obtained in the form of an infinite sequence of successive approximations. Finally, a method is suggested which allows direct determination of the linear differential equations which govern each successive approximation. No convergence proof for the infinite sequence is attempted.

In section I, a solution for the temperature time history of a spacecraft, with uniform temperatures, is established. From the solution it is found that the time-averaged temperature, of a spacecraft, is reduced by large temporal temperature fluctuations. A parameter, which governs the normalized temperature fluctuations is also found.

Temperature solutions are found for a cylinder, which has both temporal and space (temperature) fluctuations in section J. It is established from the solution that both the temporal and space temperature fluctuations reduce the average temperature of the cylinder. Finally, it is shown how the temperature of a body, enclosed by a second body, will tend to two different temperatures dependent on how heat from the first body is transferred to the second body. This last fact shows that neither the temperature of a spacecraft's internal structure nor its electronic package can be calculated without some knowledge of the (temperature) fluctuations on the spacecraft's external surfaces.

The perturbation method, used in this thesis, to solve the nonlinear differential equations, is used to obtain the solution of a linear

differential equation with nonlinear boundary conditions (in section K). The method is general, in its nature, and can be used to solve many other nonlinear problems. Its main usefulness lies in the fact that nonlinear problems, having no small perturbation parameter, can be solved by it.

Section L gives a comparison between the exact and approximate solutions to a nonlinear differential equation. The sole purpose of this section is to (roughly) indicate the accuracy of the perturbation scheme employed in this thesis. It is necessary that the comparison between the exact and approximate solutions be made since no convergence proof of the perturbation method has been established here. The numerical example given in section L suggests that the perturbation method employed through accuracy of

$$T_0 + T_1 + T_2$$

is acceptable for

$$T_1 \leq \frac{1}{4} T_0$$

Finally, section M outlines an approach to the problem of thermal design for spacecraft which use passive temperature control techniques.

Not all the problems encountered in the thermal design of spacecraft are discussed in this thesis. For example, the problem of multiple reflections between sections of a spacecraft has been carefully avoided. If one is interested in this problem, he should consult reference 3. The problem of multiple reflections is usually encountered when the radiation coefficients ($R_{i,j}$) are being calculated.

Another problem commonly encountered in thermal design and not covered here, is the high resistance to conductive heat flow at the junctions between two bodies. If two bodies are held together by interface contact pressure only then their common boundary will, in general, have a very high resistance to conductive heat flow. The mode of heat transfer through these interfaces is not well understood and their heat-transfer characteristics are usually determined experimentally. Unfortunately, such experimental data are unreliable because of data scatter and the general inability to reproduce experimental results. The usual method of avoiding such interface connections is to resort to welding or bonding techniques. The silicon grease used for 'high vacuum' applications can also be used to greatly reduce interface resistance to heat flow. Interface resistance to conductive heat flow must be considered when calculating the 'conductive heat-transfer' coefficients ($h_{i,j}$).

There are many other problems, of considerable importance in spacecraft thermal design, which cannot be mentioned here because of space limitations.

As a conclusion, some of the more important problems encountered in the spacecraft thermal design (but not realistically considered in the literature) have been solved without reference to a specific body shape whenever possible. Also, some solution methods for nonlinear problems (not having small perturbation parameters) are given.

VIII. ACKNOWLEDGMENTS

The author wishes to express his appreciation for the permission to use material in this thesis that was obtained from a research project conducted at the Langley Research Center of the National Aeronautics and Space Administration.

In particular, the author wishes to express his gratitude to Mrs. Beverly Latimer for the programing and running of the temperature time histories shown in figures 18(a) through 18(f); and to

for evaluating the albedo integrals.

The author also wishes to express his gratitude to

for preparing the thesis figures, and to for the many long hours spent in typing the manuscript.

He also wishes to thank , head of the Aerospace Engineering Department for his advice, patience, and open mind during the preparation of this thesis.

IX. REFERENCES

1. Hibbs, A. R.: The Temperature of an Orbiting Missile. Progress Rep. No. 20-294 (Contract No. DA-04-495-Ord 18), Jet Propulsion Lab., C.I.T., Mar. 28, 1956.

2. King-Hele, D. G., and Gilmore, D. M. C.: The Effect of the Earth's Oblateness on the Orbit of a Near Satellite. Tech. Note No. G.W. 475, British R.A.E., Oct. 1957.

3. Eckert, E. R. G., and Drake, R. M., Jr.: Heat and Mass Transfer. McGraw-Hill Book Company, 1959.

4. McLachlan, N. W.: Ordinary Non-Linear Differential Equations in Engineering and Physical Sciences. Oxford at the Clarenden Press, 1958.

5. Woods, F. S.: Advanced Calculus. Ginn and Company, 1954.

6. Charnes, A., and Raynor, S.: Solar Heating of a Rotating Cylindrical Space Vehicle. ARS Jour., vol. 30, No. 5, May 1960, pp. 479-484.

7. Katzoff, S.: The Electromagnetic Radiation Environment of a Satellite, Part I. Range of Thermal to X-Radiation. Technical Note D-1360, Langley Research Center.

8. Hastings, Earl C., Jr.: The Explorer XVI Micrometeoroid Satellite Supplement II, Preliminary Results for the Period March 3, 1963, Through May 26, 1963. NASA TM X-899, Langley Research Center, 1963.

9. Nichols, Lester D.: Surface Temperature Distributions on Thin-Walled Bodies Subjected to Solar Radiation in Interplanetary Space. Technical Note D-584, Lewis Research Center, 1961.

The vita has been removed from the scanned document

TABLE 1.- EVALUATION OF INTEGRALS APPEARING IN THE ALBEDO CALCULATIONS

	θ_0 (deg)								
	10	20	30	40	50	60	70	80	
F_{00}, F_{22}, F_{45}	0.01126	0.04927	0.11747	0.21609	0.34223	0.49048	0.65397	0.82567	1.00000
F_{10}, F_{34}	.01119	.04793	.11012	.19184	.28251	.36921	.43965	.48473	.50000
F_{11}, F_{35}	.00119	.00813	.02227	.04027	.05525	.05946	.04780	.02212	.00000
F_{20}, F_{43}	.01111	.04664	.10339	.17127	.23678	.28804	.31906	.33152	.33333
F_{21}, F_{44}	.00014	.00262	.01408	.04482	.10544	.20243	.33490	.49414	.66666
F_{23}, F_{48}	.00117	.00779	.02021	.03368	.04129	.03812	.02477	.00825	.00000
F_{30}	.01090	.04306	.08640	.12586	.15147	.16299	.16621	.16665	.16666
F_{31}	.00014	.00252	.01288	.03809	.08115	.13717	.19357	.23498	.25000
F_{32}	.00116	.00747	.01836	.02829	.03122	.02521	.01387	.00379	.00000
F_{33}	.00002	.00065	.00391	.01197	.02402	.03425	.03393	.01833	.00000
F_{40}	.01097	.04421	.09159	.13875	.17355	.19219	.19877	.19995	.20000
F_{41}	.00014	.00243	.01180	.03252	.06322	.09585	.12029	.13156	.13333
F_{42}	.00000	.00019	.00227	.01230	.04221	.10658	.21460	.36258	.53333
F_{46}	.00115	.00717	.01670	.02587	.02391	.01721	.00839	.00208	.00000
F_{47}	.00002	.00062	.00351	.00981	.01738	.02091	.01637	.00617	.00000

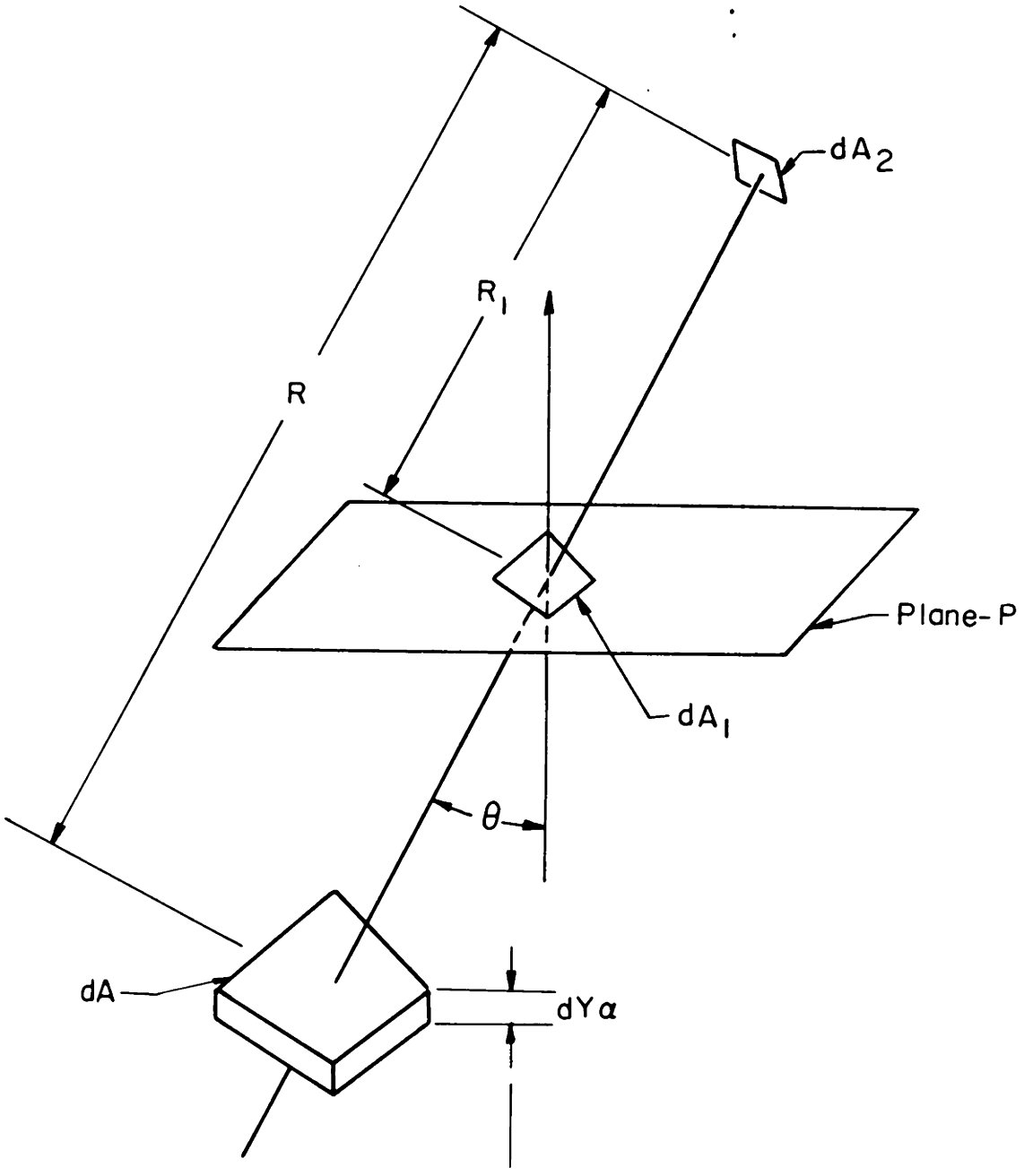

Figure 1.- Sketch showing radiative heat transfer.

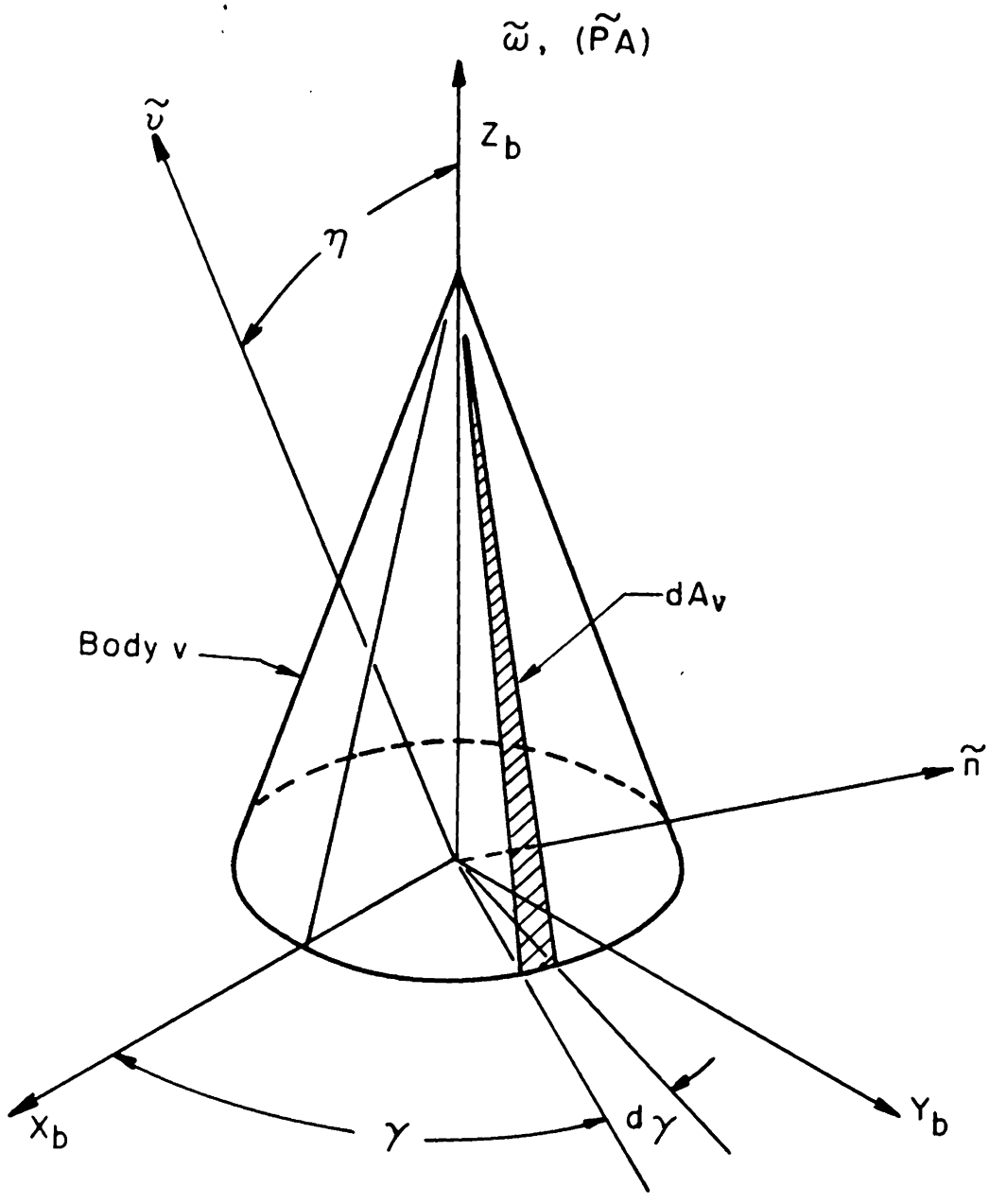

The spin vector $(\tilde{\omega})$ is aligned with the rotational axis of symmetry $(\tilde{PA})$.

Figure 2.- Sketch relating a cone to a viewer $(\tilde{v})$.

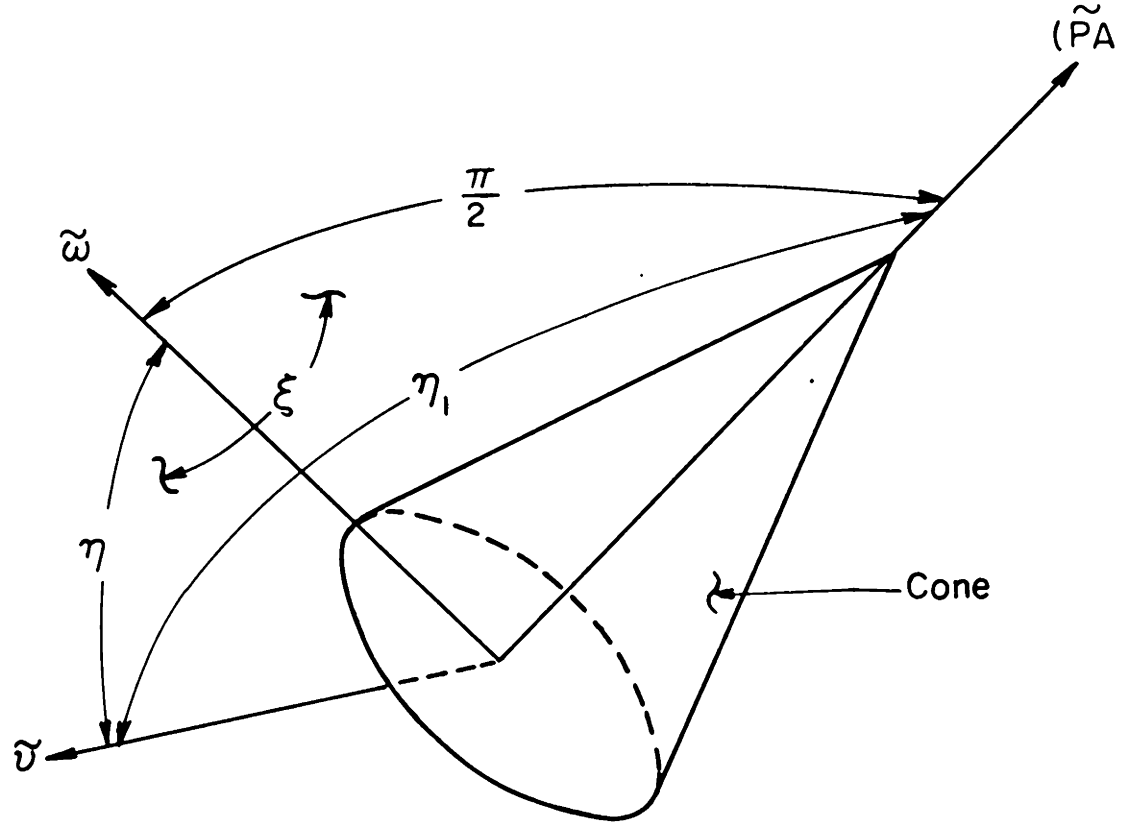

Figure 3.- Sketch showing the relation between η, η_1, and ξ.

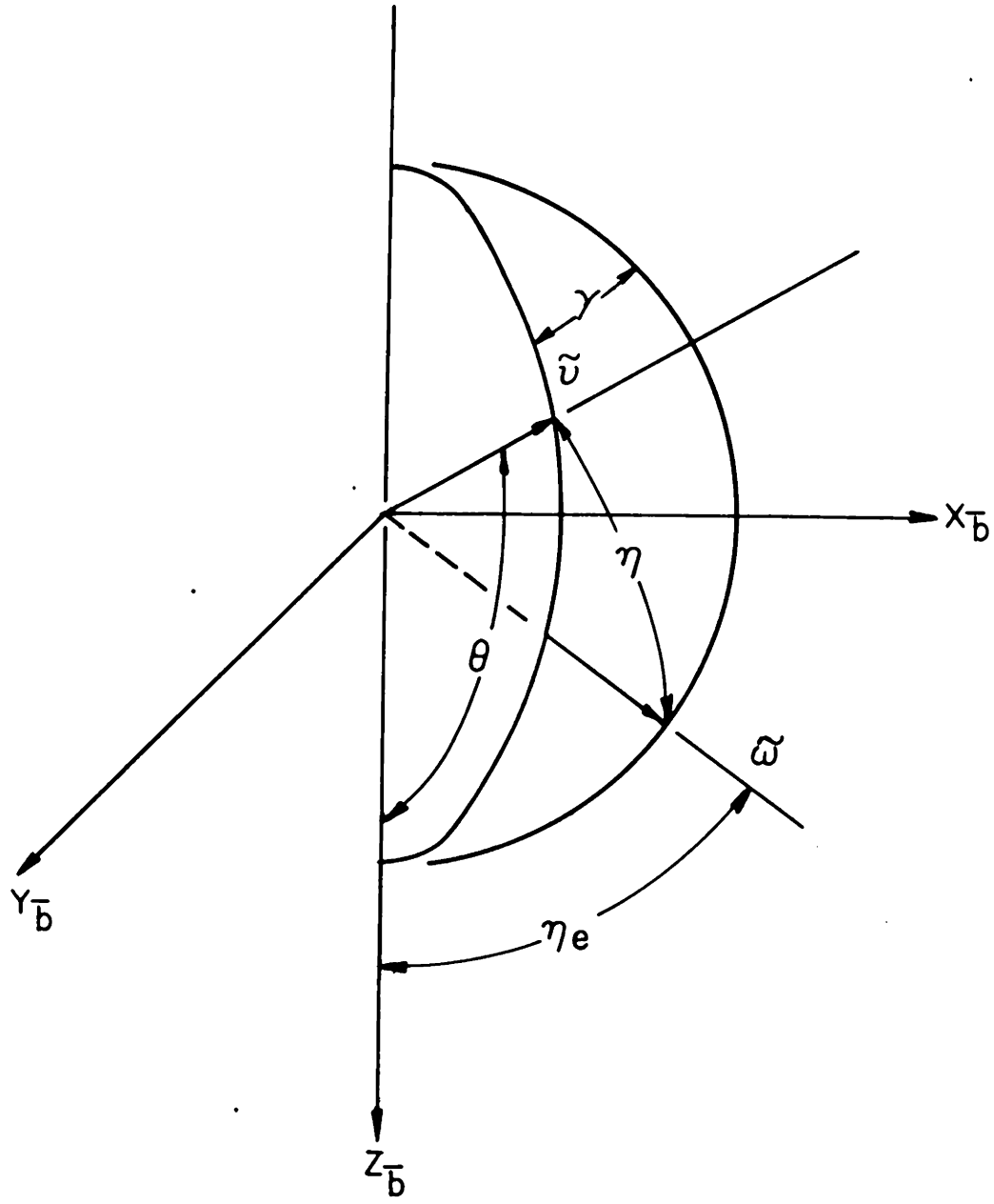

Figure 4.- Sketch relating earth and viewer to the spacecraft spin vector.

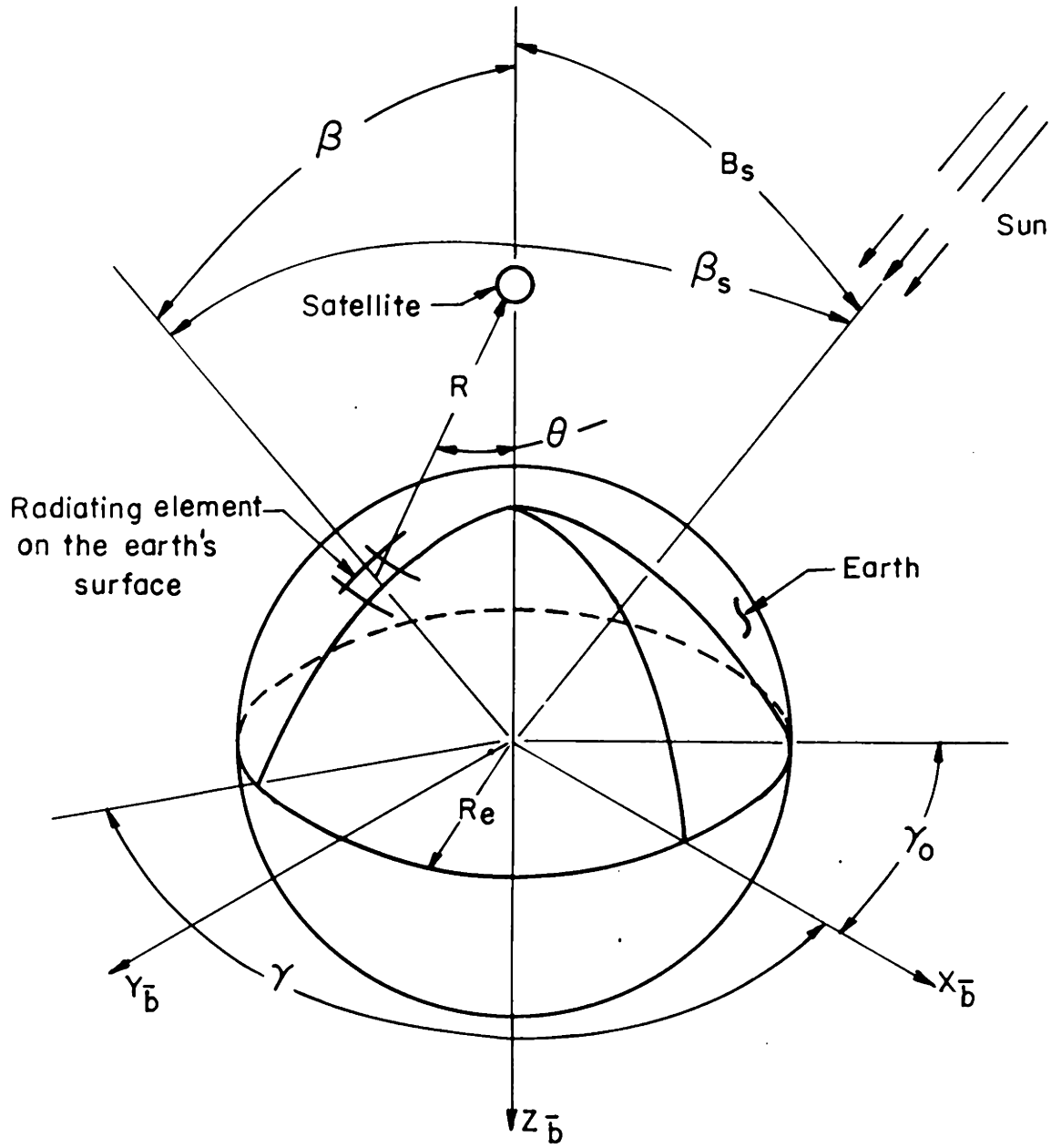

Figure 5.- Sketch relating a satellite to the earth.

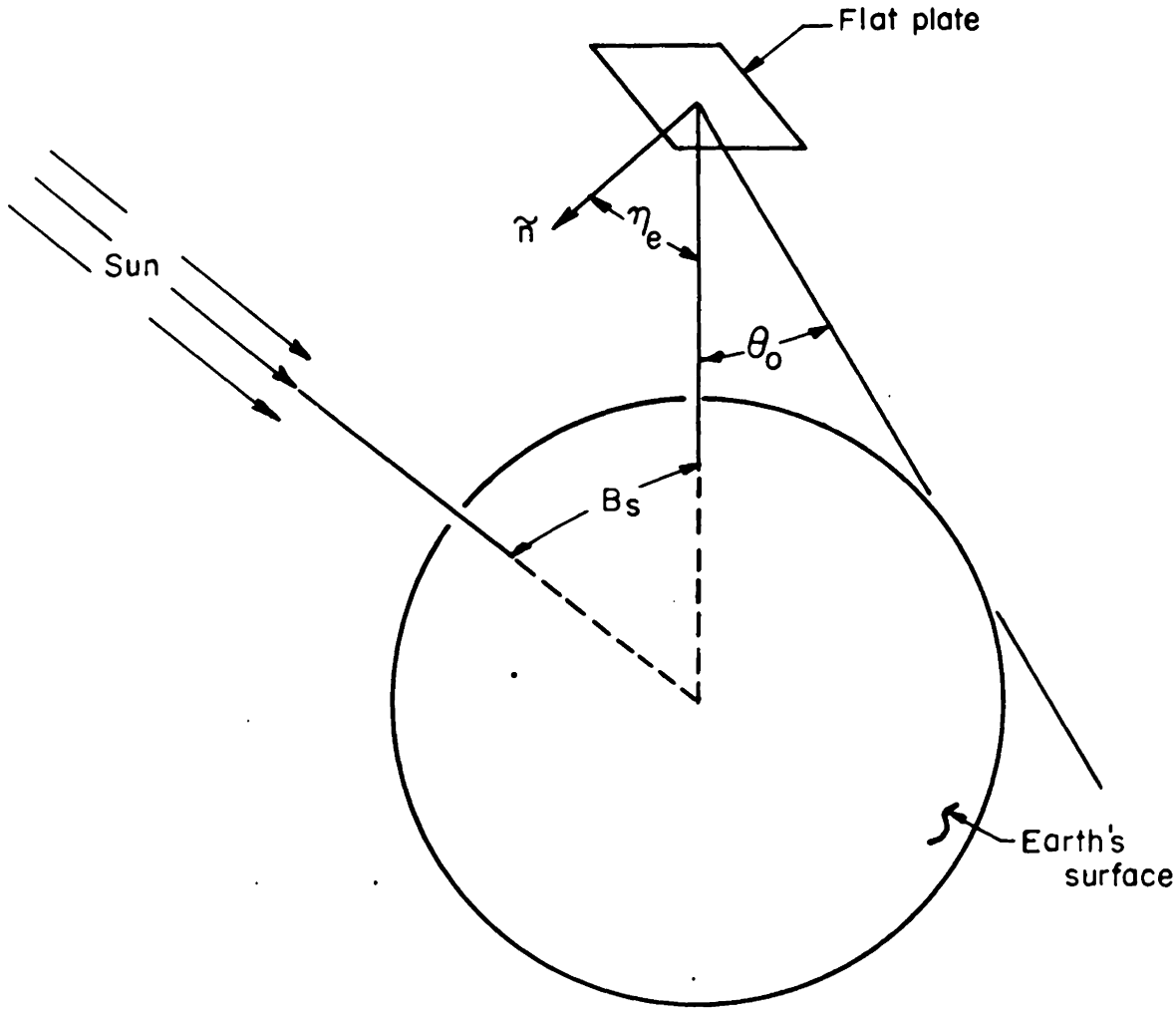

Figure 6.- Sketch showing a flat plate relative to the earth.

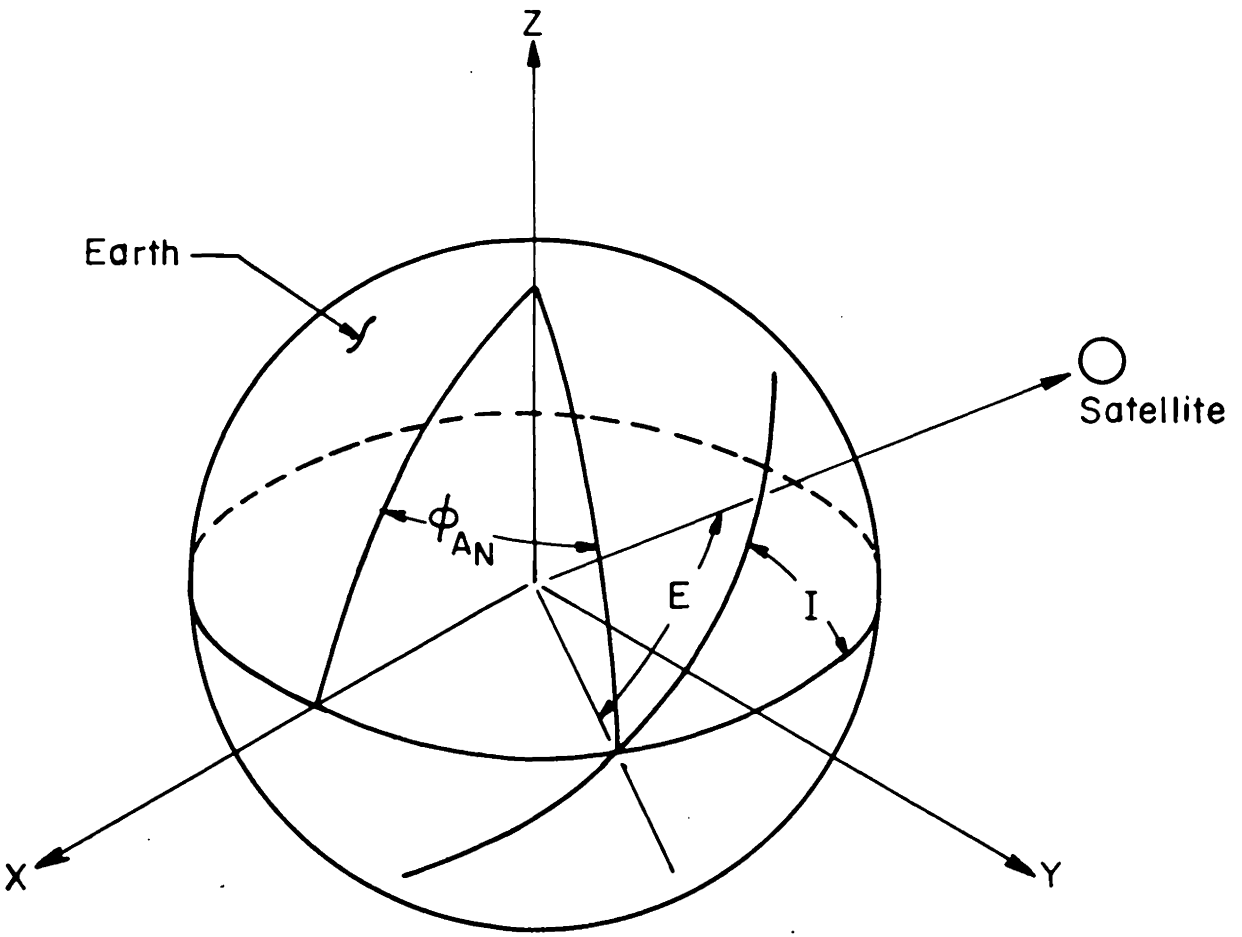

Figure 7.- Sketch relating an orbit plane to the earth.

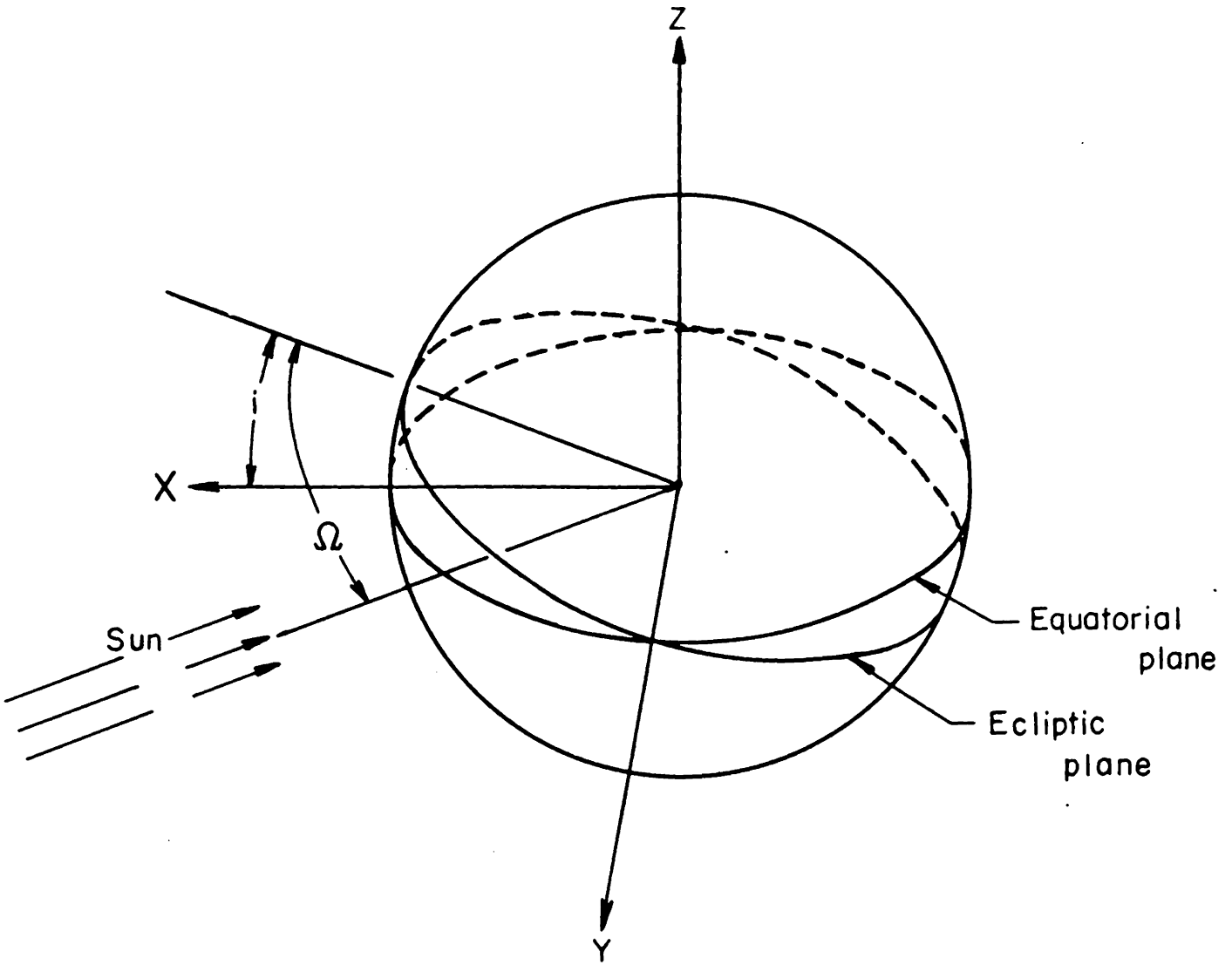

Figure 8.- Sketch showing sun relative to inertial coordinate system.

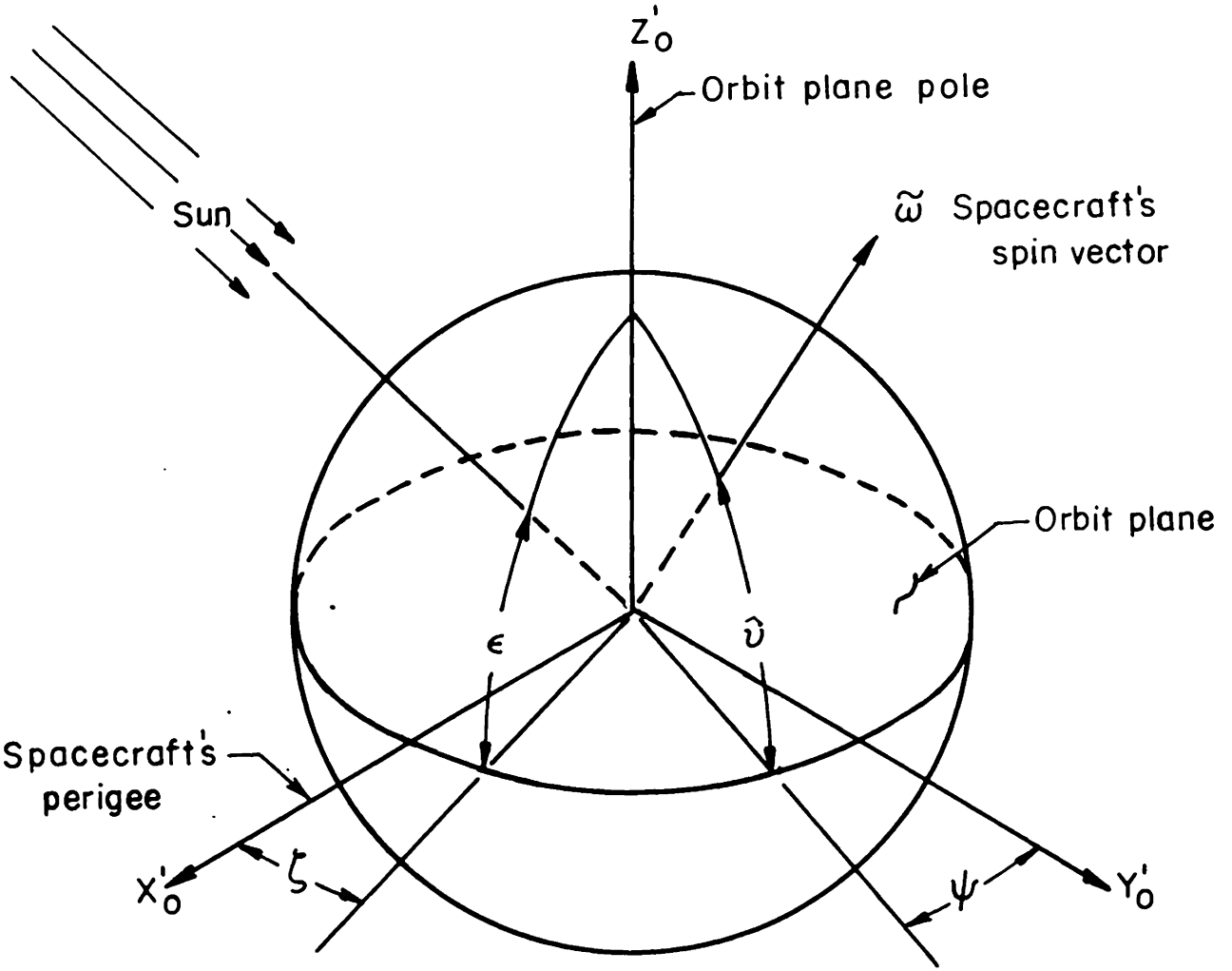

Figure 9.- Sketch showing the (X_0', Y_0', Z_0') coordinate frame.

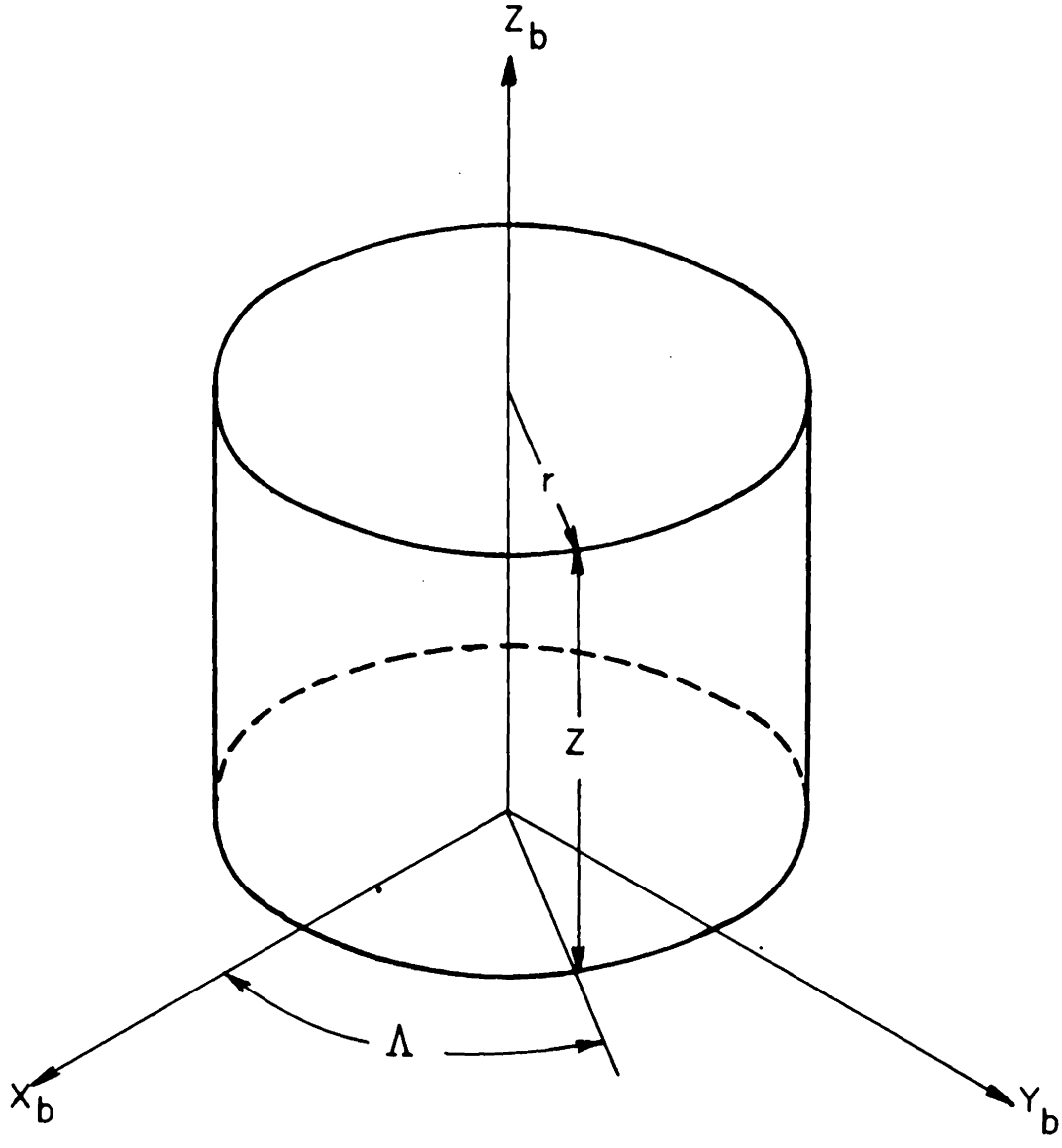

Figure 10.- Sketch showing cylindrical polar coordinate frame.

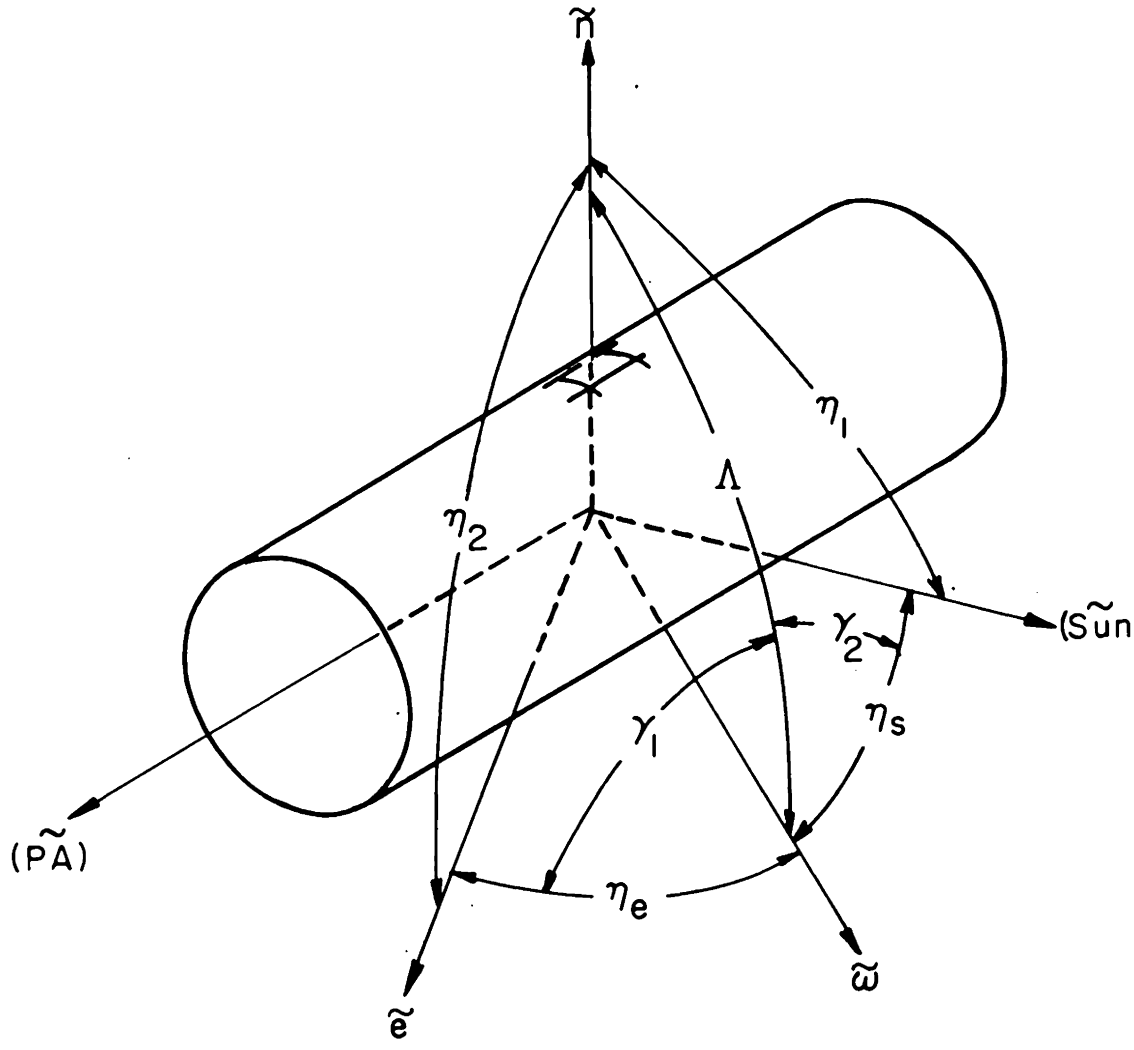

Figure 11.- Sketch relating a surface element on a cylinder to the earth and sun.

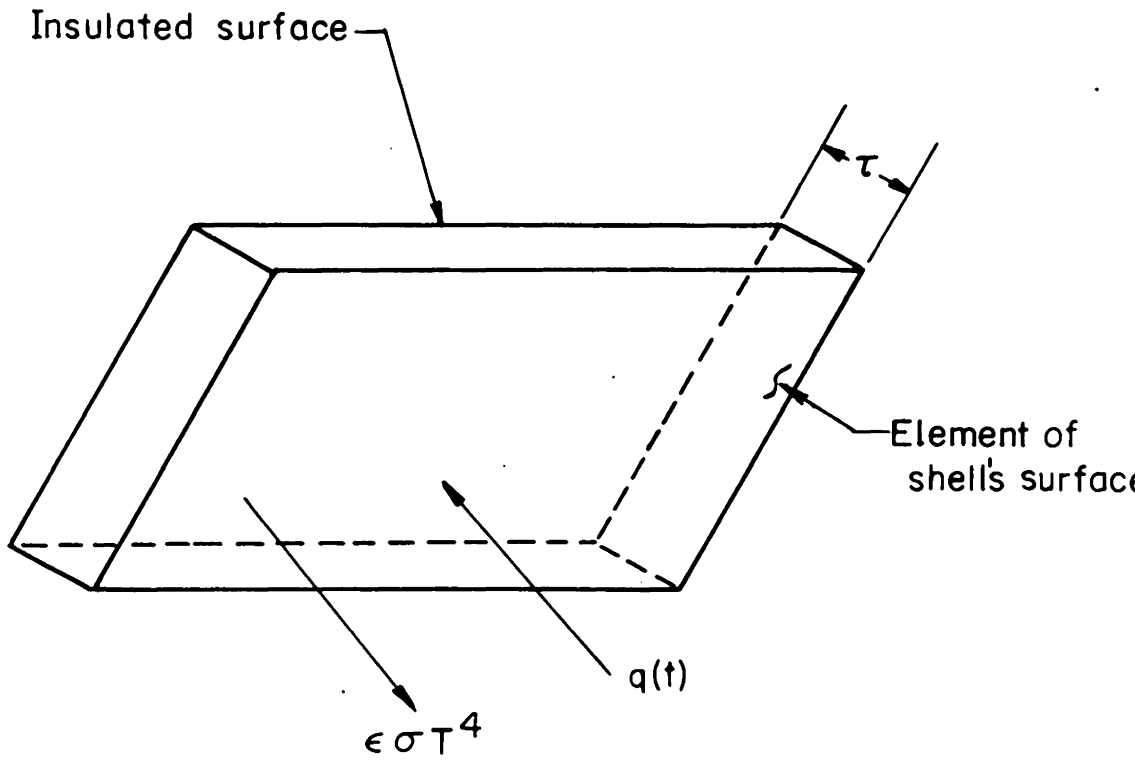

Figure 12.- Sketch showing an element of a shell's surface.

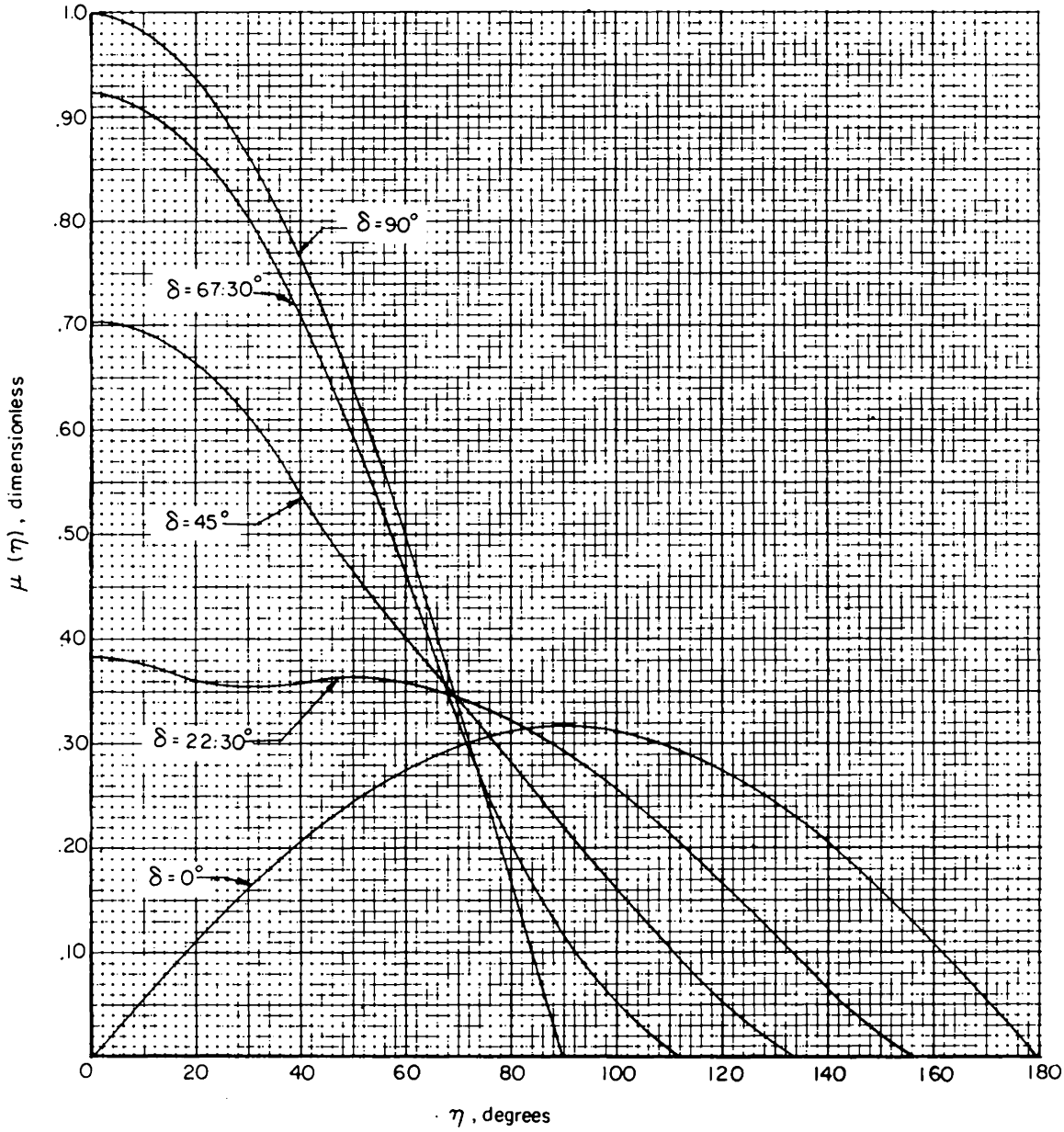

(a) Unit area projections of various cones, in short-term spin mode, versus view angle η.

Figure 13.- Area distributions for cones of various half angles.

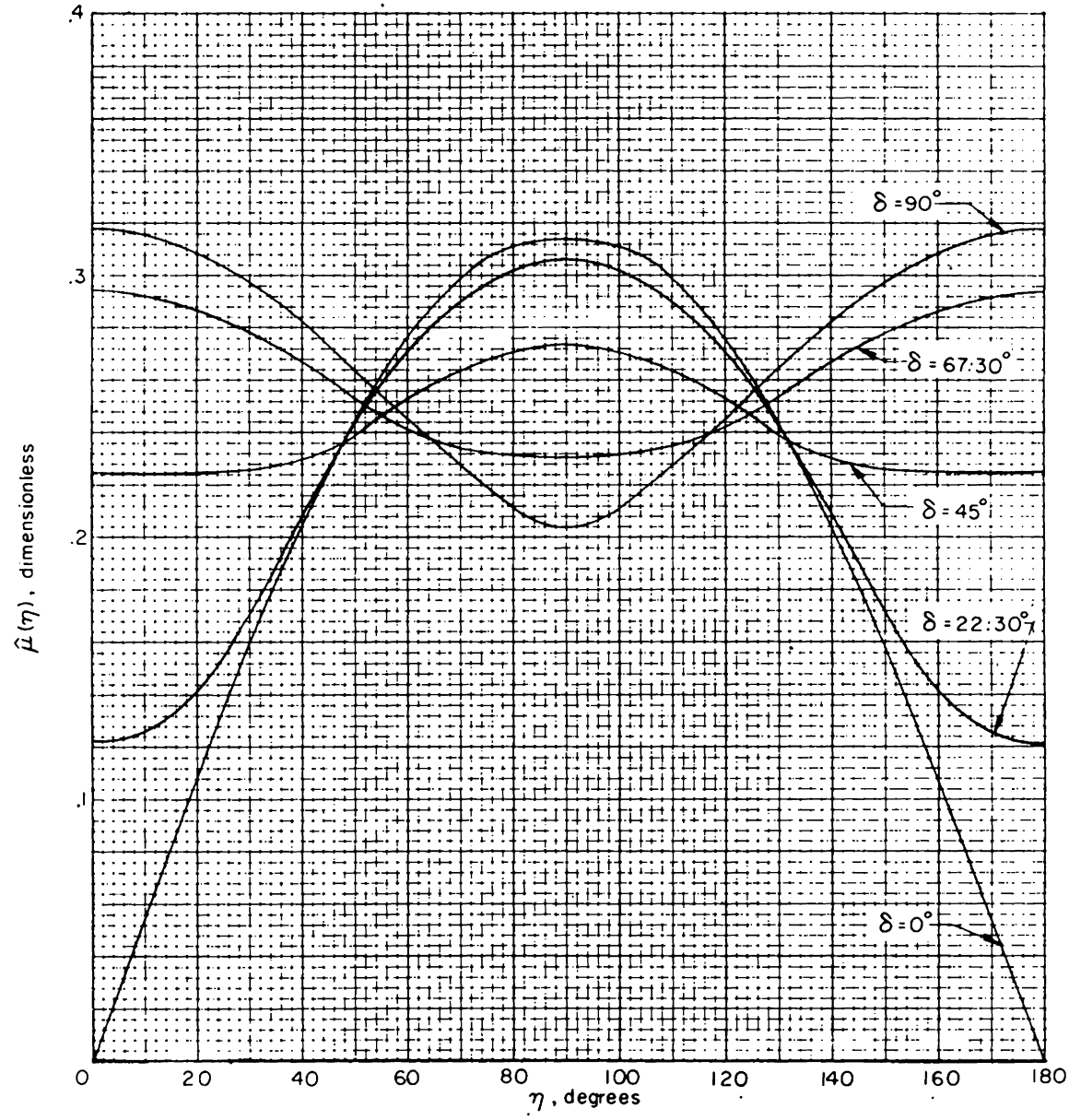

(b) Unit area projections of various cones, in long-term spin mode, versus view angle η.

Figure 13.- Concluded.

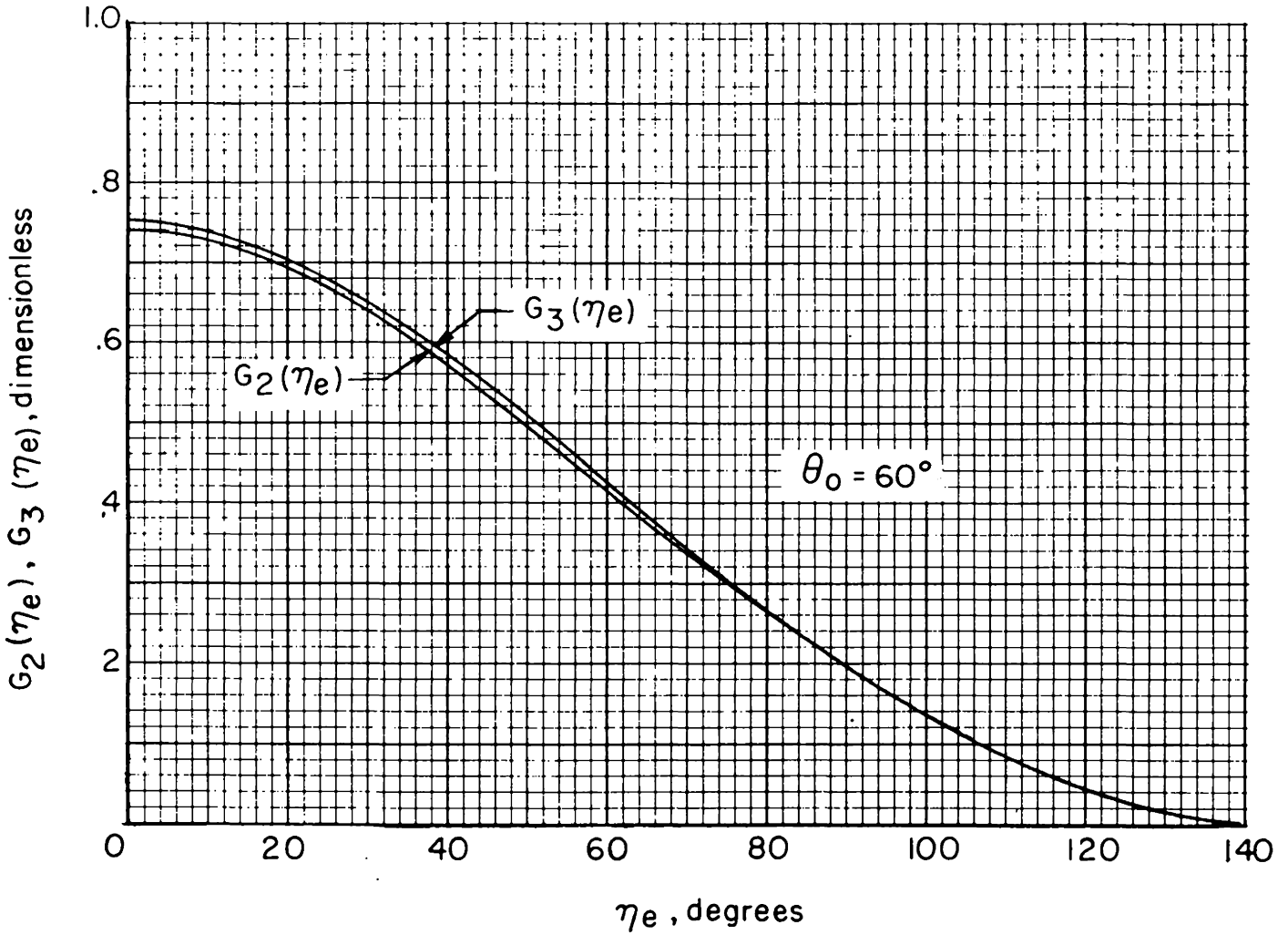

(a) Comparison of earth thermal heat and the even part of albedo heating.

Figure 14.- Earth thermal and albedo heat on a unit area flat plate.

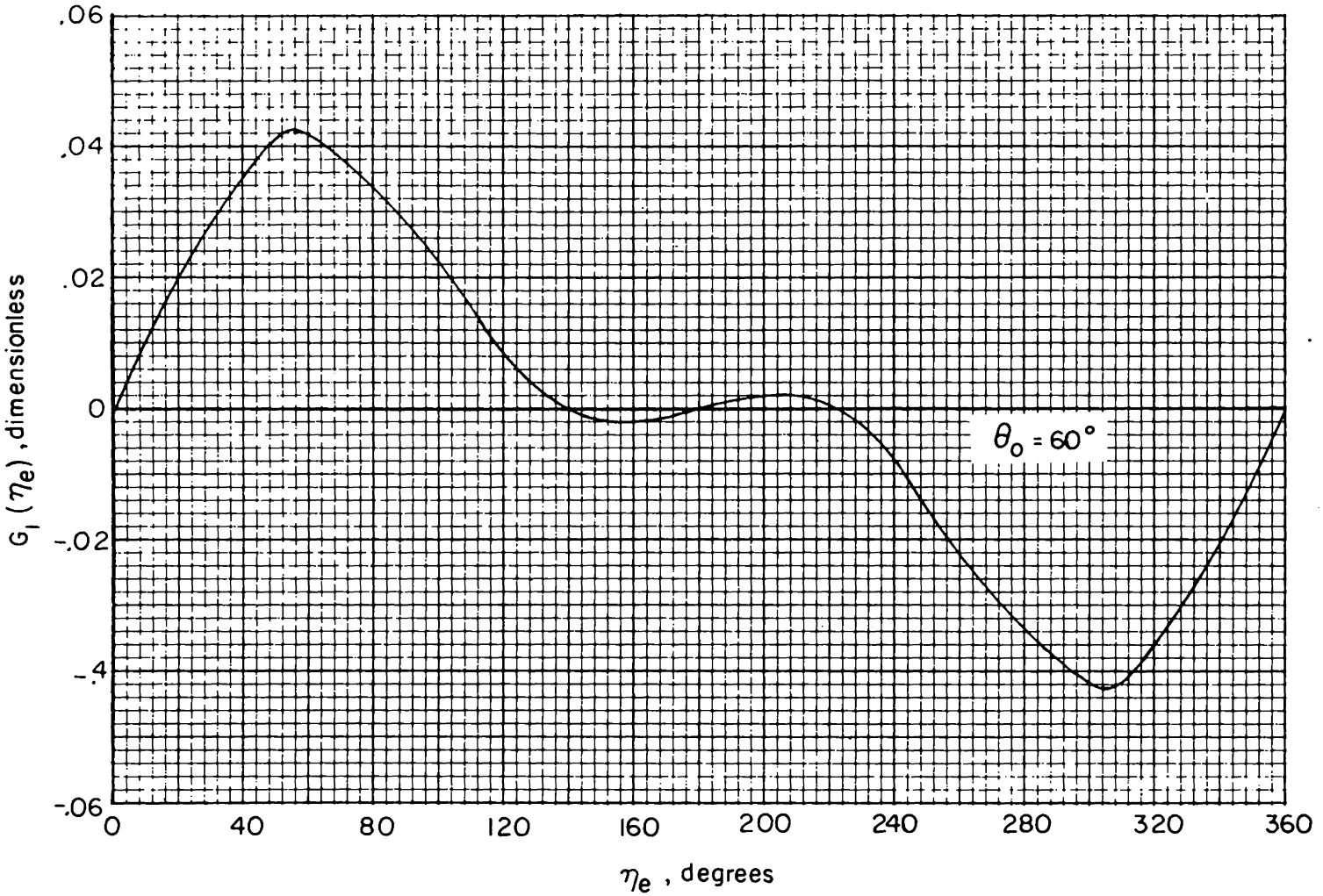

(b) Odd part of albedo heating.

Figure 14.- Concluded.

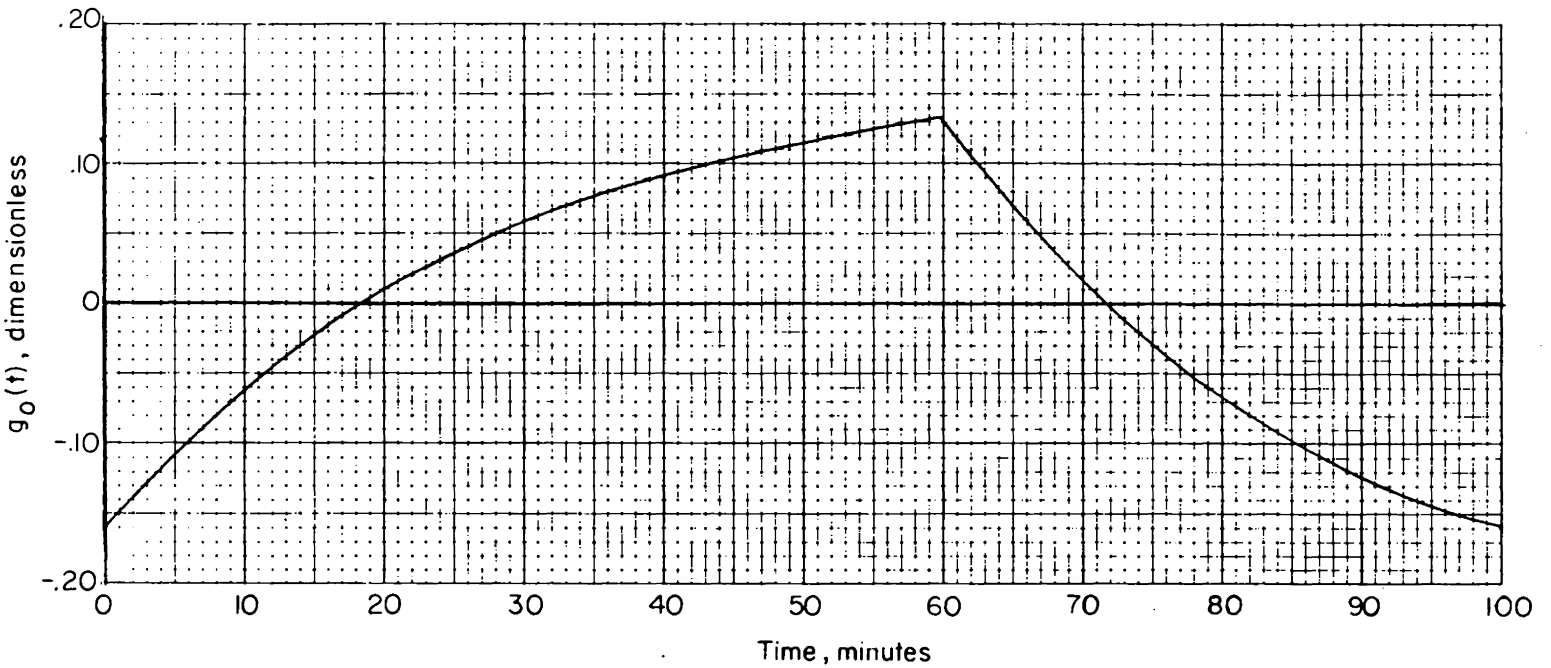

(a) $g_0(t)$ versus time.

Figure 15.- Illustration of the time-dependent temperature distributions.

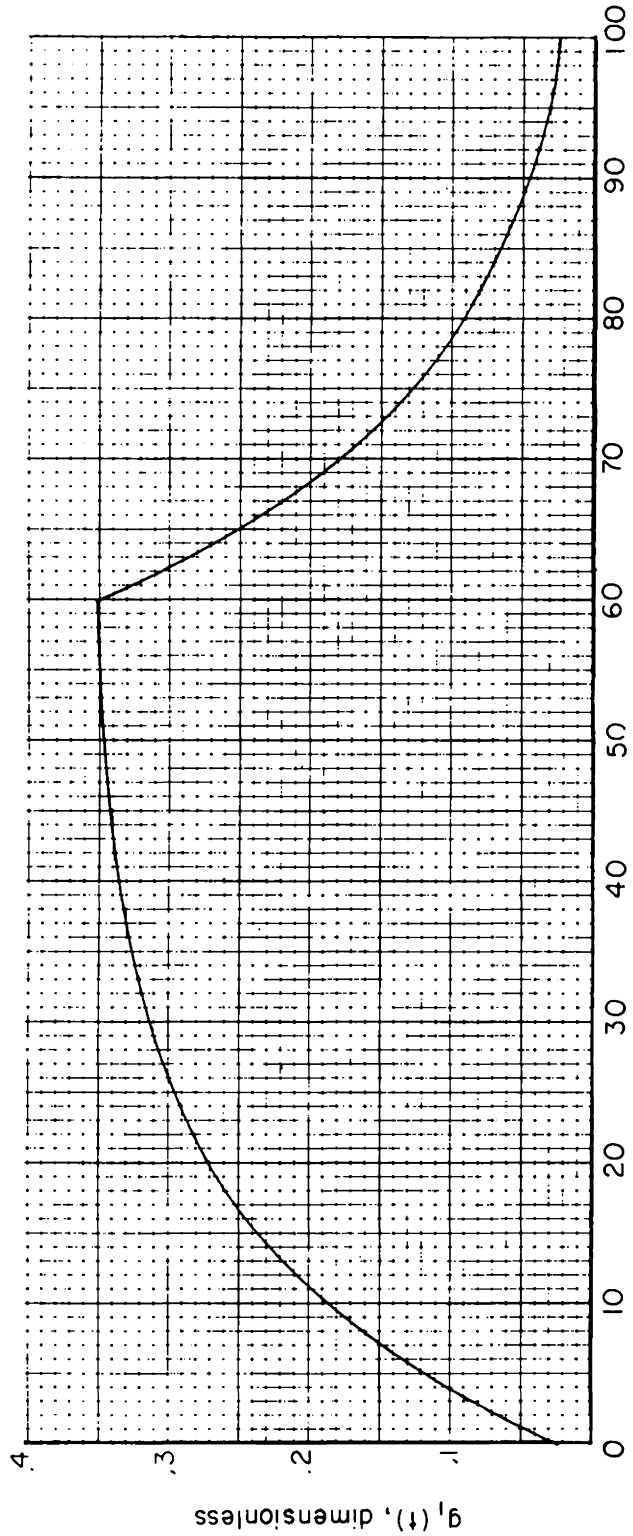

(b) $g_1(t)$ versus time.

Figure 15.- Continued.

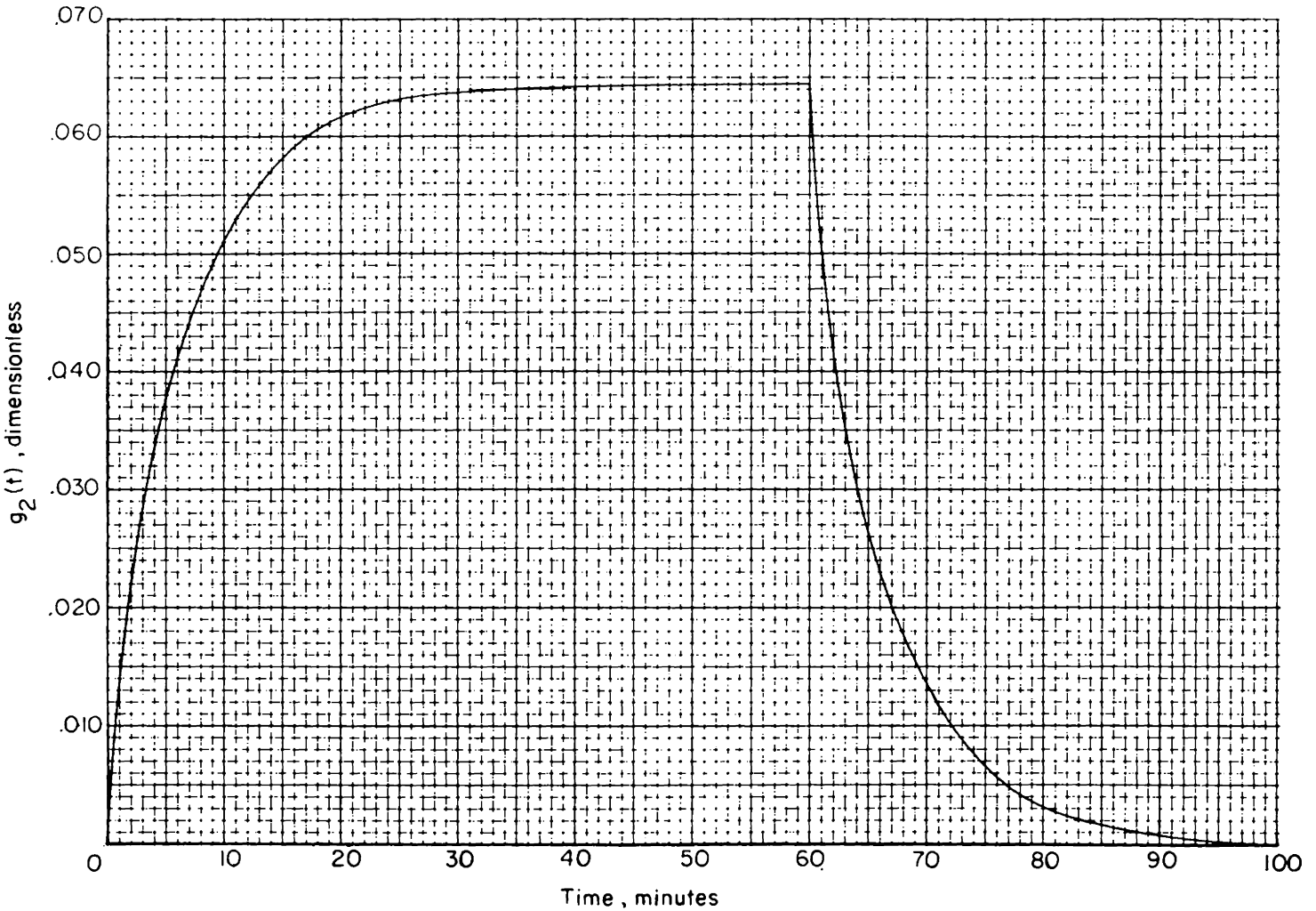

(c) $g_2(t)$ versus time.

Figure 15.- Continued.

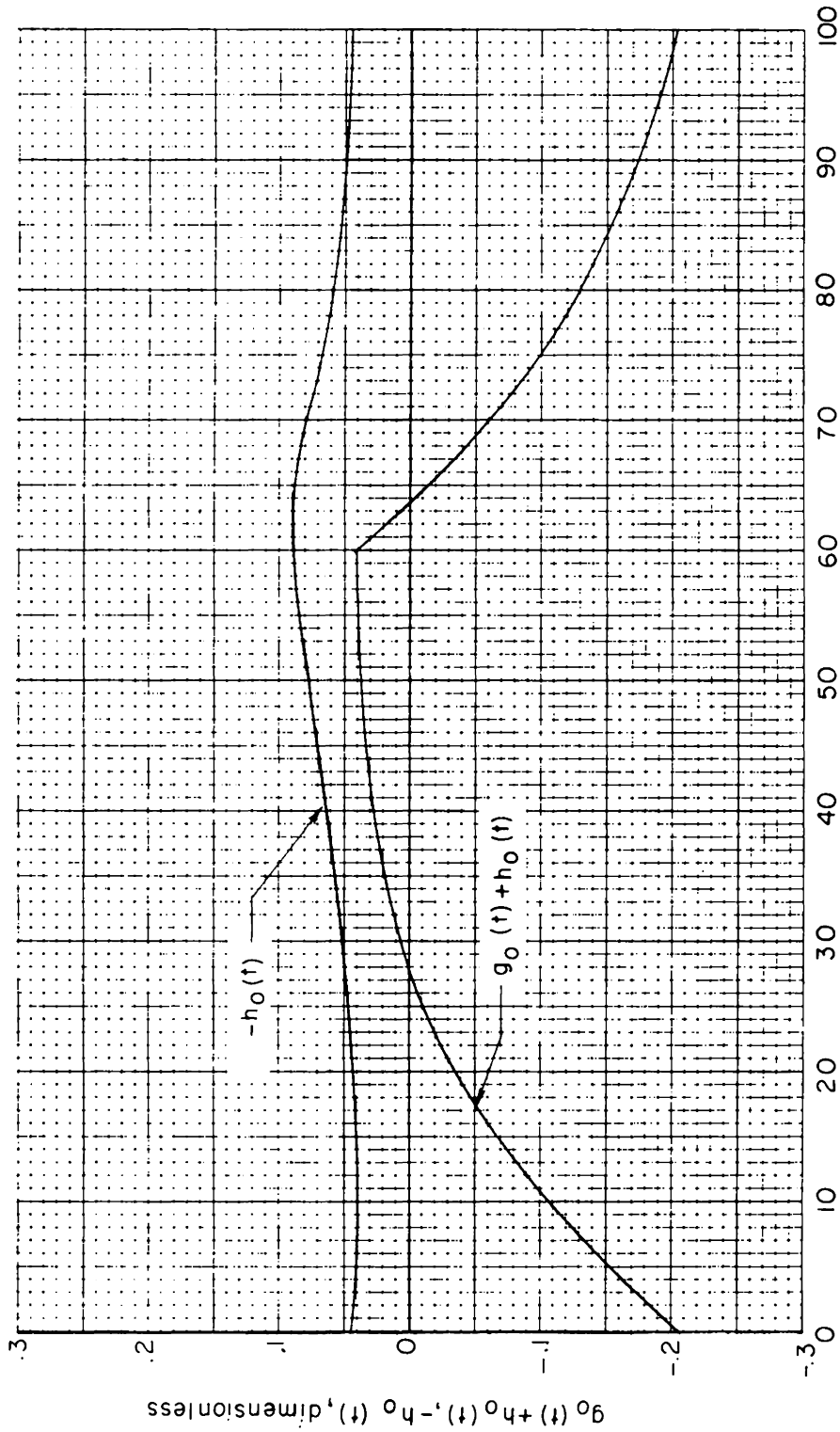

(d) $g_o(t) + h_o(t)$ and $h_o(t)$ versus time.

Figure 15.- Continued.

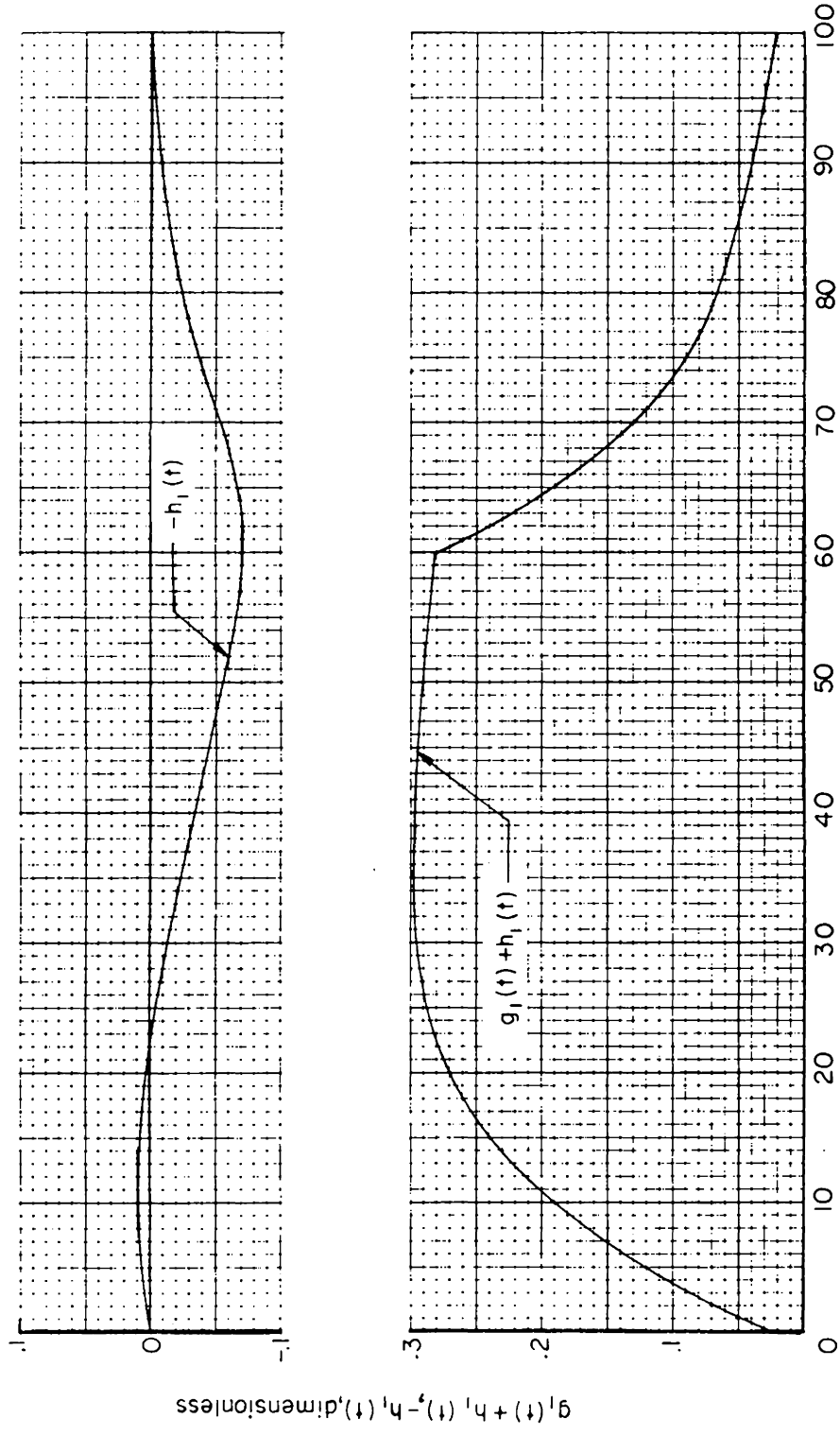

(e) $g_1(t) + h_1(t)$ and $h_1(t)$ versus time.

Figure 15.- Continued.

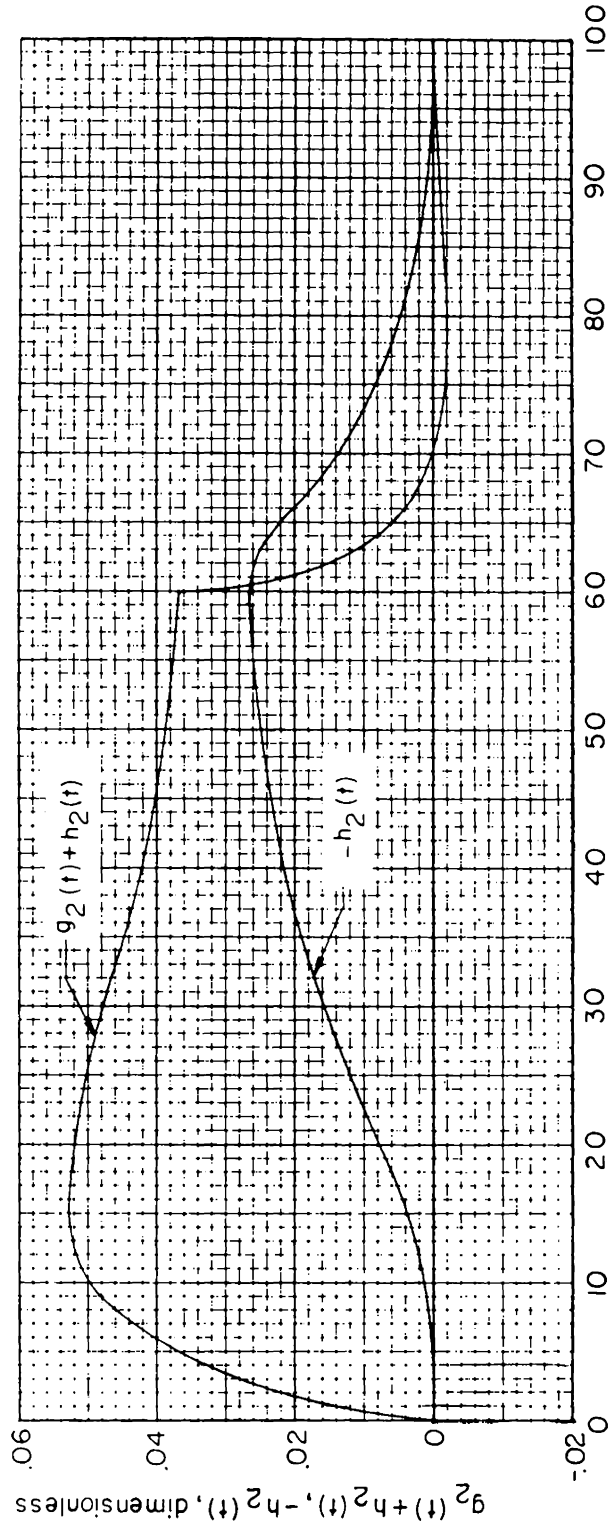

(f) $g_2(t) + h_2(t)$ and $-h_2(t)$ versus time.

Figure 15.- Continued.

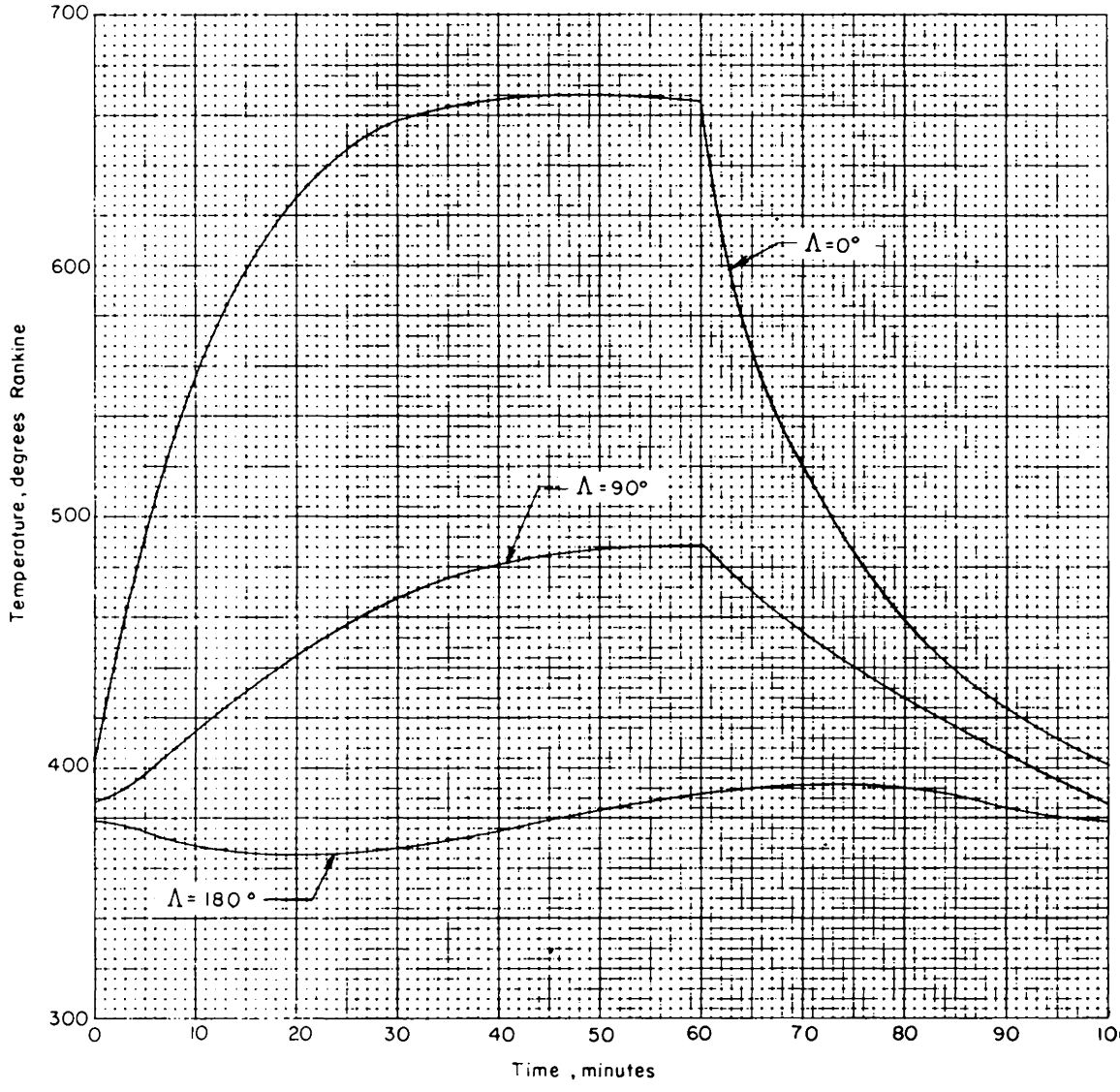

(g) Temperature time history at several positions around a cylinder exposed to periodic solar heating.

Figure 15.- Concluded.

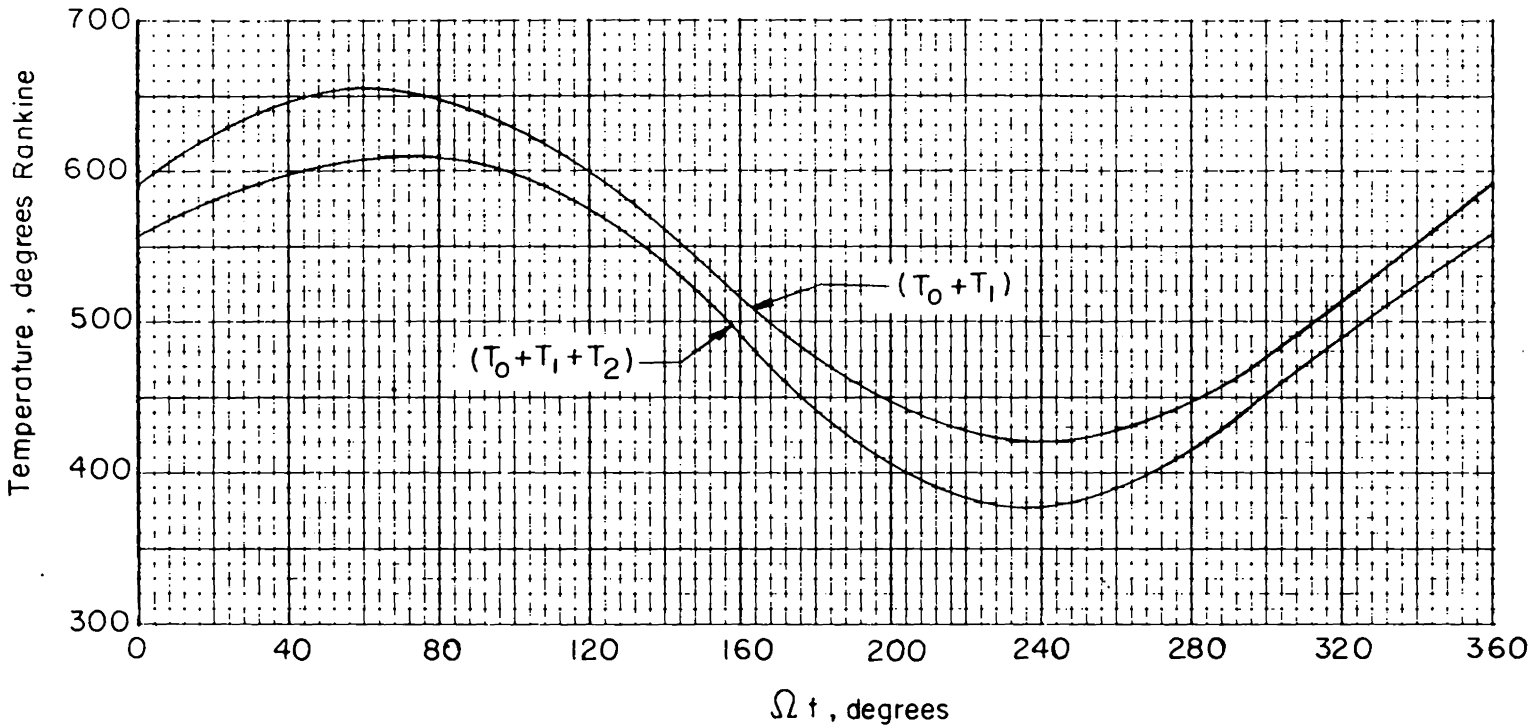

(a) Temperature time history on the back face of a plastic block exposed to thermal radiation.

Figure 16.- Temperature time history on a plastic block with periodic radiative heat input.

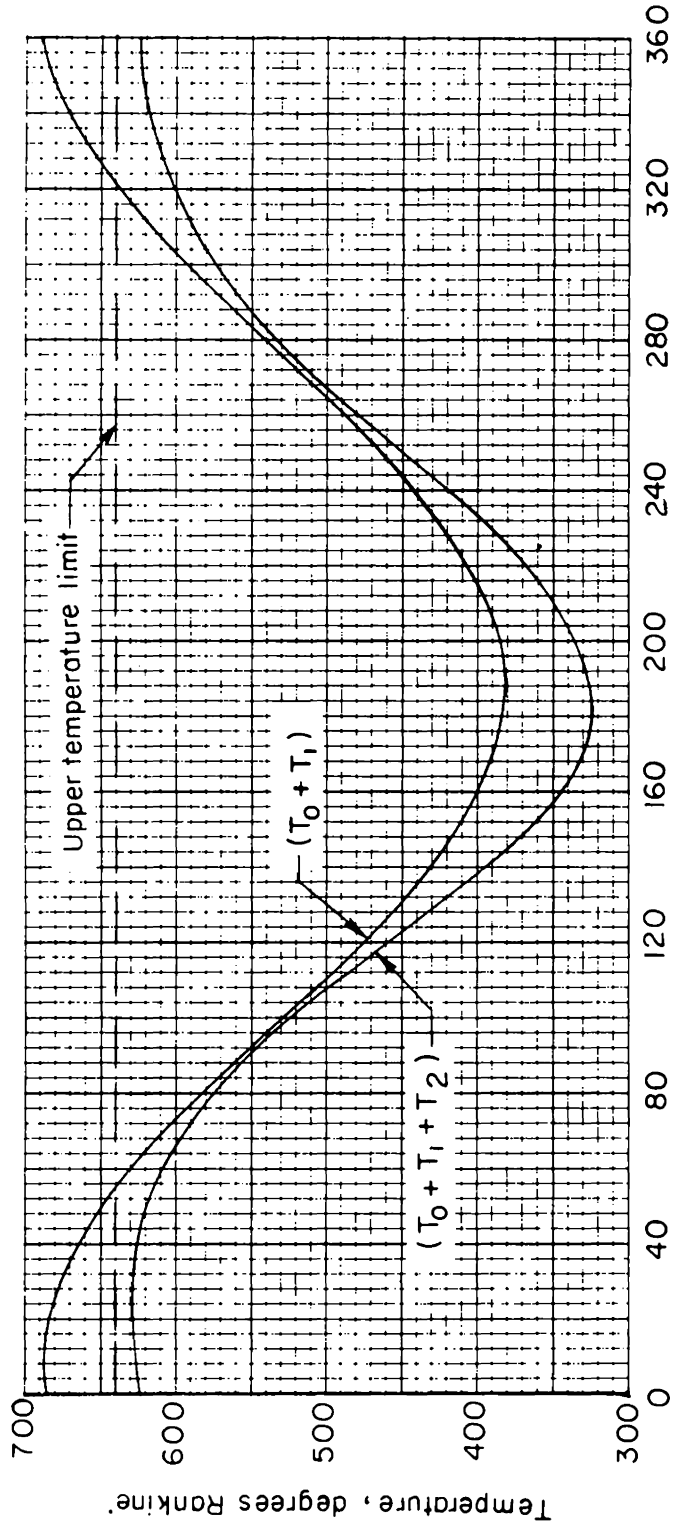

(b) Temperature time history on the front face of a plastic block exposed to thermal radiation.

Figure 16.- Concluded.

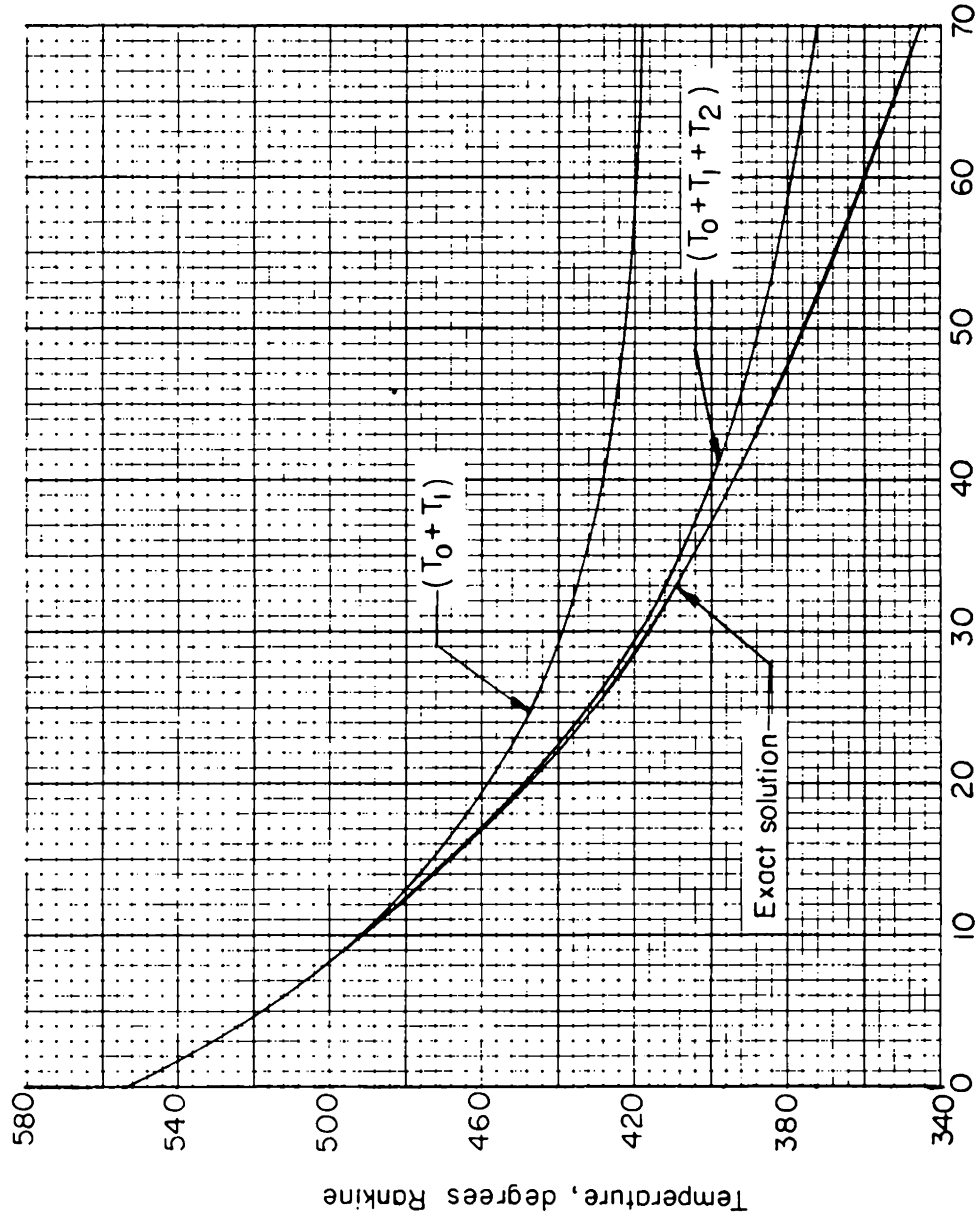

(a) Cooling curves for exact, linearized, and perturbation solutions.

Figure 17.- Comparison of exact solutions with approximate solutions.

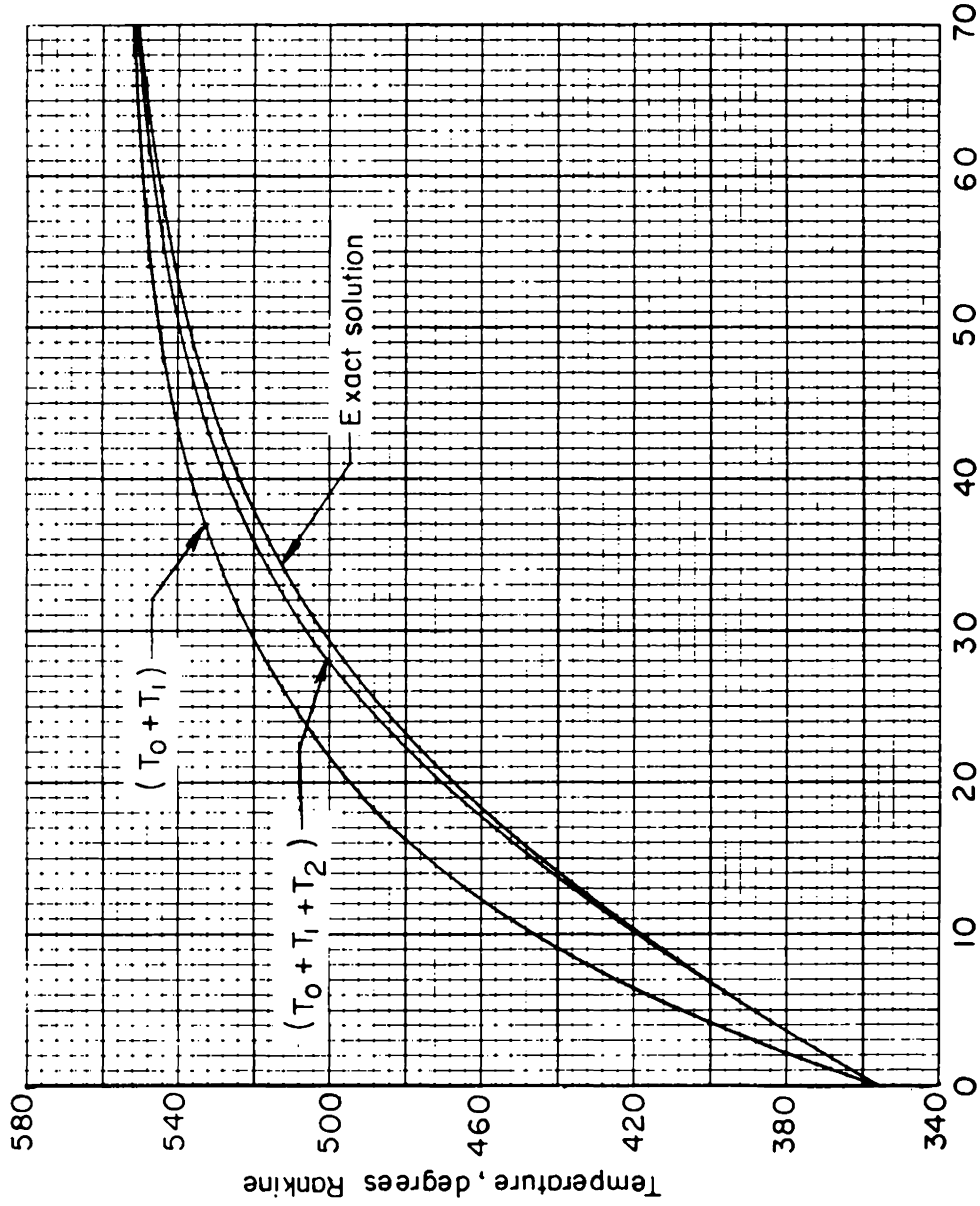

(b) Heating curves for exact, linearized, and perturbation solutions.

Figure 17.- Concluded.

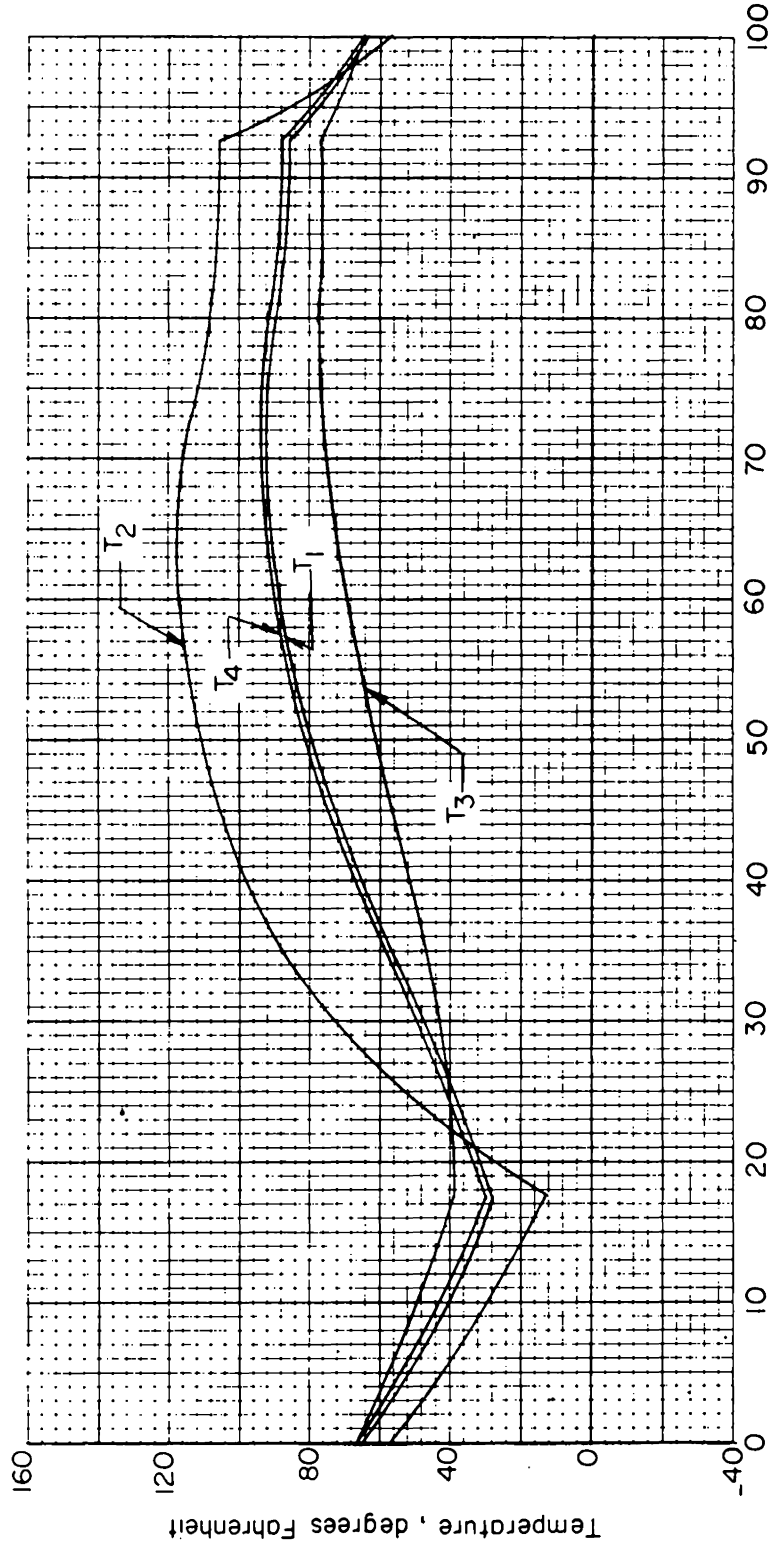

(a) Temperature time histories of sections 1, 2, 3, and 4 in orbital conditions leading to lowest telemetered temperatures.

Figure 18.- Predicted temperature time histories for various parts of Explorer XVI.

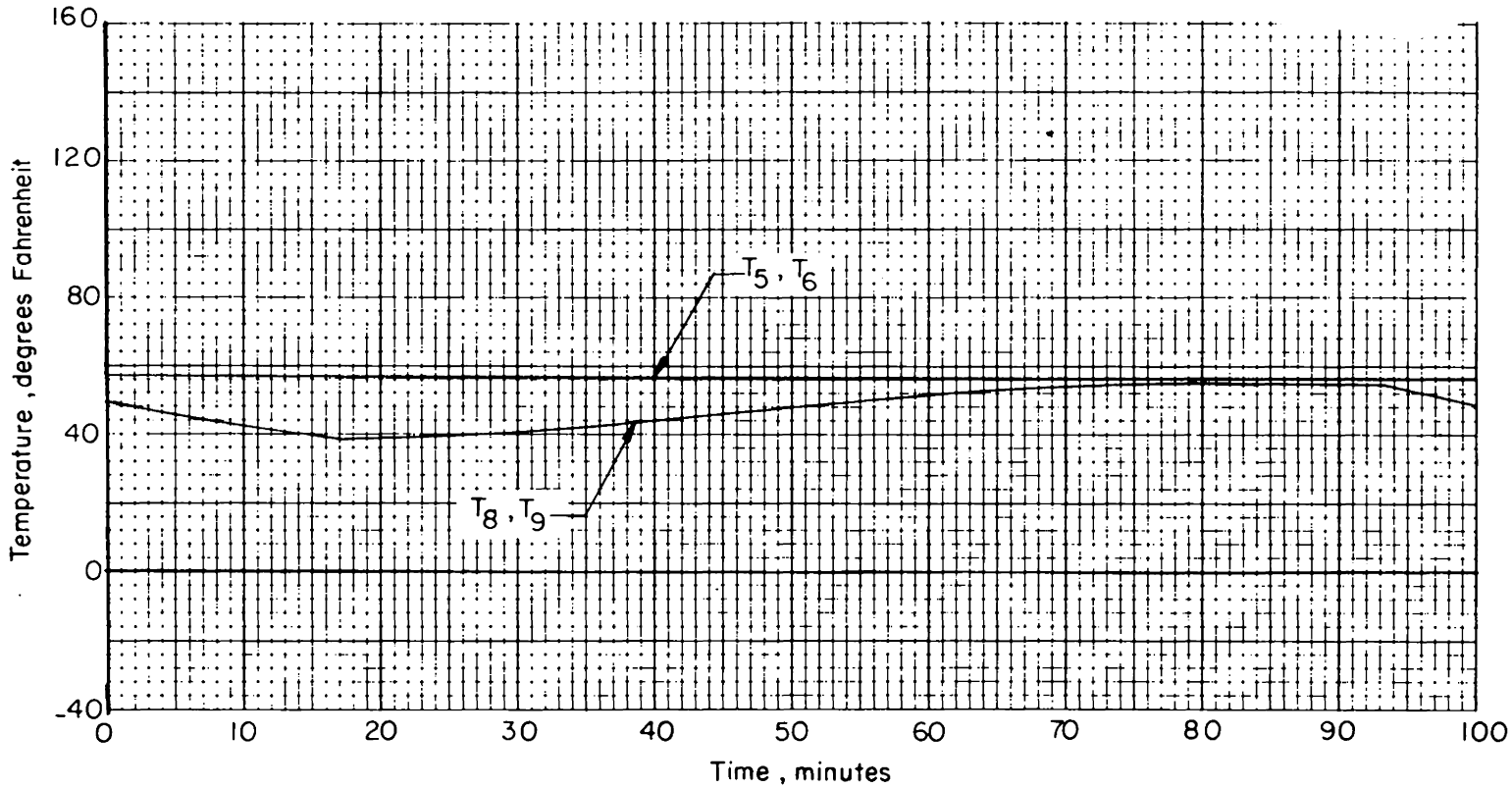

(b) Temperature time histories of sections 5, 6, 8, and 9 in orbital conditions leading to lowest telemetered temperatures.

Figure 18.- Continued.

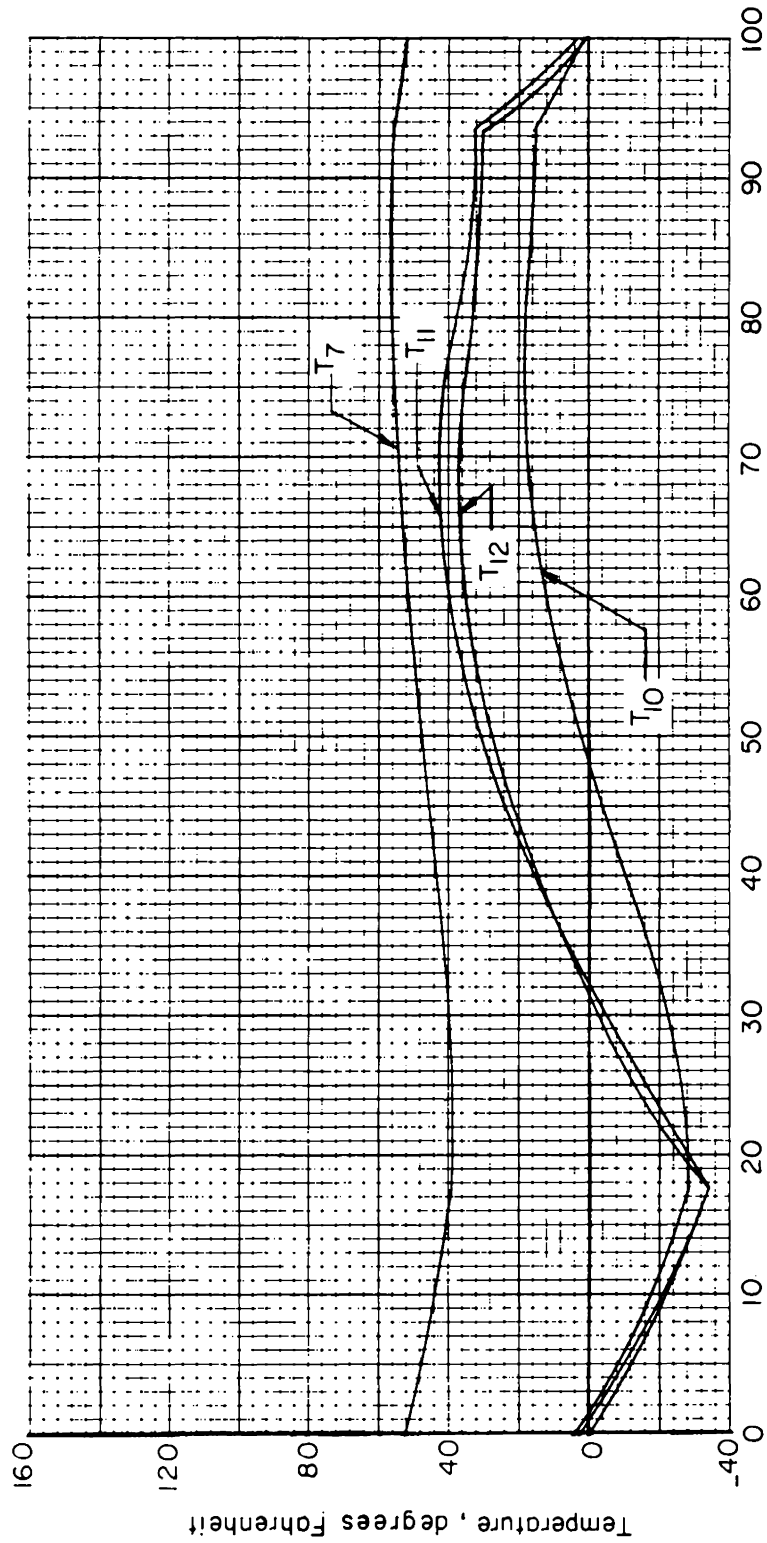

(c) Temperature time histories of sections 7, 10, 11, and 12 in orbital conditions leading to lowest telemetered temperatures.

Figure 18.- Continued.

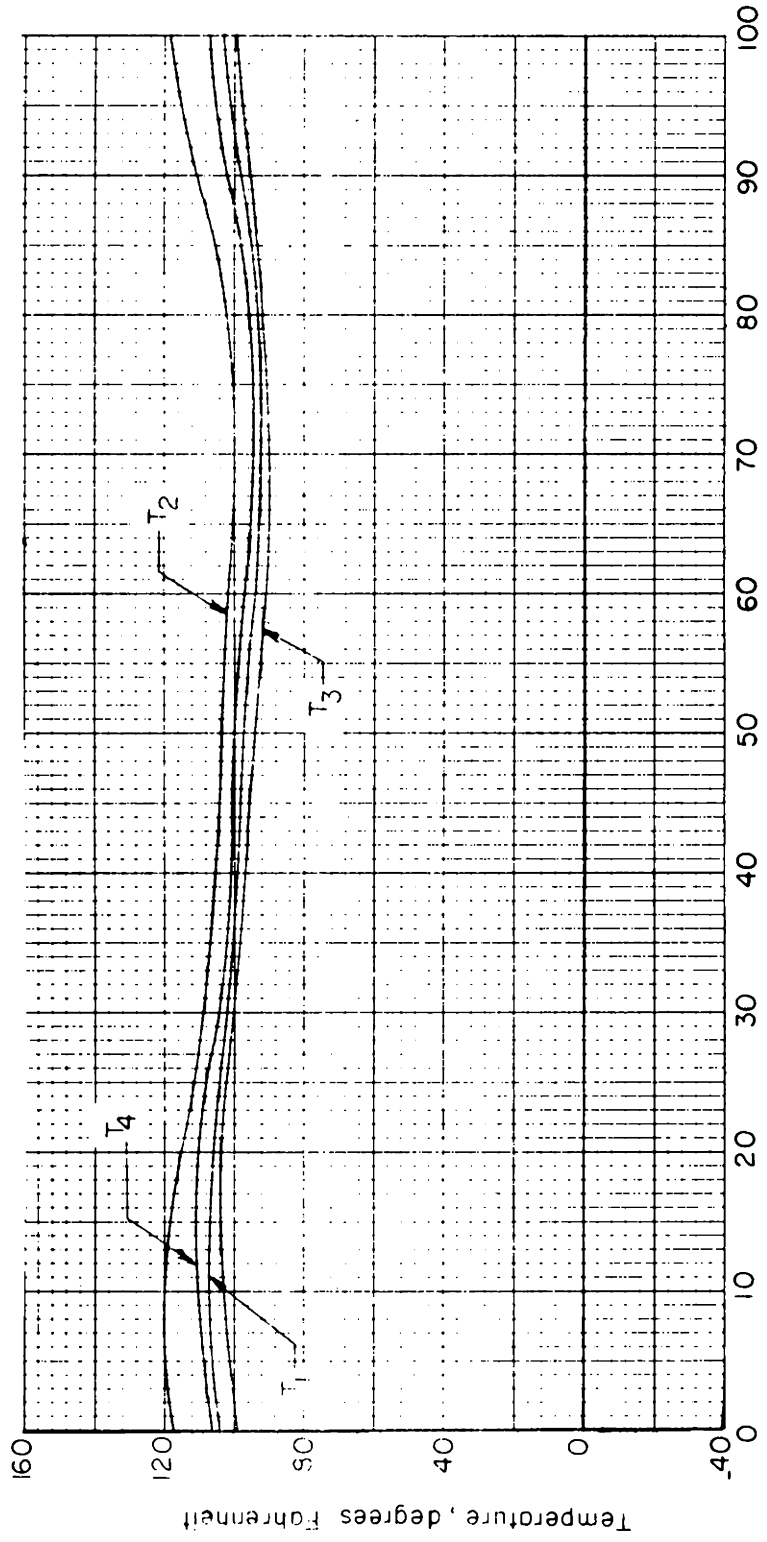

(d) Temperature time histories of sections 1, 2, 3, and 4 in orbital conditions leading to highest telemetered temperatures.

Figure 18.- Continued.

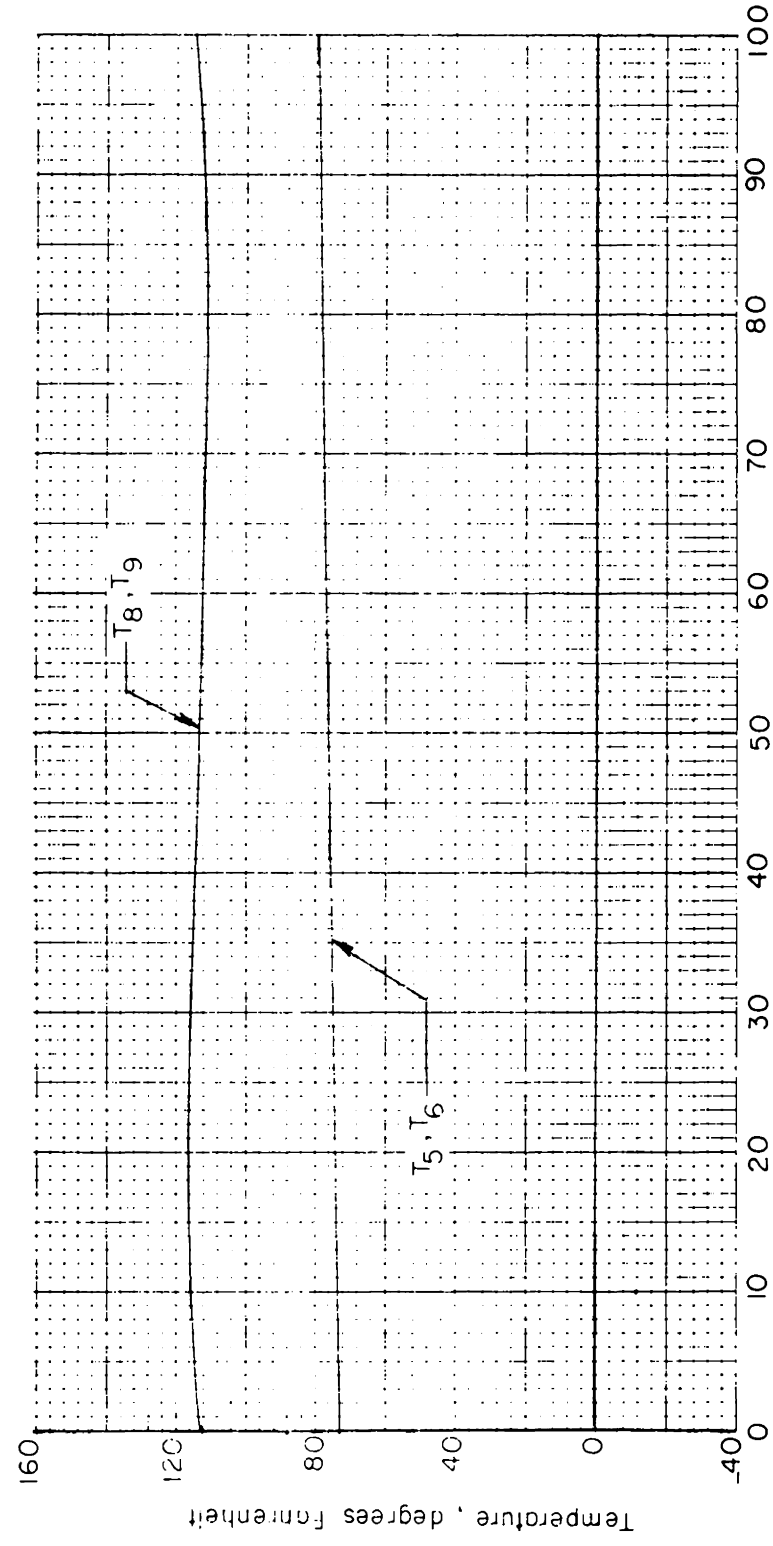

(e) Temperature time histories of sections 5, 6, 8, and 9 in orbital conditions leading to highest telemetered temperatures.

Figure 18.- Continued.

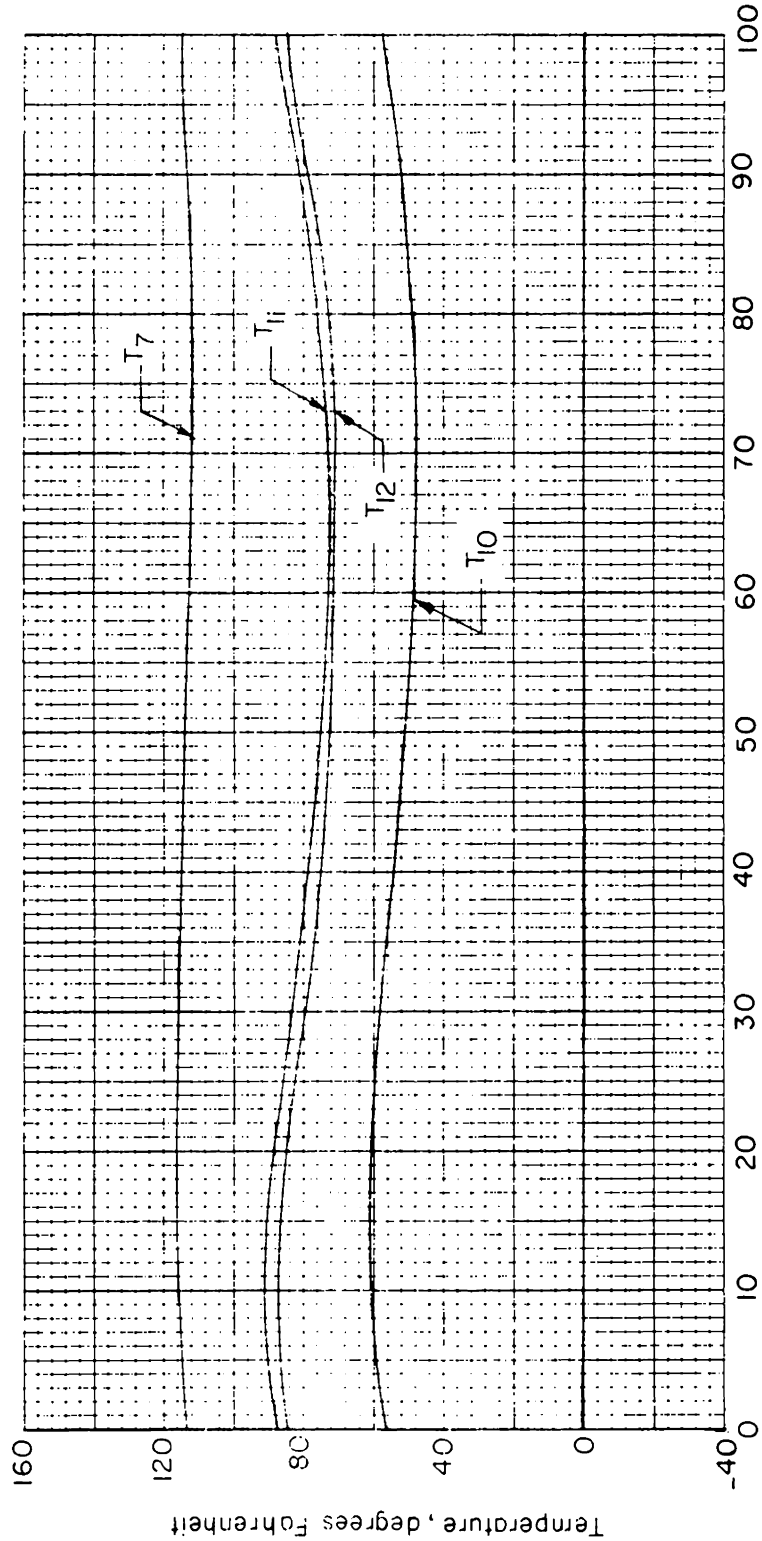

(f) Temperature time histories of sections 7, 10, 11, and 12 in orbital conditions leading to highest telemetered temperatures.

Figure 18.- Concluded.

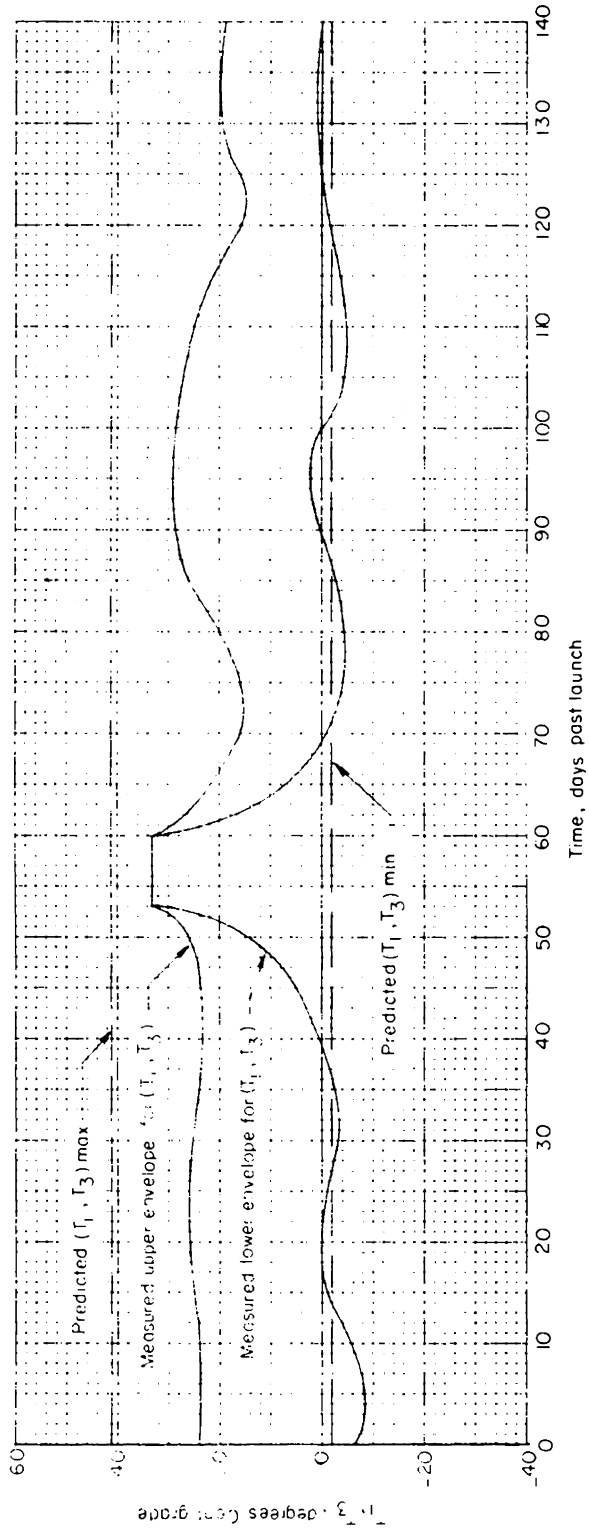

(a) Predicted upper and lower temperature bounds compared with measured flight temperature envelopes for sections 1 and 3.

Figure 19.- Comparison of upper and lower predicted temperature bounds with upper and lower temperature envelopes obtained from flight data for several sections of Explorer XVI micrometeorite satellite, S-55B.

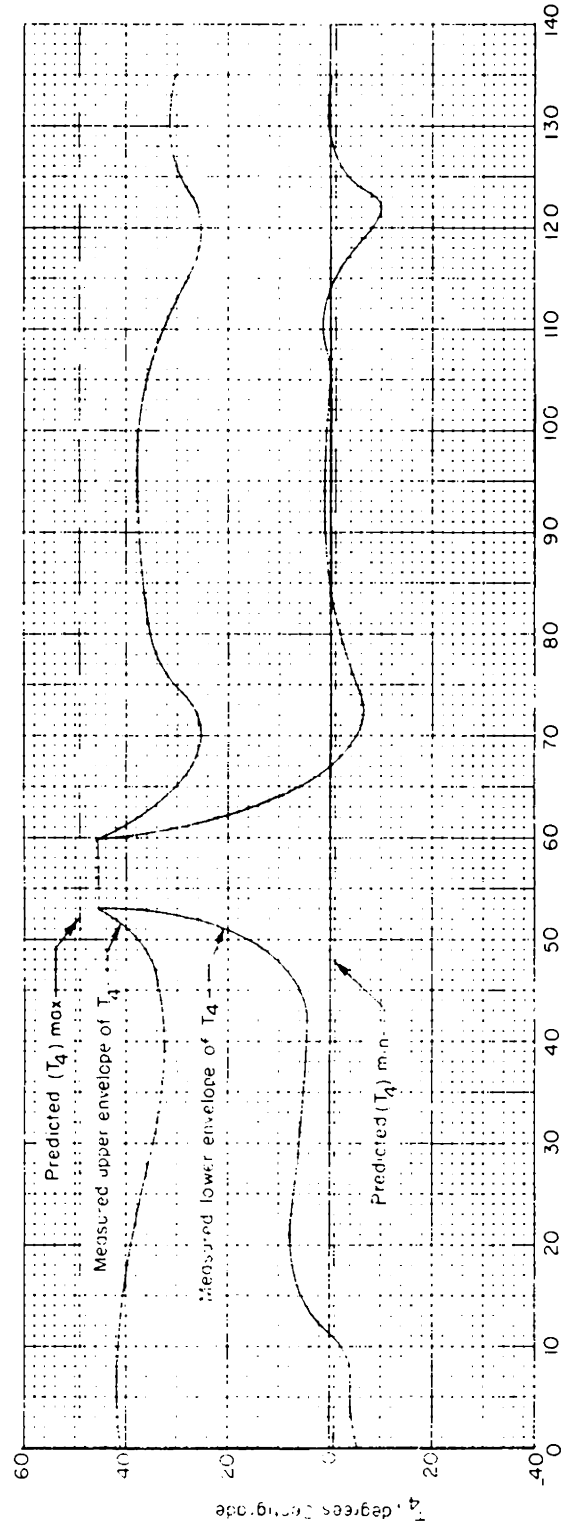

(b) Predicted upper and lower temperature bounds compared with measured flight temperature envelopes for section 4.

Figure 19.- Continued.

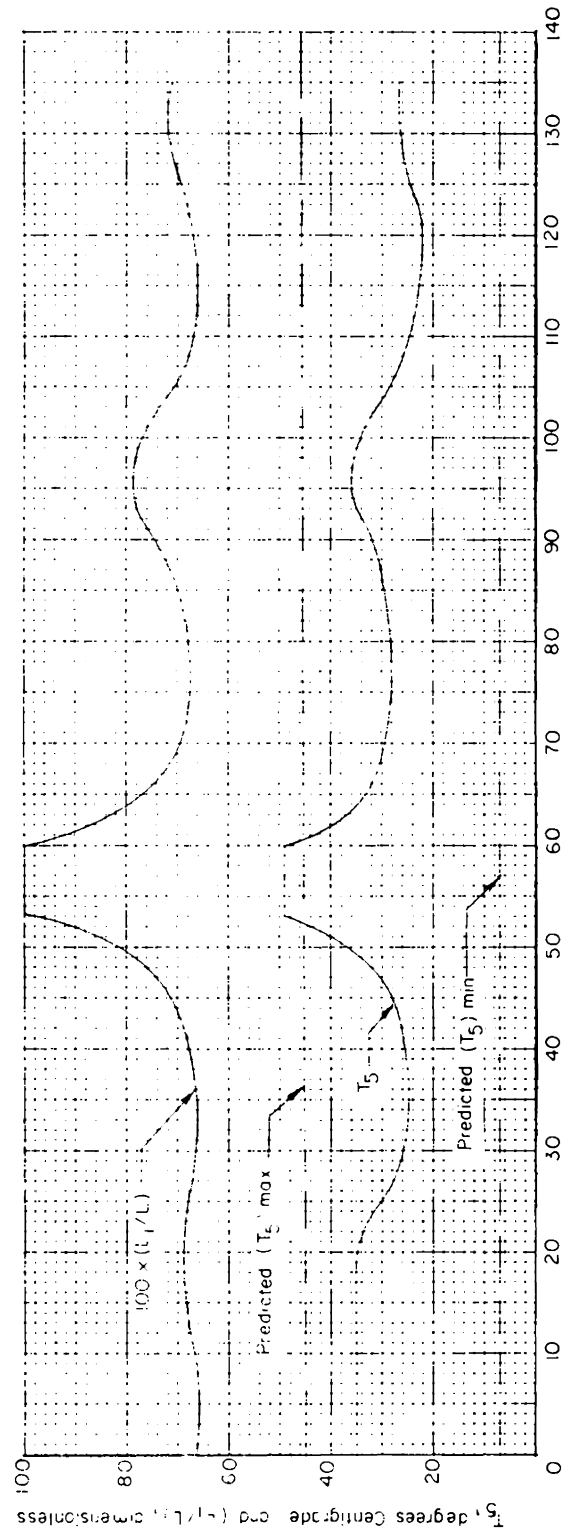

(c) Predicted upper and lower temperature bounds compared with measured flight temperature envelopes for section 5.

Figure 19.- Continued.

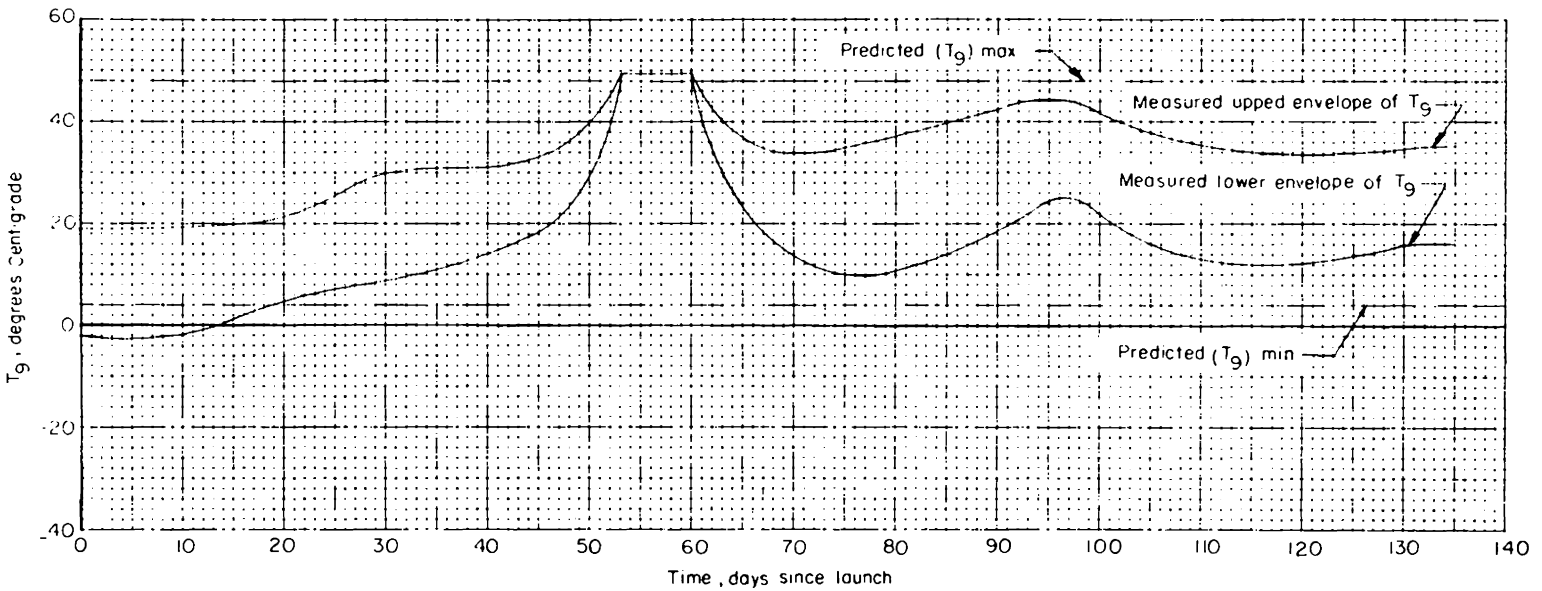

(d) Predicted upper and lower temperature bounds compared with measured flight temperature envelopes for section 9.

Figure 19.- Continued.

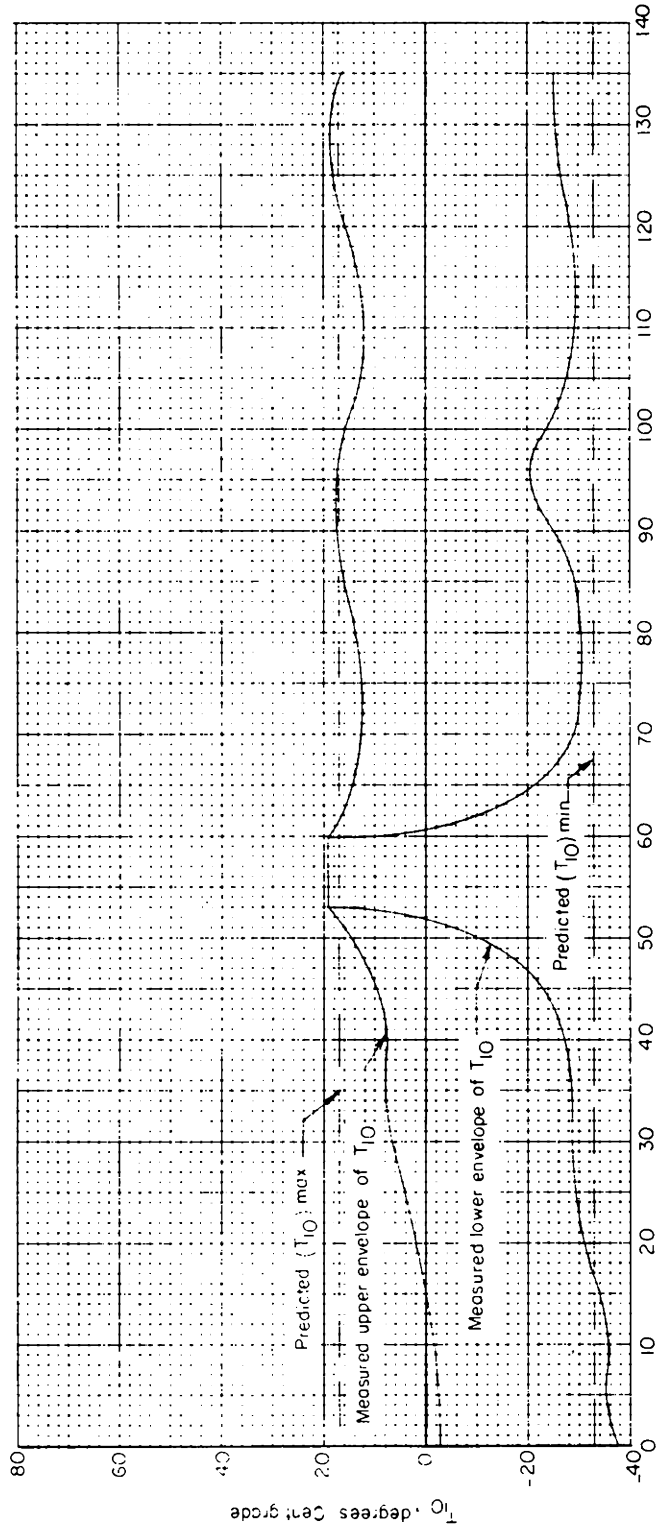

(e) Predicted upper and lower temperature bounds compared with measured flight temperature envelopes for section 10.

Figure 19.- Continued.

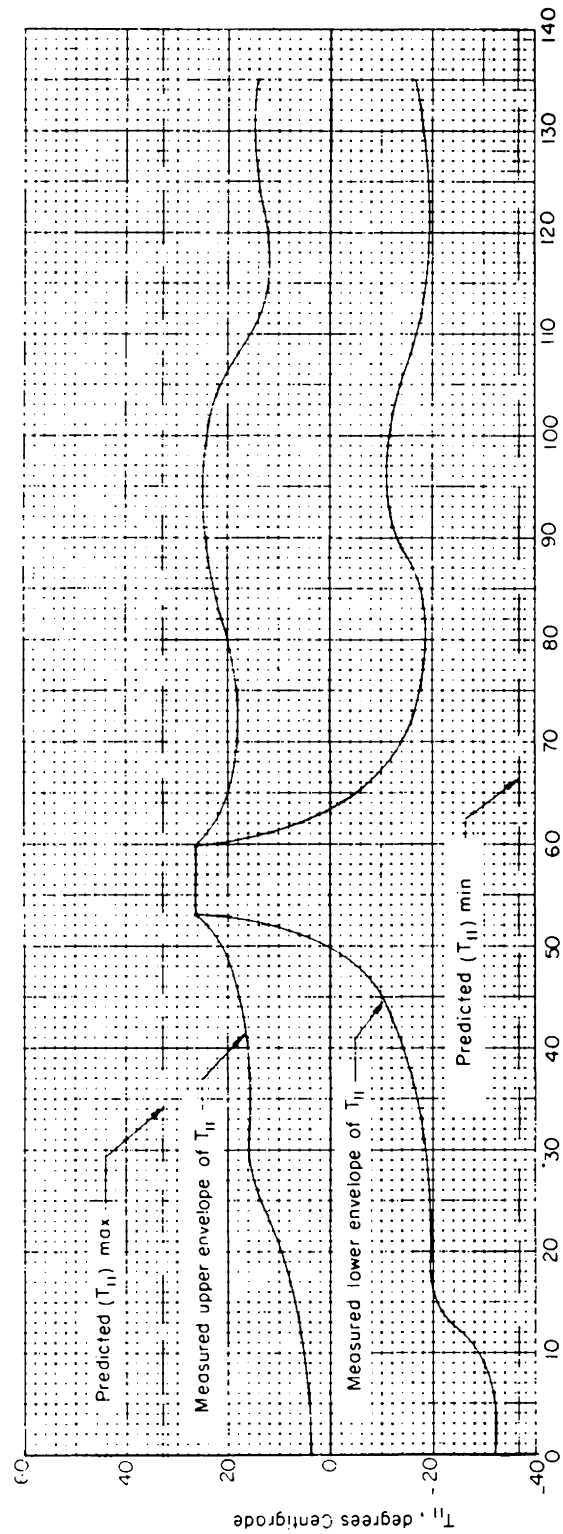

(f) Predicted upper and lower temperature bounds compared with measured flight temperature envelopes for section ll.

Figure 19.- Concluded.

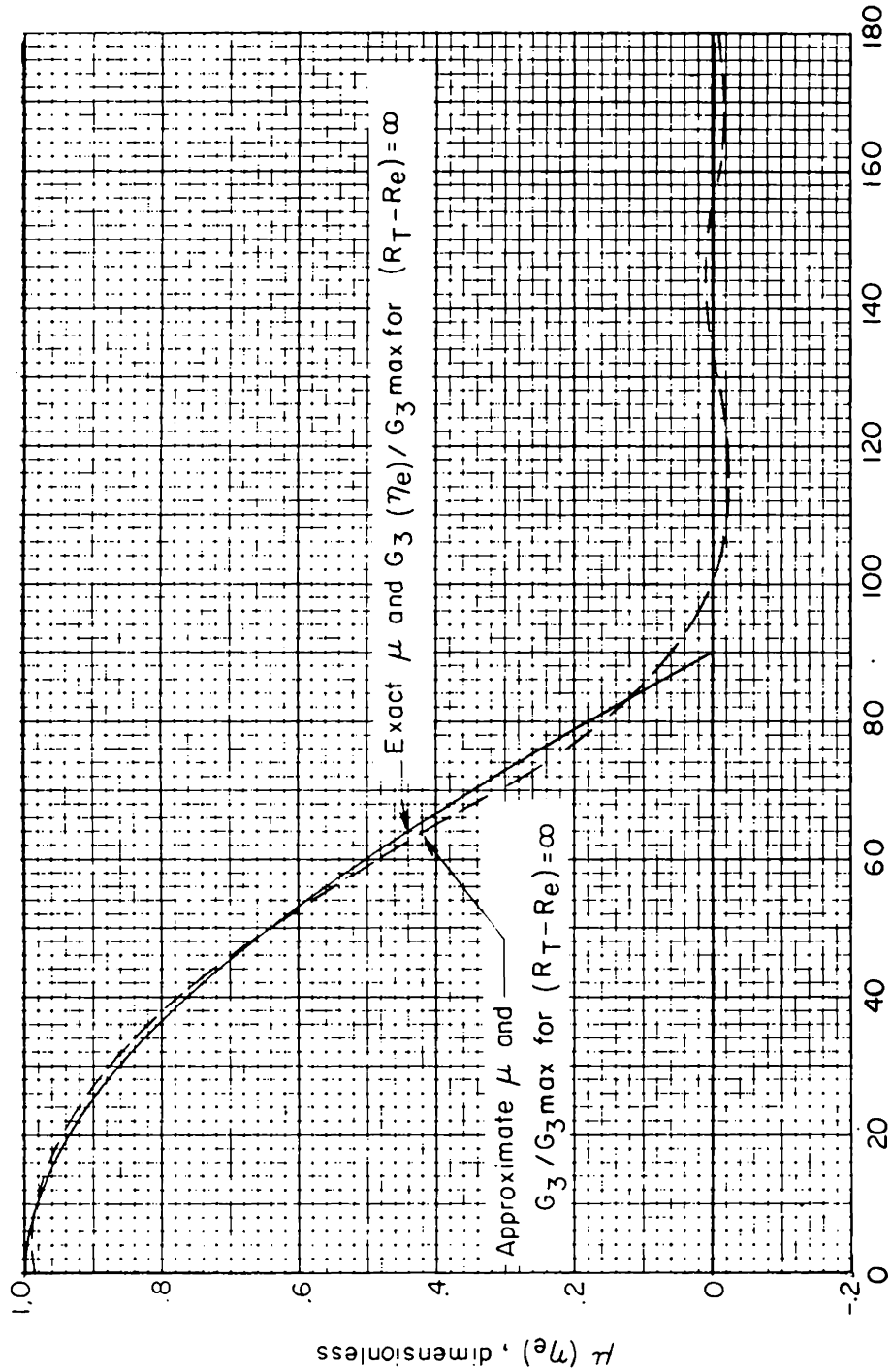

(a) Comparison of exact μ and approximate μ solutions.

Figure 20.- Illustration of truncated series solutions for G_3 and μ through terms of cos $4\eta_e$ when $\mu = \cos {}^*\eta_e$.

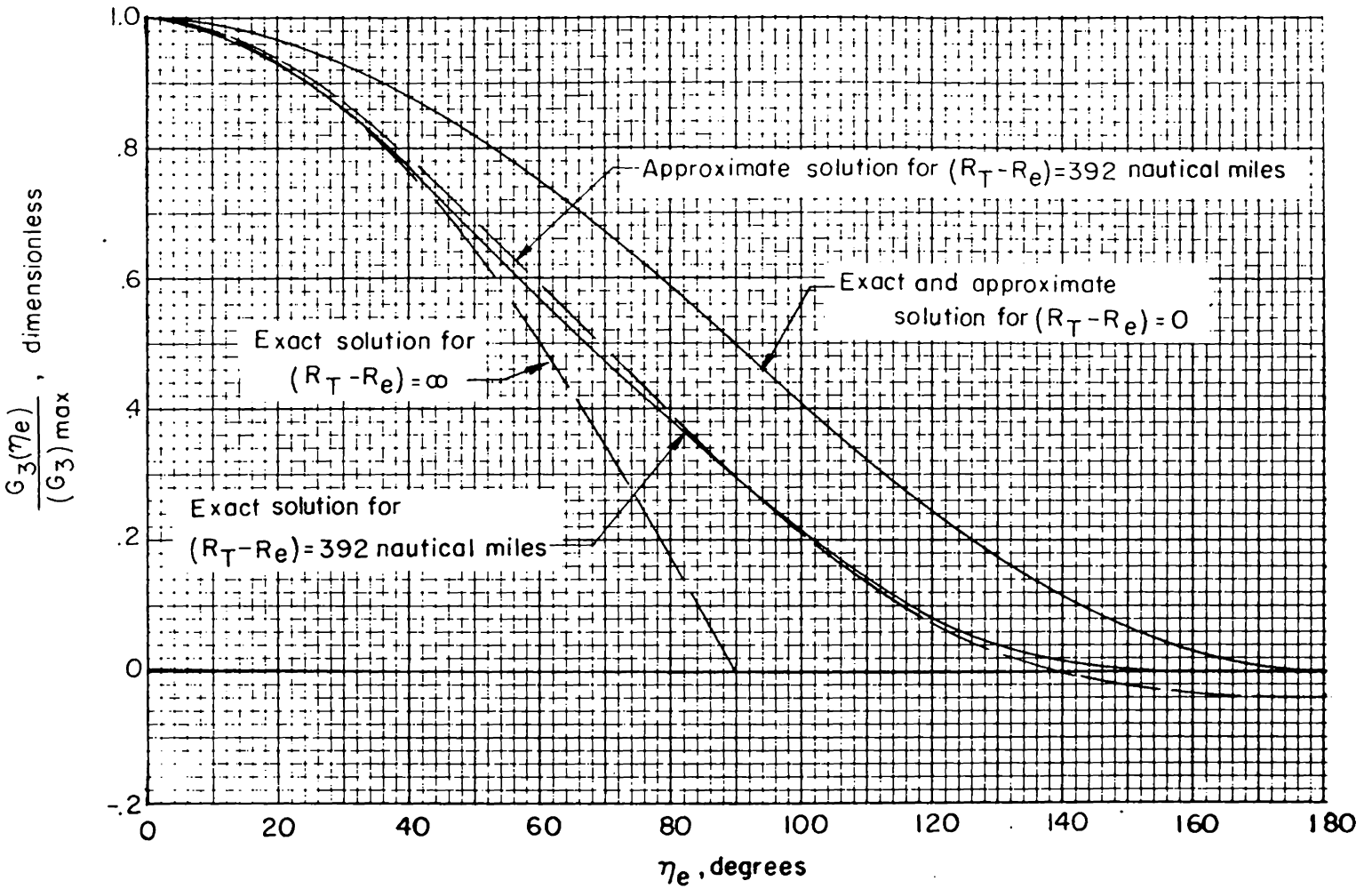

(b) Comparison of exact and approximate solutions of $G_3(\eta_e)$ for different altitudes.

Figure 20.- Concluded.

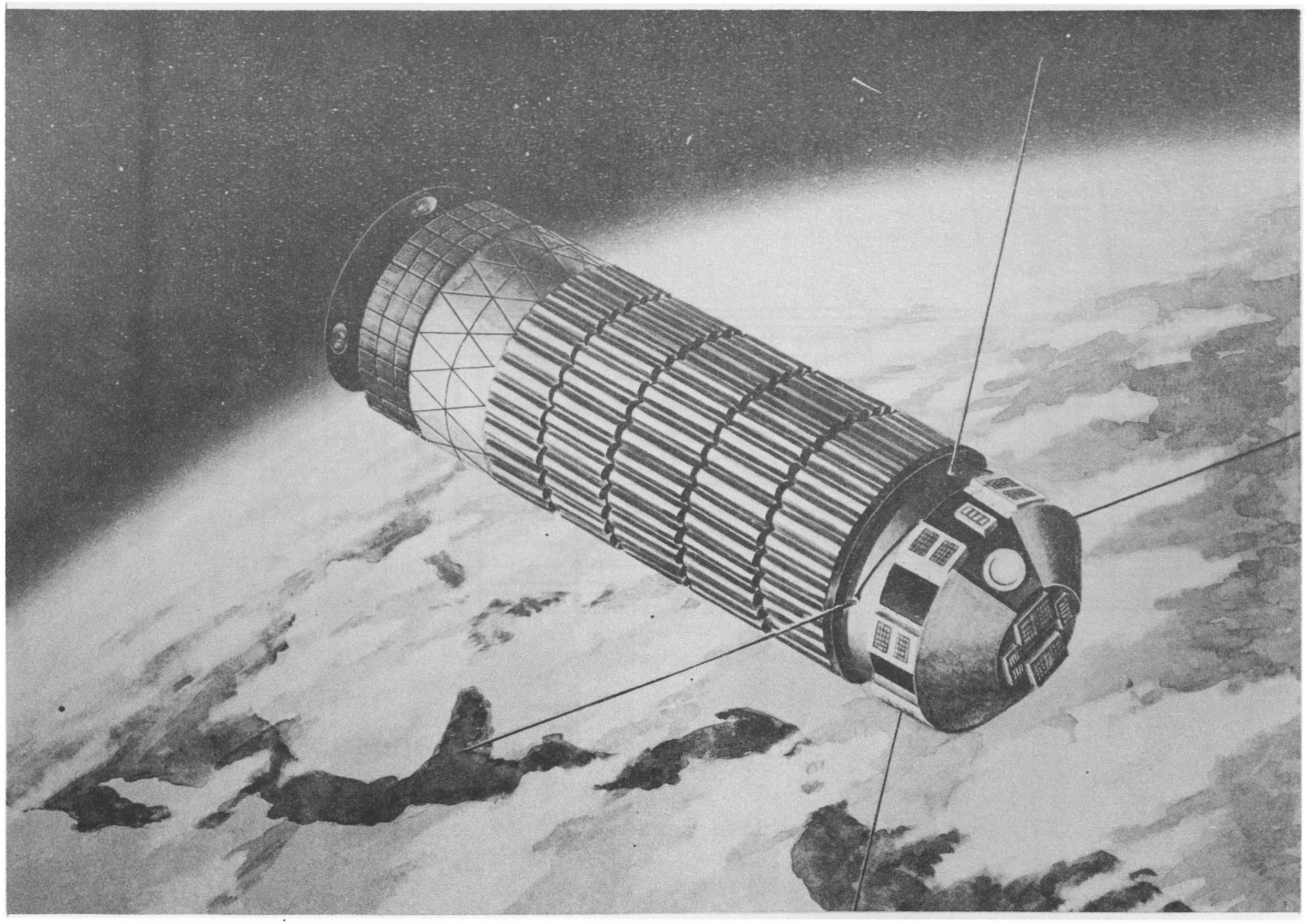

(a) Illustration of Explorer XVI in orbit.

Figure 21.- Illustration of Explorer XVI.

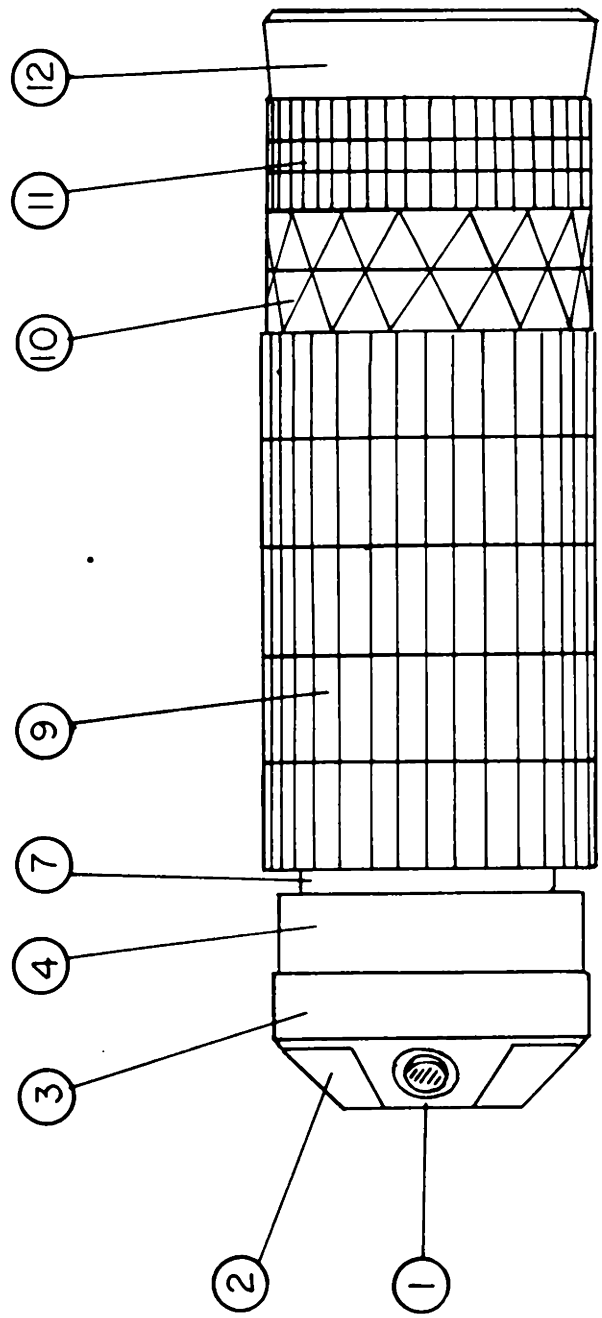

(b) Illustration of the thermal sections of Explorer XVI.

Figure 21.- Concluded.

SOLUTIONS AND METHODS OF SOLUTIONS FOR PROBLEMS ENCOUNTERED IN THE THERMAL DESIGN OF SPACECRAFT

ABSTRACT

The analytical theory of the "passive thermal design of spacecraft" can be divided into two parts. The first part is concerned with the description of the radiant heat transfer to spacecraft external surfaces. The second part is concerned with calculating temperature over a spacecraft when the radiant heat incident, on the spacecraft's wall, is known.

The first part, the calculation of the heat incident on a spacecraft's external surfaces, has been investigated in the literature. References one, two, and three are examples of such papers. Unfortunately, the results of such papers are either numerical or else too specialized to be of general interest for the analytical study of the thermal design of spacecraft.

The second part, the calculation of temperatures over a spacecraft when the incident radiant heat is known, is also dealt with in the literature. References four and five are examples of such papers. The heat flow, occurring in the walls of spacecraft, is nonlinear because of thermal radiation and few exact solutions are known. This problem is usually attacked by "linearizing" the nonlinear term or by directly employing power series. The solution of the nonlinear heat equation by the linearization process is valid only for small temperature variations. When temperature differences are large, the linearized solutions do not properly account for the nonlinear radiation terms and

series error can result. When power series are employed directly to solve the nonlinear heat flow equation, the labor required to solve the time dependent problem is generally excessive because the elementary functions cannot be used efficiently.

In this thesis, the radiant heat transferred to spacecraft is found by the use of Fourier series. The resulting solutions are simple and are valid for spacecraft of very general geometry. Heat transfer calculations which previously required extensive integration on electronic computers can be calculated by the results of this thesis with only trivial labor. Also, the results have the advantage of being well suited for use in the solution of the nonlinear heat transfer equation.

The problem of heat flow including nonlinear radiation is also attacked in this thesis. The method of solution used is closely related to the well known method of successive approximations and allows solution of nonlinear equations which do not have the classical "Small pertubation parameter". Also, the method of solution used makes good use of the elementary functions so that time dependent problems can be solved without excessive labor. The problems solved in this thesis includes: the temperature time history of a body at uniform temperature but exposed to periodic radiative heating, the temperature time history of a body having nonuniform temperatures and exposed to periodic radiative heating, and finally the problem of linear heat flow with nonlinear boundary conditions.

In each case it is shown how linearized solutions neglect the important results of nonlinear radiation heat transfer.

REFERENCES

1. Cunningham, F. G.: Earth-Reflected Solar Radiation Incident Upon Spherical Satellites In General Elliptical Orbits. NASA Technical Note TN D-1472, Goddard Space Flight Center, February 1963.

2. Swalley, Frank E.: Thermal Radiation Incident On An Earth Satellite. NASA Technical Note TN D-1524, George C. Marshall Space Flight Center, December 1962.

3. Cunningham, F. G.: Power Input To A Small Flate Plate From A Diffusely Radiating Sphere With Application To Earth Satellites: The Spinning Plate. NASA Technical Note TN D-1545, Goddard Space Flight Center, February 1963.

4. Nichols, Lester D.: Surface-Temperature Distributions On Thin-Walled Bodies Subjected To Solar Radiation in Interplanetary Space. Technical Note D-584, Lewis Research Center, 1961.

5. Charnes, A., and Raynor, S.: Solar Heating of a Rotating Cylindrical Space Vehicle. ARS Journal, Vol. 30, No. 5, May 1960, pp. 479-484.